NOVEL FUNCTIONS OF B7-H4 IN β-CELL PHYSIOLOGY AND STRESS RESPONSE

by

Annika C. Sun

B.Sc., The University of British Columbia, 2012

A THESIS SUBMITTED IN PARTIAL FULFILLMENT OF

THE REQUIREMENTS FOR THE DEGREE OF

MASTER OF SCIENCE

in

THE FACULTY OF GRADUATE AND POSTDOCTORAL STUDIES

(Experimental Medicine)

THE UNIVERSITY OF BRITISH COLUMBIA

(Vancouver)

April 2015

Abstract

Stress-induced failure and death of pancreatic β-cells are integral steps in the pathogenesis of type 1 and type 2 diabetes. Better understanding of the molecular interactions that influence β-cell function and stress signaling may therefore identify therapeutic targets to protect endogenous β-cells or transplanted islet grafts. B7-H4 is a negative co-stimulatory molecule that is expressed on the cell membranes of antigen presenting cells and down-regulates the immune response. Interestingly, pancreatic β-cells also express high levels of B7-H4 mRNA and moderate levels of B7-H4 protein. Of note, various tumor cells have up-regulated levels of B7-H4, which has been linked to metabolic and anti-apoptotic effects. This raises the intriguing possibility that B7-H4 may also regulate β-cell function, stress signaling, and survival independent of immune-regulation. In this study, we used mice with β-cell-specific overexpression of B7-H4, as well as B7-H4 knockout mice to examine the possible roles of B7-H4 in β-cell physiology and responses to endoplasmic reticulum (ER) stress. Cytosolic Ca^{2+} imaging showed that B7-H4 transgenic islets had increased sensitivity to sub-maximal glucose stimulation. Additional experiments indicated no differences in ER Ca^{2+} uptake/release or glucose metabolism, but revealed that B7-H4 transgenic islets are sensitized to tolbutamide and are resistant to diazoxide, suggesting changes at the ATP-sensitive potassium channels. The B7-H4-induced amplification of glucose-stimulated Ca^{2+} did not translate into detectable differences in *in vitro* insulin secretion or *in vivo* glucose tolerance, suggesting secondary control between rise in intracellular calcium and exocytosis of insulin granules. ER stress was induced *in vitro* using thapsigargin, and gene expressions were compared by real time quantitative PCR. Moderate ER stress induced the expression of key unfolded protein response genes, BiP, CHOP, and XBP1s to significantly higher levels in B7-H4 transgenic islets compared with wild type. However, the death of dispersed B7-H4 and wild type islet-cells did not differ following more severe and prolonged ER stress. Together, our findings demonstrate that over-expression of B7-H4 amplifies β-cell glucose-stimulated Ca^{2+} responses and the unfolded protein response during ER stress, revealing novel roles for B7-H4 in the pancreatic β-cell.

Preface

The content presented in this thesis is the original and unpublished work by the author, Annika C. Sun. Dr. Michal Aharoni-Simon performed the experimental procedures outlined in 2.2.11; data analysis was carried out by Annika Sun.

All animal work conducted for this study was approved by the University of British Columbia Animal Care Committee. Animal Care Service's Rodent Biology and Husbandry course was completed by Annika Sun through the UBC Animal Care Center (RBH-239-12). Animal Care Service's Principles of Rodent Anesthesia course was completed by Annika Sun through the UBC Animal Care Center (RA-115-12). Animal Care Service`s Principles of Rodent Surgery course was completed by Annika Sun through the UBC Animal Care Center (RSx-84-12). Ethics training requirement for animal work was completed by Annika Sun, and met the requirements of the Canadian Council on Animal Care/National Institutional Animal User Training Program (CCAC, certificate #3706-10).

Table of Contents

List of Tables

List of Figures

List of Abbreviations

$[Ca^{2+}]_i$	Intracellular Ca^{2+} concentration
$[Ca^{2+}]_{ER}$	ER Ca^{2+} concentration
18s rRNA	18s ribosomal RNA
ATF4	Activating transcription factor 4
ATF6	Activating transcription factor 6
AUC	Area under the curve
B7-H4 Ig	B7-H4 immunoglobulin
B7-H4 KO	B7-H4 knock-out
B7-H4 Tg	B7-H4 transgenic
B7-H4 WT	B7-H4 wild type
Bak	Bcl-2 homologous antagonist killer
Bax	Bcl-2-associated X protein
Bcl-2	B-cell lymphoma 2
BiP	Binding immunoglobulin protein
CBD	Common bile duct
Cch	Carbachol
CHOP	C/EBP-homologous protein
CPT1	Carnitine palmitoyltransferase I
DAG	Diacyl glycerol
DMSO	Dimethyl sulfoxide
DP5	Death protein 5

DZ	Diazoxide
ECAR	Extracellular acidification rate
eIF2α	Eukaryotic translation initiation factor 2α
ELISA	Enzyme-linked immunosorbent assay
ER	Endoplasmic reticulum
ERAD	Endoplasmic reticulum-associated protein degradation
GAPDH	Glyceraldehyde 3-phosphate dehydrogenase
GCK	Glucokinase
GDH	Glutamate dehydrogenase
GIP	Gastric inhibitory peptide
GLP-1	Glucagon-like-peptide 1
Glut-2	Glucose transporter 2
GPCR	G protein-coupled receptor
IgC	Constant immunoglobulin domain
IgV	Variable immunoglobulin domain
IL-2	Interleukin-2
IP_3	Inositol triphosphate
IPGTT	Intraperitoneal glucose tolerance test
IRE1α	Inositol-requiring protein 1α
JNK	c-Jun N-terminus kinase
K_{ATP} channel	ATP-dependent K^+ channel
K_v channel	Voltage-gated K^+ channel

LC-CoA	Long-chain fatty acyl-CoA
MODY	Maturity onset diabetes of the young
NOD	Non-obese diabetic
OCR	Oxygen consumption rate
Pen/Strep	Penicillin/Streptomycin
PERK	protein kinase RNA-like endoplasmic reticulum kinase
PLC	Phospholipase C
PUMA	P53 upregulated modulator of apoptosis
qPCR	Quantitative polymerase chain reaction
RIP	Rat insulin promoter
RPLP0	60S acidic ribosomal protein P0
SDS-PAGE	sodium dodecyl sulfate polyacrylamide gel electrophoresis
SERCA	Sarco/endoplasmic reticulum Ca^{2+}-ATPase
SNARE	Soluble NSF attachment protein receptor
SNP	Single-nucleotide polymorphism
STS	Staurosporine
T1D	Type 1 diabetes
T2D	Type 2 diabetes
Th1	T helper cell 1
Thap	Thapsigargin
Tol	Tolbutamide
UPR	Unfolded protein response

VGCC	Voltage-gated Ca^{2+} channel
VTCN-1	V-set domain containing T cell activator inhibitor 1
XBP1	X-box binding protein 1
XBP1s	Spliced X-box binding protein 1

Acknowledgements

In the blink of an eye, I am approaching the end of my graduate studies. Looking back, this journey has been an experience that has at times frustrated me, angered me, excited me, and most importantly, challenged me. I have not only gained a pair of nifty hands for islet picking and an addiction to caffeine, but also an appreciation for scientific research, and new-found respect for those who are able to persevere on this path. I would like to thank my supervisor Dr. Garth Warnock, for providing me with the opportunity to work on project, and for his continued support throughout this experience. I would also like to thank Dr. Dan Luciani, who has taken on the role of my co-supervisor and allowing me to integrate myself into the Luciani lab, as well as providing both guidance and support for my studies. Thanks to my committee members, Dr. Bruce Verchere, Dr. Lucy Marzban, and Dr. Alice Mui for their guidance and scientific inputs. I am grateful to be working at both VGH and CFRI, where I have easy access to a vast intellectual knowledge base in the form of all the graduate students, PIs, and research staff. The CIHR Training Program provided both funding support for my studies, and an opportunity to gain a better understanding of the clinical side of research in organ transplantation.

I am lucky to have the continued support of my friends that have been there for me since our high school and university days where we sat on dirty floors of school hallways during lunch time, and fell off bunk beds in university dorms. Of course, this experience would not have been the same without the many new friends that I have worked and bonded with over the two and half years since the start of my graduate studies. Alexis Shih, for suffering it all along with me, and being my awesome HK-counterpart- lab life would not be nearly as much fun if not for her. Dan Wu, for listening to me rant incessantly at times, and for lending a hand whenever I needed. Thilo Speckman, for always providing a good laugh, even when it may be at his own expense. Sigrid Alvarez, for much goodies that I have consumed over the years, and as she puts it, for "introducing" me to the world of CFRI.

I also owe many thanks to the lab members at both the Warnock and Luciani lab for their technical support and advice. Jianqiang Hao, for isolating all the mouse islets used for my experiments, Crystal Roberson, for administrative assistance, and Ziliang Ao, for providing the human islets through the Ike Barber Human Transplant Laboratory. I also thank Rose Shumiatcher for being a great lab manager, and Queenie Hui for fulfilling all the little requests that I have tossed her way despite her hectic workload. I would especially like to thank Sarah White, for teaching me almost all the technical skills required for my project, and for helping me trouble-shoot whenever I encounter problems with my assays.

Finally, thanks to Mom and Dad for their unconditional love and support, and for encouraging me along this journey.

CHAPTER 1: INTRODUCTION

1.1 Diabetes as a Global Epidemic

Diabetes mellitus, commonly referred to as diabetes, is a growing global epidemic that affects 382 million people world-wide today. It has been projected that this number will reach 592 million by the year 2035[1]. Diabetes is a chronic metabolic disease characterized by elevated blood glucose level due to insufficient insulin production or inability of peripheral tissues to efficiently utilize insulin[2]. Control of euglycemia is largely maintained by a cluster of hormone-producing cells residing in the islets of Langerhans, which constitutes the endocrine pancreas. Each subset of endocrine cells differs in its percent distribution in the islet and the hormones that it produces/secretes. Alpha (α) cells produce and secrete glucagon, which stimulates glycogenolysis and gluconeogenesis in the liver to elevate blood glucose concentrations[3]. Beta (β) cells, on the other hand, help remove excess glucose from blood via production and secretion of insulin[3], which acts on peripheral tissues such as muscles and adipocytes to stimulate glucose uptake[3]. There are also small percentages of delta (δ) cells, PP cells, and epsilon (ε) cells, which secrete somatostatin, pancreatic polypeptide, and ghrelin, respectively[3,4]. Somatostatin suppresses the release of both insulin and glucagon, while pancreatic polypeptide and ghrelin are neuropeptides that are linked to the control of food intake, body weight, and energy expenditure[3,4,5]. In diabetes, failure and/or loss of β-cells are significant factors that contribute to the development of chronic hyperglycemia[2,6,7]. Persistently high blood glucose leads to both acute metabolic and long-term vascular complications such as diabetic retinopathy, nephropathy, and neuropathy, stroke, and cardiovascular diseases[6-8]. Management of diabetes places enormous socioeconomic strains on the healthcare system, with a global estimate of 612 billion USD in

health expenditure in 2014 alone[1]. It is therefore essential to generate improved therapies that can alleviate both health and socioeconomic burdens caused by diabetes.

1.2 Disease Etiology of T1D and T2D

Diabetes is a multi-faceted disease with various forms and disease etiologies. The two major forms- type 1 diabetes (T1D) and type 2 diabetes (T2D), account for almost all diagnosed cases. Less prevalent forms of diabetes include gestational diabetes and monogenic diabetes[9,10]. T1D has been identified as an autoimmune disease, and is usually diagnosed in children and young adults. In T1D, hyperglycemia occurs as β-cells are targeted and destroyed by the body's own immune system in genetically susceptible individuals[7]. Current studies suggest that environmental factors initially trigger the recruitment of immune cells to pancreatic islets[11]. Targeted attacks are mounted against β-cell autoantigens, resulting in massive cell death and insulin deficiency[7,8]. T2D amounts to 90% of all diabetes cases, and is primarily diagnosed in the adult population. In recent years there has also been a surge in T2D cases in children and teens largely contributed by high-calorie diets and sedentary lifestyles[12]. T2D is closely linked to obesity, and is characterized by insulin resistance in peripheral tissues, which leads to β-cell stress, dysfunction, and its eventual demise[7,13,14]. Recent studies suggest that T1D and T2D to some extent converge on similar β-cell stress and death pathways despite their distinct disease origins[2]. One such common pathway is endoplasmic reticulum (ER) stress, which activates a series of signaling cascades collectively termed the unfolded protein response (UPR)[2], as will be discussed in more detail in section. In T2D, a pressing demand for increased insulin production to compensate for the progressive insulin insensitivity, combined with continuous exposure to elevated levels of glucose and fatty acids, induces prolonged β-cell ER stress and cell death by

apoptosis[13-15]. Growing evidence also implicates ER stress as a contributing factor in T1D[16-18]. Pro-inflammatory cytokines secreted by infiltrating immune cells could disrupt ER homeostasis, leading to UPR dysregulation and β-cell death[2,19,20]. The partial overlap in pathophysiology of T1D and T2D present the possibility that therapeutics have the potential to target instigators common to both forms of the disease.

1.3 Treatment of Diabetes

Current treatment regimens aim to restore euglycemia and alleviate diabetic complication. T1D patients rely mainly on exogenous insulin injections to regulate their blood glucose levels. Several on-going clinical trials for T1D are also focused on immunomodulation strategies to preserve β-cell function and delay disease progression into full blown diabetes[21]. Transplantation of insulin-secreting tissue is another option to restore glycemic control. With the establishment of the Edmonton Protocol, islet cell transplantation has become a relatively safe and reliable alternative to whole pancreas transplant[22,23]. However, shortage of donor islets, as well as graft failure and rejection continue to be major challenges to this treatment option[24]. It is therefore vital to develop β-cell immunoprotective strategies that can maintain functionality of implanted grafts, but lacks the toxicity of immunosuppressive drugs. Treatment options for T2D are more varied compared to T1D, and ranges from lifestyle and diet modifications to pharmacological agents such as insulin sensitizers, insulin secretagogues, incretin-based therapies, and insulin analogues[15].

1.4 Mechanism of Insulin Secretion in β-Cells

Insulin is critical for the maintenance of blood glucose homeostasis, and is synthesized and secreted by pancreatic β-cells. In mammals, β-cells are the main endocrine cell type in the pancreatic islet, whose spherical architecture offers structural support and facilitates paracrine signaling between cells[4,25].

1.4.1 The canonical K_{ATP} channel-dependent triggering pathway for insulin secretion

Under physiological conditions, the main secretagogue for insulin is glucose. Within the islets, β-cells rapidly convert small fluctuations in blood glucose level to insulin output by exocytosis of insulin granules. In response to meal-induced glucose rise, only a small fraction of β-cell's total insulin granules is needed to restore blood glucose concentration to within the normal physiological range[26]. Therefore, this process is tightly controlled to not only prevent hyperglycemia, but also to avoid hypoglycemic episodes which can have life-threatening consequences.

Two pathways are implicated in glucose-stimulated insulin secretion[27]. The more well-defined pathway, also termed the triggering pathway, relies on actions of ATP-dependent K^+ (K_{ATP}) channels to generate a triggering Ca^{2+} signal[27,28]. Glucose entry and metabolism denotes the first step in the insulin secretion pathway. The main glucose transporter in rodent islets is GLUT2 while human islets predominantly express GLUT1[28,29]. After glucose enters the cell, it is phosphorylated to glucose-6-phosphate by glucokinase (GCK), which constitutes the rate-limiting step in the glycolysis reactions[29]. The importance of GCK in glucose-sensing is demonstrated by human GCK mutations, which accounts for defective insulin secretion in maturity onset diabetes of the young-2 (MODY-2)[30]. Phosphorylated glucose enters the

glycolytic and oxidative pathways to generate ATP, which increases cytosolic ATP/ADP ratio, leading to the closure of K_{ATP} channels[27,31]. Inhibition of K^+ efflux raises cell membrane potential from a resting potential of -70mV due to unbalanced positive charge build-up from Na^+ ion influx. As the plasma membrane depolarizes, action potentials are fired, accompanied by activation of voltage-gated Ca^{2+} channels (VGCCs) to admit inflow of Ca^{2+} ions[28]. Intracellular Ca^{2+} is a key regulator of vesicle fusion via interactions with fusion regulatory proteins such as synaptogamin[32]. This is followed by activation of secretory granule-associated small N-ethylmaleimide-sensitive factor receptor (SNARE) proteins that drive granule fusion to the plasma membrane and release of insulin[32,33]. As blood glucose concentration is lowered, K_{ATP} channels re-open due to decreased ATP/ADP ratio, returning the cell to its hyperpolarized state and terminating insulin secretion. This coupling of glucose metabolism to insulin secretion gives rise to the β-cell's unique ability to secrete insulin in response to changes in blood glucose concentrations, thereby preserving euglycemia under both fed and fasting states. The integral component of this process is the K_{ATP} channel, which convert changes in the cellular "energy currency" ATP into changes in electrical activities and ultimately, insulin secretion. The critical involvement of K_{ATP} channels in insulin secretion is highlighted by inactivating and activating mutations, which are major causes of persistent hyperinsulinemia and neonatal diabetes, respectively[34,35]. Genetic studies have also identified K_{ATP} variants that are risk factors for T2D[34,36]. For example, the E23K variant has been associated with reduced glucose tolerance and mild β-cell dysfunction, and was predicted to predispose individuals to T2D[36].

While this classical triggering pathway is undisputed, it is now considered an incomplete picture of glucose-stimulated insulin secretion in β-cells. It has been suggested that glucose-

stimulated insulin secretion would be reduced by 50% if the triggering pathway is not subject to further amplification[27].

1.4.2 The metabolic amplifying pathway

Although still an area of active research, there is strong evidence to suggest the existence of another glucose-sensing pathway for insulin secretion independent of K_{ATP} channel closure. The existence of a metabolic amplifying pathway was established in 1992 when it was discovered that glucose-dependent insulin secretion occurs even in the absence of K_{ATP} channel activity[37]. Independent studies demonstrated that glucose can increase insulin secretion in the presence of pharmacological agents such as diazoxide and sulfonylurea, which prevents the closure of, and constitutively activates, K_{ATP} channels, respectively[37,38]. These observations were confirmed by extended studies using rodent islets, human islets, perfused rat pancreas, as well as β-cell lines[39,40], suggesting that cytosolic Ca^{2+} -mediated signal is not the only mechanism by which glucose metabolism induces insulin secretion. An alternative pathway, called the amplifying pathway, was proposed to augment K_{ATP}-dependent insulin secretion via intermediates arising from glucose, amino acids, and lipid metabolism[41].

Central to the amplifying pathway is anaplerosis, which is the process of replenishing and accumulating tricarboxylic acid cycle (TCA cycle) intermediates[29,41]. Metabolic intermediates such as malate, citrate, and isocitrate can exit the mitochondrial matrix and act as coupling factors via generation of cytoplasmic NADPH[41]. This was supported by studies showing that dose-dependent rise in NAD(P)H content was correlated with glucose-stimulated insulin secretion[42]. One potential molecular target for NADPH was proposed to be glutaredoxin, which regulates post-translational modification of various proteins, including those involved in

exocytosis[43,44]. Another probable target is the voltage-dependent K^+ (K_v) channel, which contributes to cellular repolarization and termination of Ca^{2+} signaling. A binding site for NADPH was discovered on the β subunit of K_v channels, and binding of NADPH was shown to decrease efficacy of K_V channels in repolarizing the cell membrane following action potentials[28].

Closely linked to insulin secretion is the process of lipid metabolism. In the fasting state, cytosolic non-esterified fatty acids are converted to long chain acetyl CoA (LC-CoA) and shuttled into the mitochondria by carnitine palmitoyltransferase I (CPT1) to be metabolized via β-oxidation[29,41]. In the presence of elevated glucose, malonyl-CoA, derived from TCA cycle intermediates, inhibits CPT1 activity, and thereby elevates cytosolic LC-CoA[29,31,45]. Accumulation of cytosolic LC-CoA was proposed to act as a coupling factor for glucose-induced insulin secretion[29,31,45]. Studies have shown that overexpression of a mutant CPT-1that is insensitive to malonyl-CoA resulted in impaired insulin secretion in the INS-1 rat β-cell line[46] . Moreover, LC-CoA was found to alter the activity of regulatory ion channel proteins, directly stimulate vesicle exocytosis, and augment L-type Ca^{2+} channel activity[29,47,48]. However, fatty-acid dependent coupling to insulin secretion occurs only in the presence of elevated glucose, as β-oxidation dominates in the absence of carbohydrate metabolism[41].

In addition to glucose and fatty acid, amino acid metabolism was also reported to amplify insulin secretion. One such coupling factor is glutamate, a metabolite of the amino acid glutamine[28,41, 29]. Maechler *et al.*[49] showed that insulin exocytosis was accompanied by elevated glutamine levels in permeabilized β-cells during high glucose challenge. Gain-of-function mutations in glutamate dehydrogenase, the enzyme that catalyzes the conversion of α-ketoglutarate to glutamate, resulted in hyperinsulinemia and hypoglycemia in patients[50,51]. However, Bertrand *et al.*[52] observed that despite an increase in glutamate level following high

glucose stimulation, insulin secretion was unaffected. Therefore the relative importance of glutamate in enhancement of glucose-stimulated insulin secretion is still a topic of controversy.

1.4.3 The neurohormonal amplifying pathway

Glucose-stimulated insulin secretion is regulated by neurohormonal amplifying pathways via neurotransmitters and incretins, and other hormones[53,54]. The endocrine pancreas is innervated by inputs from both the parasympathetic and the sympathetic systems[55]. The sympathetic response acts on endocrine cells to increase glucagon secretion and decrease insulin secretion[55]. Conversely, parasympathetic vagal efferents synapse with post-ganglionic neurons, which release acetylcholine that binds to β-cell muscarinic receptors to potentiate insulin secretion[53,55]. Similarly, pharmacological muscarinic agonists such as carbachol can also augment glucose-induce insulin secretion in β-cells[56]. Muscarinic receptors are G-protein coupled receptors (GPCRs) that activate phospholipase C (PLC)/ diacyl glycerol (DAG) signaling pathway to generate the 2nd messenger inositol 1,4,5-triphosphate (IP_3), which binds to IP_3 receptors on the ER to induce Ca^{2+} release[55]. Mobilization of ER Ca^{2+} stores can then contribute to insulin secretion during glucose stimulations.

Incretins are a group of metabolic hormones secreted by the gut in response to nutrient ingestion. The two major incretin hormones in humans are glucagon-like-peptide-1 (GLP-1) and gastric inhibitory peptide (GIP)[53]. Both hormones are synthesized by specialized endocrine cells located in the intestine[54]. GLP-1, produced by L-cells, binds to GPCRs on β-cells to enhance glucose-stimulated insulin secretion[53,54]. Furthermore, it stimulates glucagon secretion from α-cells[57]. Studies demonstrated that GLP-1 also induces β-cell mass expansion by stimulating β-cell proliferation and differentiation[58]. GIP, secreted by K cells, exerts insulinotropic effects via GPCRs as well[54,59,60]. Contrary to the actions of GLP-1, GIP suppresses glucagon secretion by α-

cells[57,60]. Other hormones involved in the regulation of insulin secretion include ghrelin, aldosterone, 17β-estradiol, and melatonin[53].

The neurohormonal amplification pathway provides another layer of regulatory control on insulin secretion, which further ensures normoglycemic range is maintained in the blood.

1.4.4 The kinetics of glucose-induced of Ca^{2+} response and subsequent insulin secretion

Insulin release from an islet has been found to closely follow intracellular Ca^{2+} responses. *In vitro* perfusion studies demonstrate that the kinetics of glucose-stimulated Ca^{2+} changes in pancreatic islets occur as several distinct phases[61]. The earliest changes in islet intracellular Ca^{2+} concentration ($[Ca^{2+}]_i$), termed phase 0, can be detected approximately 1 min after raising glucose levels[61,62]. Phase 0 is characterized by a decline in $[Ca^{2+}]_i$ that persists for 3-5 min[61,62]. This is attributed to glucose-activated sequestration of Ca^{2+} into the ER via sarco/endoplasmic reticulum Ca^{2+}-ATPase (SERCA)[61]. Intracellular Ca^{2+} interacts with SERCA via a high affinity binding site, and upon phosphorylation of SERCA by ATP, Ca^{2+} transport into the ER lumen is initiated[61]. Phase 0 is followed by a rapid and transient increase in $[Ca^{2+}]_i$ that reaches a peak value for 2-5 min before declining (phase 1)[62]. The rise in cytosolic Ca^{2+} is dependent on depolarization-driven Ca^{2+} influx through voltage- gated channels. Following this period, the islet $[Ca^{2+}]_i$ reaches a steady-state (phase 2), and displays either sinusoidal oscillations or a plateau[62]. These oscillations arise due to waves of action potentials called bursting, which results from oscillatory metabolic processes and periodic electrical activity of ion channels and pumps on β-cells[63]. Simultaneous measurements of intracellular Ca^{2+} changes and insulin secretions from single islets showed that glucose-induced Ca^{2+} oscillations were consistently followed by

peaks in insulin release[64], illustrating the importance of Ca^{2+} in driving pulsatile insulin secretion[64].

In response to a rapid and sustained glucose stimulus, insulin is secreted in a bi-phasic manner. The first phase corresponds to rapid insulin release immediately occurring within 10 minutes of glucose stimulation before slowing down and stabilizing into sustained insulin release, marking the second phase[28,41,65]. Interactions between the triggering and amplifying pathway are critical for sustained insulin release. Interest in the bi-phasic pattern of glucose-stimulated insulin secretion was generated when clinical studies indicated that the first phase of insulin secretion was impaired or lost in T2D patients[65,66]. Traditionally, this first phase of insulin secretion was thought to be attributed mostly by the triggering signal, while amplifying signals were necessary for the second phase[26,27,67]. However, recent studies suggested that the amplifying signals account for approximately 50% of insulin secretion in both phases[65]. In fact, interactions between the triggering and amplifying pathway exert temporal and amplitude control over the biphasic kinetics of insulin secretion. It was determined that time course of the triggering Ca^{2+} signal may be more involved in temporal control, where synchronization of cytosolic Ca^{2+} oscillations via gap junctions between β-cells contribute to pulsatility of insulin secretion [65,68]. Amplifying pathways, on the other hand, are associated with amplitude modifications of insulin secretion pulses[65]. Combined regulation of time and efficacy in glucose stimulations by both signaling pathways is key to stimulus-secretion coupling in pancreatic β-cells.

1.5 Endoplasmic Reticulum Stress and the Unfolded Protein Response

Pancreatic β-cells possess highly developed ER, which is central to its role in insulin synthesis and secretion. Maintenance of ER homeostasis is therefore essential for preservation of β-cell health and function. The ER is a factory for protein synthesis, which is dependent on its stored Ca^{2+} [69]. Resident ER chaperone proteins need high ER Ca^{2+} to function, and depletion of ER Ca^{2+} can lead to inappropriate folding, aggregation, and accumulation of unassembled proteins[70,71]. In addition, low ER calcium concentration ($[Ca^{2+}]_{ER}$) impairs proinsulin processing and transport, leading to insufficient insulin secretion[70]. ER Ca^{2+} homeostasis is maintained by 3 different types of proteins- Ca^{2+} pumps for the sequestration of Ca^{2+} from the cytosol into the ER lumen against its electrochemical gradient, luminal Ca^{2+} binding proteins for storage of Ca^{2+}, as well as Ca^{2+} channels for controlled release of Ca^{2+} back to the cytosol[70]. Perturbations of ER Ca^{2+} homeostasis can lead to manifestation of disease phenotype. For example, when ER Ca^{2+} is dysregulated due to mutations in the WFS1 gene, Wolfram syndrome results, which is characterized by juvenile onset diabetes[71]. Recent studies also suggested that palmitate may exert its lipotoxic effects in part via ER Ca^{2+} depletion, resulting in ER stress[72].

As β-cells are secretory in nature, they are highly susceptible to ER stress. Indeed, β-cell ER stress has been identified as a causal factor in T2D, where compensatory increase in insulin production due to peripheral insulin resistance, combined with chronic exposure to elevated glucose and fatty acid levels can trigger ER-stress induced cell apoptosis[2,13-15,73,74]. Although greater emphasis has been placed on autoimmunity in the pathogenesis of T1D, accumulating data suggest that the inflammatory milieu generated by infiltrating immune cells can also attribute to ER stress and β-cell death in T1D[17,75-77]. One model proposed that ER stress initiated β-cell damage can promote the release of β-cell antigens that secondarily induce autoimmunity[16].

While it is debatable whether ER stress alone is sufficient to drive β-cell autoimmunity, there is growing consensus that ER stress is implicated in autoimmune-mediated β-cell destruction.

A number of insults can lead to the accumulation of unfolded proteins in the ER lumen, thereby triggering ER stress. These include nutrient deprivation, inflammation, alterations in oxidation-reduction balance, glucotoxicity, lipotoxicity, and glucolipotoxicity[2,72,74,78,79]. In response to accumulation of unfolded or misfolded proteins in the ER lumen, a series of signaling cascades, known collectively as the unfolded protein response (UPR), is activated as a protective strategy to mitigate ER stress[69,73,80] The UPR serves to restore ER homeostasis by attenuating protein translation, increasing the expression of chaperone proteins, and activating ER-associated degradation (ERAD) to clear misfolded proteins[79,81]. However, failure to absolve ER stress during sustained UPR shifts these compensatory measures toward pro-apoptotic pathways, ultimately resulting in β-cell death[79,81]. The UPR operates via 3 arms mediated by the transmembrane signal transducers PKR-like ER kinase (PERK), inositol-requiring protein 1α (IRE1α), and activating transcription factor 6 (ATF6)[80]. Under physiological conditions, they are rendered inactive by association with the ER chaperone binding immunoglobulin protein (BiP). During ER stress, BiP binds to misfolded proteins in the ER lumen, and is thus released from complexes with the ER stress sensors to allow activation of the UPR[80].

1.5.1 PERK

As an immediate response to ER stress, the PERK branch of the UPR prevents further increase in the translational load of the ER. PERK is a serine/threonine kinase, which upon release from BiP, dimerizes and autophosphorylates to facilitate its activation[81]. Activated PERK attenuates protein translation by phosphorylation of eukaryotic translation initiator factor 2α

(eIF2α)[73,80]. The importance of PERK in relieving ER protein load was demonstrated in knock-out mouse models which developed diabetes due to chronic ER stress[82,83]. Phosphorylated eIF2α leads to up-regulation of activating transcription factor 4 (ATF4), which promotes various adaptive responses through transcription of pro-survival genes involved in redox balance, amino acid metabolism, protein folding, and autophagy[80]. The PERK-ATF4 axis is also a positive regulator of C/EBP-homologous protein (CHOP), which is the main inducer of apoptosis during the pro-apoptotic shift in the UPR[80].

1.5.2 IRE1α

IRE-1α is a kinase and endoribonuclease that dimerizes and autophosphorylates following ER stress induction. Once activated, it cleaves a 26-bp intron from the mRNA encoding X box-binding protein 1 (XBP1) to produce the active transcription factor, spliced XBP1 (XBP1s)[73,80,81]. Translocation of XBP1s to the nucleus promotes the transcription of chaperone and ERAD proteins, as well as phospholipid synthesis for ER expansion[73,80,81]. Under physiological conditions, IRE1α can potentiate insulin biosynthesis in response to acute high glucose, suggesting a role for IRE1α in normal β-cell function[84]. This function was confirmed in conditional IRE1α knock-out mice, which exhibited hypoinsulinemia accompanied by hyperglycemia[85].

1.5.3 ATF6

ATF6 is a transcription factor that is transported to the Golgi apparatus upon activation of the UPR and processed by site 1 protease (S1P) and S2P to release the fragment containing its cytosolic domain, ATF6αf. This activated form of ATF6 enters the nucleus to directly upregulate

gene transcription of XBP1, ER resident chaperones such as BiP/ GRP78, as well as ERAD response proteins[80]. Interestingly, the active ATF6αf was also detected in unstressed β-cells, while knock-down of ATF6α reduced cellular expression of GRP78 and resulted in apoptosis in INS-1 cells[86]. These observations allude to a role for ATF6 in sustaining chaperone expression and β-cell survival in the absence of ER stress.

1.5.4 ER stress-induced apoptosis

While the UPR is a protective strategy to restore ER homeostasis during stress conditions, failure to absolve chronic ER stress switches its pro-survival signaling to pro-apoptotic mechanisms. Apoptosis is regulated by the B-cell lymphoma 2 (Bcl-2) family of proteins, which are further categorized into pro and anti-apoptotic proteins. Under unstressed conditions, the pro-apoptotic BH3-only proteins of the Bcl-2 family are sequestered by anti-apoptotic proteins. Commitment to ER-stress induced apoptosis is initiated by activation of downstream signaling molecules such and CHOP and c-Jun N-terminal kinase (JNK)[81]. CHOP is a downstream transcriptional target of both ATF6 and PERK/eIF2α/ATF4 pathways, while JNK activation is mediated by signaling events in the IRE1α pathway[80]. CHOP inhibits expression of anti-apoptotic Bcl-2 protein through transcriptional repression, and stimulates the transcription of pro-apoptotic BH3-only protein Bcl-2-like protein 11 (BIM) [80,81]. JNK phosphorylates Bcl-2 and BIM to repress, and enhance its functionality, respectively[80]. Studies by Cunha *et al.*[87] also indicated that during lipotoxic β-cell death induced by palmitate, two BH3-only proteins, death protein 5 (DP5) and p53 upregulated modulator of apoptosis (PUMA) were both up-regulated. DP5 functions as a "sensitizer" protein that neutralizes anti-apoptotic Bcl-2 proteins, while PUMA is an "activator" protein that facilitates initiation of apoptosis[87]. An overall increase in

the proportion of BH3-only "activator" proteins induces insertion of Bcl-2 associated X protein (Bax) and Bcl-2 homologous antagonist/killer (Bak) into the mitochondrial membrane[88]. These two proteins form oligomeric pores on the outer mitochondrial membranes to allow release of cytochrome c into the cytosol, which trigger caspase cascade that implements the execution of apoptosis[88,89]. In the ER stress-induced diabetic mouse model, the Akita mouse, elevated levels of CHOP was detected in pancreatic β-cells, which contributed to cell apoptosis[90]. Targeted disruption or deletion of the CHOP gene was able to prevent ER-stress induced cell death in multiple models of T2D, further solidifying its role in UPR-mediated cell death[90,91].

1.6 The B7 Family of Immuno-regulatory Ligands

While a variety of therapeutic options are offered to T2D patients to combat insulin resistance and relative insulin deficiency, so far there is limited success on β-cell protection in a T1D setting. Efforts to design immune-protective strategies have focused on mechanisms of immune suppression and tolerance. B7-H4 (B7x) is an immune-regulatory molecule belonging to the B7 immunoglobulin family, which has been widely studied for their interactions with putative receptors on T cells to modify immune responses[92-94]. Currently there are 7 known family members, all of which deliver co-stimulation signals to T cells to up or down-regulate T cell response: B7.1, B7.2, PD-L1, PD-L2, B7-H2, B7-H3, and B7-H4[95,96]. Two well-known T cell co-stimulatory molecules, B7.1 and B7.2, engage with CD28 receptors on T cells to promote cell expansion and differentiation[97]. Upon binding to the negative co-signaling CTLA-4 receptor, B7.1 and B7.2 switch to an inhibitory phenotype, and terminate T cell activation[98]. Similarly, coordination of ligands and receptors of other B7 family members all act to fine-tune the T cell response. As a negative co-signaling molecule, B7-H4 has the potential to down-regulate

autoreactivity in autoimmune diseases such as T1D as well as offer allograft protection in islet transplants, which will be further discussed in section 1.5.2.

1.6.1 Gene organization of B7-H4

B7-H4 was identified as a negative co-signaling molecule in 2003 by several groups[92-94]. Genomic B7-H4 is encoded by the V-set domain-containing T-cell activation inhibitor 1 (VTCN1) gene, which is located on chromosome 1 and 3 in human and mouse, respectively[94]. Mature B7-H4 is a 50 kDa-80 kDa trans-membrane protein consisting of one variable immunoglobulin (IgV) region and one constant immunoglobulin (IgC) region, which are encoded on exons III, IV, and part of V[92-94]. Consistent with established functions of the B7 family, this ligand is up-regulated on cell membranes of activated antigen presenting cells, and binds to its counter-receptor on T cells to inhibit T cell activation[92-94]. However, to date, the receptor for B7-H4 remains unidentified.

1.6.2 Immune-modulatory roles of B7-H4 in T1D and islet transplantation

The suppressive activity of B7-H4 on T cell immunity marks it as a potential candidate to limit autoreactivity in autoimmune diseases such as T1D. Indeed, inhibition of B7-H4 has been shown to up-regulate T cell proliferation and exacerbate disease progression in experimental autoimmune encephalomyelitis[92]. Genome-wide association studies have also identified single nucleotide polymorphisms (SNPs) within the VTCN1 gene associated with autoimmune diabetes, further implicating B7-H4 as a potential regulator of T1D[99].

Immuno-suppressive functions of B7-H4 in models of T1D were investigated by recombinant protein technology. Soluble B7-H4 recombinant immunoglobulin (B7-H4 Ig) can

be derived from fusion of the immunoglobulin constant region to the extracellular domain of B7-H4[100,101]. Both intraperitoneal injections of B7-H4 Ig and cell-associated B7-H4 inhibited proliferation and cytotoxicity of $CD4^+$ and $CD8^+$ T cells *in vitro.*[92-94,102]. While the exact mechanism by which B7-H4 interferes with T cell activation is not fully understood, it has been proposed that B7-H4 inhibits AKT, JNK, and ERK kinase activation, which are involved in essential signaling pathways for T cell proliferation and interleukin-2 (IL-2) production[103]. In conjunction with its inhibitory functions on T cell proliferation, B7-H4 can slow and even arrest progression of diabetes. Juvenile non-obese diabetic (NOD) mice treated with B7-H4 Ig exhibited significantly delayed onset as well as reduced incidence of diabetes[101]. This was accompanied by reduced proliferation and activation of $CD4^+$ and $CD8^+$ subsets of T cells in the islet infiltrates[101]. Furthermore, B7-H4 reversed established T1D. Return of glycemic control was observed in newly-onset diabetic NOD mice following B7-H4 Ig injections[104]. Interestingly, restoration of normoglymemia was due to arrested advancement of insulitis to overt diabetes following treatment in NOD mice[101,105]. It was proposed that B7-H4 modulates immune balance at the transition point between insulitis and diabetes by limiting the shift of T cells toward the pathogenic type 1 T helper cell (Th1) phenotype, which are key mediators of autoimmune diseases.[101]

B7-H4 also promotes viability of islet grafts, and thus has significant potential for improving clinical islet transplantation as a treatment for diabetes[106-108]. Roles of B7-H4 in allograft rejection was initially demonstrated in NIT cells, a functional NOD-derived β-cell line, where survival of NIT cells allotransplanted into diabetic mice was prolonged by B7-H4 transfection[107]. The protective effects of B7-H4 in allotransplantation were further observed in B7-H4 adenovirus-transduced islets and B7-H4 transgenic islets[106,109]. Mice that received islets

transduced with recombinant B7-H4 adenovirus achieved longer allograft survival with significantly reduced infiltrates compared with control recipients, suggesting that B7-H4 may alter the immune environment at the graft site to induce tolerance[106]. Similarly, B7-H4 transgenic islets promoted islet allograft survival, which was concurrent with migration of Tregs to the graft site[109]. Moreover, when the primary B7-H4-transduced islet graft was removed and replaced with a secondary graft, survival of the new graft was higher if it was obtained from the same donor strain as the primary graft donor, as opposed to a graft from a third-party donor strain[110]. Isolated splenic leukocytes from recipient mice showed decreased IL-2 levels due to reduced number of IL-2 secreting cells, thereby reducing inflammation in the grafts[110]. These results indicate that B7-H4 is able to induce donor-specific tolerance as opposed to general unresponsiveness towards foreign antigens, which can be of great benefit in islet transplantation.

1.6.3 Tissue distribution and expression patterns of B7-H4

Interestingly, expression pattern of B7-H4 is unique amongst the B7 family members. Both B7-H4 mRNA and protein are expressed in various peripheral tissues such as the spleen, lung, liver, and pancreas, but its role in these tissues is subject of debate[93,111,112]. In the pancreas, B7-H4 has been shown to be more abundantly expressed in the endocrine cells than the exocrine tissues, and immunohistochemical analyses revealed co-localization of B7-H4 with insulin[105,111]. Furthermore, B7-H4/insulin co-localization was dramatically reduced in both T1D islets and insulinomas compared with healthy islets[111]. These observations suggest the possibility that B7-H4 may have endogenous functionality in the pancreatic islets independent of immune-modulation.

1.6.4 Potential non-immune mediated roles of B7-H4 in cell function and survival

Expression of B7-H4 in peripheral tissues led to speculation for its alternative modes of action independent of T cell modulation. Evidence from several cancer types suggested a link between up-regulation of B7-H4 expression in tumor cells and enhanced oncogenicity[113-115]. It has been proposed that B7-H4 promoted tumorigenesis by mediating escape from immunosurveillance as well as being a direct tumorigenic factor [116,117]. In support of these data, Zhang *et al.*[117] identified a nuclear localization sequence within the human B7-H4 protein. They proposed that B7-H4 has the ability to shuttle between the cytoplasm and the nucleus, and may regulate transcription of genes involved in cell cycle progression and proliferation. In pancreatic cancer cells, *in vitro* B7-H4 gene silencing reduced cell proliferation rate and increased apoptosis[116]. Studies by Kim *et al.* using knock-down models in HeLa cells suggested that B7-H4 may also participate in regulation of metabolic functions[118]. Specifically in the β-cells, endogenous B7-H4 may regulate stress responses via cell-autonomous signaling pathways. Preliminary data from our lab suggested that *in vivo* administration of B7-H4 Ig affected the age-dependent expression of key UPR genes in NOD mouse islets (unpublished-shown below). In light of the recent findings, it is plausible that B7-H4 may play an essential role in cell survival.

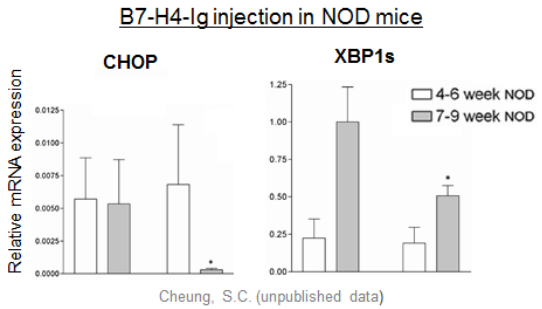

Image 1 Gene expression of CHOP and XBP1s following soluble B7-H4 Ig injection in NOD mice at 4-9 weeks of age

1.7 Thesis Objective: Investigating B7-H4 Functionality in Pancreatic β-Cells

The present study aims to examine potential endogenous roles of B7-H4 in pancreatic β-cells by employing over-expression and knock-out mouse models. Our first objective is to investigate whether B7-H4 can modulate β-cell function in terms of glucose-induced Ca^{2+} signaling, metabolism, and insulin secretion, as well as *in vivo* glucose tolerance. We investigate the involvement of B7-H4 in β-cell biology by examining islet responses to a variety of stimuli, including various levels of glucose, direct depolarization with potassium chloride (KCl), and stimulation with the sulfonylurea tolbutamide. Our second goal is to determine whether B7-H4 affects the β-cell ER stress response and cell death during chronic stress.

Our findings demonstrate roles of B7-H4 in regulating the β-cell response to glucose and tolbutamide, and are in agreement with evidence suggesting that functions of B7-H4 are not only limited to T cell regulation. Moreover, we show that B7-H4 overexpression amplifies the islet UPR during moderate levels of ER stress. These results are the first to demonstrate that B7-H4 affects β-cell function, as well as β-cell ER stress signaling. Given that β-cell stress and dysfunction are critical steps propelling disease progression in diabetes, a better understanding of these novel roles of B7-H4 may suggest new approaches for promoting the function of endogenous β-cells as well as improving islet function in a transplant setting.

CHAPTER 2: METHODS

2.1 *In Vivo* Studies

2.1.1 Mouse model & breeding

C57BL/6 mice were purchased from The Jackson Laboratory and housed in the animal facility at Jack Bell Research Center. Further breeding was carried out at the facility. B7-H4 transgenic (B7-H4 Tg) mice were previously generated by the Warnock lab[109]. Systemic homozygous B7-H4 knock-out (B7-H4 KO) mice of C57BL/6 X 129/Ola mixed background were kindly supplied to us by the Mak lab (University of Toronto)[119]. Disruption of the B7-H4 locus was confirmed previously with Southern blot analyses and RT-PCR. These mice were backcrossed for 5 generations with C57BL/6 mice in our lab to create the B7-H4 global KO line and WT littermates of C57BL/6 background. All animals were cared for according to the Canadian Council on Animal Care guidelines and University of British Columbia regulations.

2.1.2 Mouse Genotyping

Genotype verification was conducted on ear notch tissues obtained from newly-weaned mice. Briefly, two ear notche samples from each mouse were placed in a 1.5 mL microcentrifuge tube (VWR, Mississauga, ON, CA, 89000-028), and digested overnight at 56˚C in tissue lysis (ATL) buffer (Qiagen, Toronto, ON, CA, 19076) containing proteinase K (Qiagen, 19131). DNA was isolated from samples using the DNeasy Blood & Tissue Kit (Qiagen, 69504) according to manufacturer's instructions, and stored at -20˚C. Polymerase chain reactions (PCR) were carried out on isolated DNA samples for the B7-H4 transgene (B7-H4 Tg), the disrupted B7-H4 locus (B7-H4 KO), or the WT B7-H4 gene (B7-H4 WT). Each PCR reaction mixture contained 2x PCR Taq MasterMix (Abm, Vancouver, BC, CA, G013), DNAse and RNAse-free water, specific

primers for each B7-H4 gene variant (Table 1), and sample DNA. PCR reactions were run on the Applied Biosystems thermocycler (Life Technologies) for 30 cycles according to the PCR Taq MasterMix amplification protocol. Electrophoresis of amplifed DNA was then done on a 1.2% agarose gel (UltraPure Agarose, Invitrogen/Life Technologies, 16500500) using The PowerPac™ HC (Biorad, Mississauga, ON, CA) , stained with SYBR Safe DNA Gel Stain (Invitrogen/LifeTechnologies, S33102), and visualized on BioSpectrum 310 MultiSpectral Imaging System (UVP, Upland, CA, USA).

Table 1 PCR primer pairs for genotyping

Gene	Sense	Antisense
B7-H4 (WT)	GCCGTTCAGCAAGTCAAGTTT	CCCGTCCTCTCCAATGTTTC
B7-H4 (KO)	GGCATGGGTCCTTCCTGAA	CCTTCTATCGCCTTCTTG
B7-H4 (Tg)	AGTGACCAGCTACAGTCGGAA	ATCTGCCCCAAGGAAGCCA

2.1.3 Intraperitoneal glucose tolerance test (IPGTT)

After a 6 hr fast, mice were intraperitoneally injected with 20% glucose (Sigma-Aldrich, St. Louise, MO, USA, G8270 in saline (0.9% NaCl) at 2 g/kg body weight. Tail vein blood samples were drawn at 0, 15, 30, 60, 90, and 120 min following glucose injections, and assessed for blood glucose level using a OneTouch glucometer and Ultra Blue Test Strips (Lifescan, Burnaby, BC, CA).

2.2 *In Vitro* Studies

2.2.1 Human tissue collection & culture

Pancreatic islets were isolated from adult cadaveric organ donors and provided to us by the Ike Barber Clinical Human Islet Transplant Laboratory and the Alberta Clinical Islet Transplant Program. Human pancreata were processed as described previously [120]. Upon receipt, we further hand-picked the islets into clean 100 mm petri dish (VWR, 25384-088) prior to culturing at 21˚C and 5% CO_2 in CMRL media (Life Technologies, Grand Island, NY, USA, 11530-037) completed with 10% fetal bovine serum (FBS) (Life Technologies, 12483-020), 1% penicillin/streptomycin (Pen/Strep) (Life Technologies, 15140-148), and 1% glutamine (Life Technologies, 25030-081).

2.2.2 Mouse islet isolation & culture

Pancreatic islets from 16-18 week old mice were isolated via ductal collagenase injection by the research technician from the Warnock lab. Briefly, following surgical exposure of the lower abdominal cavity, the common bile duct (CBD) was clamped at the junction to the duodenum. The CBD was cannulated with a 30 gauge needle and perfused with 5 mL of collagenase (1000 U/mL) dissolved in 1x HBSS (with 5.5 mM D-Glucose and without Ca^{2+}, Mg^{2+}, phenol red, and sodium bicarbonate) (Gibco, Life Technologies, 14185-052). The inflated pancreas was removed from the mouse and placed into a 50 mL conical tube (Corning, Tewksbury, MA, USA, 352070) containing 2 mL of ice-cold collagenase solution. The pancreas was then digested at 37˚C for 8-11 minutes, followed by mechanical dispersion by vigorous shaking. The homogenized tissue was washed with 1x HBSS containing 1 mM $CaCl_2$. Islet-containing pellet was re-suspended in 1x HBSS + $CaCl_2$, filtered through a 70 µm nylon filter

(BD Biosciences, San Jose, CA, USA, 352350) into a sterile 100 mm petri dish containing 11.1 mM glucose RPMI-1640 supplemented with 10% FBS and 2% Pen/Strep. Isolated islets were further hand-picked to remove any remaining exocrine contaminations, and cultured in 60 mm petri dishes (VWR, 25384-090) with 11.1 mM glucose RPMI-1640 at 37˚C and 5% CO_2 overnight before experimentation.

2.2.3 ER stress treatments in cultured human islets

For quantitative PCR (qPCR) and Western blot analysis on ER stress-induced changes in gene and protein expressions, whole islets were cultured in 35 mm (VWR, 25373-041) or 60 mm petri dishes with treatment or control media for the time durations specified. Thapsigargin (1mM stock in dimethyl sulfoxide) was diluted in complete CMRL media with 11.1 mM glucose to achieve the desired concentrations. Equal volumes of dimethyl sulfoxide (DMSO) dissolved in complete CMRL were used as treatment controls.

2.2.4 Human islet B7-H4 protein quantification

For B7-H4 protein detection, islets were collected in 2 mL tubes (VWR, 20170-170) following 24 hrs stress or control treatment, and then lysed by high frequency sonication (amplitude: 80, 30 s pulses for 6 min). 20-30 μg proteins were loaded onto 15% sodium dodecyl sulfate- polyacrylamide gel electrophoresis (SDS-PAGE) gels, and separation was performed at 150 V for 60 min. Proteins were transferred onto PVDF membranes (Biorad, Hercules, CA, USA, 162-0177) at 100 V for 45 min, and incubated in I-block solution (Life Technologies, T2015) for 1 hr to reduce non-specific protein binding. Membranes were then incubated overnight at 4˚C in rabbit anti-B7-H4 primary antibody (Santa Cruz Biotechnology, Dallas,

Texas, USA, sc-68872) at 1:500 dilution. Subsequently, membranes were washed with PBS-T (0.1% Tween 20 in 1x PBS), and incubated with the anti-rabbit secondary antibody (Cell Signaling, Danvers, MA, USA, 7074s) at 1:10000 for 1 hr at room temperature. Protein detection was carried out with Enhanced Chemical Luminescence (ECL) (Thermo Scientific, Waltha, MA, USA, 32106), and film was exposed for 1.5 min before development.

Quantification of actin protein in each sample was done following B7-H4 detection. Membranes were re-blocked with blocking buffer, and subjected to 4˚C overnight incubation with anti-actin mouse primary antibody at 1:10000 dilution. Anti-mouse secondary antibody, diluted at 1:10000, was added to the membrane for 1 hr at room temperature. Film was subjected to ECL-mediated exposure for 1 second.

Band intensities of both B7-H4 and actin were quantified by densitometry using Adobe Photoshop, and the relative B7-H4 band intensities were normalized to that of the corresponding actin loading controls.

2.2.5 Real-time qPCR quantification of islet gene expression

Approximately 30 islets were collected from each sample for RNA quantification, and suspended in RNA*later* RNA Stabilizing Reagent (Qiagen, 76104) for storage at -80˚C. Islets were homogenized using the QIAshredder (Qiagen, 79656) as per manufacturer's instructions. Total RNA was extracted from cell lysates with the RNEasy Mini Kit (Qiagen, 74106) according to manufacturer's instructions. cDNA was synthesized from 10 ng of RNA using the qScript cDNA synthesis kit (Quanta Biosciences, VWR, 95047-500). The parameters were as follows: 22˚C for 5 min, 42˚C for 30 min, 85˚C for 5 min, and holding at 4˚C. Amplified cDNA was

diluted 1:3 in DNAse and RNAse-free water prior to real-time qPCR quantification on the Applied Biosystems 7500 Fast Real-Time qPCR machines (Life Technologies).

For verification of B7-H4 gene knock-down in B7-H4 KO animals, cDNA were first pre-amplified prior to gene expression analysis due to low natural abundance of B7-H4 in mouse islets. Diluted cDNA was pre-amplified for B7-H4 with PerfeCTa PreAmp 5x Supermix (Quanta Biosciences, 95146) (Table 2). The reaction mixtures consisted of 1x PrefecTa PreAmp Supermix, 50nM of B7-H4 forward and reverse primers in $T_{10}E_{0.1}$ buffer (10mM Tris, 1mM EDTA), 1:3 diluted cDNA, and dH_2O. Post-amplification, cDNA was diluted 1:2 in cold $T_{10}E_{0.1}$ buffer prior to real-time qPCR.

Table 2 Pre-amplification cycling protocol

Initial denaturation	95˚C- 2min
Pre-amp cycling (14 cycles)	95˚C- 10s 60˚C- 3min
Hold	4˚C

Real-time qPCR reactions were assembled in a final reaction volume of 8.25 µL containing 4 µL SYBR, 3.73 µL of 0.5 µM forward and reverse primer mix, and 0.5 µL of the diluted cDNA. Genes of interest were amplified for 35 cycles (Table 3) followed by melt curve analysis. All primers were custom ordered from IDT (Toronto, Ontario, CA) (Table 4), and validated for specificity and efficiency by standard curve serial dilutions. Gene expressions were quantified using the $2^{-\Delta CT}$ method relative to several endogenous control genes: GAPDH, 18s rRNA, and RPLP0 to maximize accuracy of gene expression profiles[121].

Table 3 Cycling protocol for real-time qPCR

Initial denaturation	95˚C- 2min
Pre-amp cycling (35 cycles)	95˚C- 10s 60˚C- 45s
Melt-curve	

Table 4 Primer Sequences for qPCR (mouse primers unless specified)

Gene	Sense	Antisense
Glucokinase (GCK)	AGCTGCACCCGAGCTTCA	GATTTCGCAGTTGGGTGTCA
Glucose transporter 2 (Glut2)	GTCCAGAAAGCCCCAGATACC	GTGACATCCTCAGTTCCTCTTAG
Sarco/endoplasmic reticulum Ca^{2+} ATPase 2b (SERCA2b)	GATCCTCTACGTGGAACCTTTG	CCACAGGGAGCAGGAAGAT
Pancreatic and duodenal homeobox 1 (Pdx1)	GAACCCGAGGAAAACAAGAGG	GTTCAACATCACTGCCAGCTC
Insulin II (Ins2)	GAAGTGGAGGACCCACAAGTG	GATCTACAATGCCACGCTTCT
Binding immunoglobulin protein (BiP)	TCATCGGACGCACTTGGAA	CAACCACCTTGAATGGCAAGA
Spliced X-box binding protein (XBP1s)	GAGTCCGCAGCAGGTG	GTGTCAGAGTCCATGGGA
C/EBP homologous protein (CHOP)	CTGCCTTTCACCTTGGAGAC	CGTTTCCTGGGGATGAGATA
Nuclear factor (erythroid-derived 2)-like 2 (Nrf2)	AGTGGATCCGCCAGCTACT	TCTCTGCCAAAAGCTGCAT
Heme oxygenase (Hmox)	CAGAAGGGTCAGGTGTCCA	CTTCCAGGGCCGTGTAGAT
60S acidic ribosomal protein P0 (RPLP0)	AGATTCGGGATATGCTGTTGGC	TCGGGTCCTAGACCAGTGTTC
18s ribosomal RNA (18s rRNA)	ACCGCAGCTAGGAATAATGG	CCTCAGTTCCGAAAACCAAC
Glyceraldehyde 3-phosphate dehydrogenase (GAPDH)	AGGTCGGTGTGAACGGATTTG	TGTAGACCATGTAGTTGAGGTCA
V-set domain-containing T-cell activation inhibitor 1 (B7-H4)	CAGCTGGAAACATTGGAGAGG	TGCGGCCTCTGAACATCTCAT
V-set domain-containing T-cell activation inhibitor (human B7-H4)	CTTCTGCCTCTCAGCCCTTA	GAAATAGTTCTGTAGATCCCTGTTG
Hypoxanthine-guanine phosphoribosyltransferase (human HPRT)	TGTATGTACGCCGCGTATTCA	GCGATGTCAATAGGACTCCAGA

2.2.6 Fluorescent imaging of islet cytosolic Ca^{2+}

Islets were seeded on sterile 25 mm glass coverslips (VWR, 16004-310), incubated in 11.1 mM glucose complete RPMI-1640, and allowed to adhere in culture for 5 days prior to imaging. The coverslips with the attached islets were transferred to magnetic perfusion chambers (2 ml volume) and incubated for 30 min with 5 μM of the Ca^{2+}-sensitive ratiometric fluorescent probe Fura 2-AM (Invitrogen, Life Technologies, F1221) in basal Ringer's solution (5.5 mM KCl, 2 mM $CaCl_2$, 1 mM $MgCl_2$, 20 mM HEPES, 144 mM NaCl, and 2 or 3 mM glucose). When bound to Ca^{2+}, Fura 2-AM is excited at 340 nm and 380 nm, and the ratio of the emissions at those wavelengths directly reflects the amount of intracellular Ca^{2+}. The magnetic chambers were then connected to a perfusion system driven by a Gilson Minipuls 3 multichannel peristaltic pump and continuously perifused at a flow rate of 2.5 mL/min during experiments. Prior to recording, islets were washed with basal Ringer's solution for 30 min. Recordings were made on a Leica DMI6000 inverted microscope equipped with a Leica HC Plan Fluotar 10x objective and images were acquired using a Leica DFC365 FX digital camera. Fura-2 loaded islets were excited alternately at 340 nm and 380 nm at 13 second intervals, and the resulting emissions were collected through a 502-538 nm emission filter for estimation of changes in cytosolic Ca^{2+}. Areas of interest containing individual islets were drawn, and analyses were conducted on individual regions on the Leica LAS AF Software. An average of 10 islets were analyzed per animal, and cytosolic Ca^{2+} levels were represented as the ratio of Fura-2 fluorescence emission intensities following excitation at 340nm and 380nm (F340/F380). In all experiments a chamber with WT islets and another with B7-H4 Tg islets were mounted side-by-side and perifused in parallel with the same buffer. A software-controlled automated microscope stage would alternate between the two chambers and images were acquired of both islet preparations at each time-

point. In section 3.2.3 the thapsigargin treatment was administered in conjunction with the 30 min Fura-2 staining. In section 3.2.4, islets were treated with thapsigargin during the 30 min pre-recording wash period, and thapsigargin was continuously infused in the buffers throughout the recording.

2.2.7 Islet dispersion into single cells

Islets were collected into 1.5 mL sterile, low retention microcentrifuge tubes (Fisher Scientific, Waltham, MA, USA, 02-681-331), and washed 3 times with Ca^{2+}, $Mg^{2+,}$, and L-glutamine-free MEM media (Mediatech, Manassas, VA, USA, 15-015-CV). Islets were then mechanically dispersed via pipetting in a 1:5 dilution of MEM with 0.05% trypsin-EDTA (Life Technologies, 25300) for 1 min. Cellular suspension was washed once prior to re-suspension in complete 11.1 mM glucose RPMI-1640 media.

2.2.8 *In vitro* stress treatments in mouse islets

Mouse islets were cultured in complete RPMI-1640 overnight as described above prior to stress treatment. For qPCR analysis of ER stress-induced gene expression changes, whole islets were cultured in 30 mm petri dishes with appropriate volumes of treatment or control media for the time periods indicated. Thapsigargin (1mM stock in DMSO) was diluted in 11.1 mM glucose RPMI 1640 to the desired final concentration. Equal volumes of DMSO were similarly dissolved in RPMI 1640 to serve as treatment control.

For cell death studies, stress and control media were added to dispersed islet cells. Thapsigargin and staurosporine were diluted in 11.1 mM glucose RPMI 1640 for single stress treatments. For thapsigargin + high glucose treatments, appropriate volumes of glucose (1M

stock in dH_2O) and thapsigargin were added to glucose-free RPMI 1640 completed with 10% FBS and 2% P/S, and cell death was quantified at various time points, as outlined below.

2.2.9 Cell death quantification

Isolated pancreatic islets were dispersed, and seeded into 96-well plates (Perkin Elmer ViewPlates Waltham, MA, USA, 6005182), and allowed to adhere for 48 hrs; individual wells contained cells from approximately 30 islets. Cells were stained with propidium iodide (PI) (0.5µg/mL) and Hoechst 33342 (0.05µg/mL) 30 minutes prior to addition of various stress treatments, as described above. The plate was kept at 37˚C with 5% CO_2 in a regular incubator over the course of the experiment. Cell death was quantified at indicated time points using the Molecular Devices ImageXpress Micro high content screening system (Molecular Devices, Sunny vale, CA, USA), and analyzed with MetaXpress software. Percentage of dead islet-cells was expressed as the number of PI positive cells relative to Hoechst positive cells.

2.2.10 Insulin secretion & islet insulin content

15 size-matched islets were collected into 1.5 mL low retention microcentrifuge tubes (Fisher Scientific, 02-681-331), and pre-incubated in Kreb's Ringers buffer (KRB, 129 mM NaCl, 4.8 mM KCl, 1.2 mM $MgSO_4$, 1.2mM KH_2PO_4, 2.5 mM $CaCl_2$, 5 mM $NaHCO_3$, 10 mM HEPES-Free Acid, 0.5% BSA) for 1 hr prior to onset of assay. Islets were then subsequently stimulated for 1 hr in 5 mM glucose KRB, 10 mM glucose KRB, and lastly incubated for 30 min with 30 mM KCl + 2 mM glucose KRB (concentration of NaCl was adjusted from 129 mM to 103.8 mM to balance osmotic stress). Supernatants from stimulations were collected, and centrifuged for 5 min at 200xg to eliminate remaining cellular debris. Islets were counted at the

end of each incubation period to account for islet loss during supernatant collection. Immediately following insulin secretion assay, islets were incubated with acetic acid lysis buffer overnight at -80˚C. They were freeze-thawed at 100˚C for 10 min the next day, and supernatants were collected following centrifugation at 12000 rpm for 10 min. All samples were stored at -20˚C prior to protein quantification via enzyme-linked immunosorbent assay (ELISA).

Quantifications of insulin secretion and insulin content were carried out using the Mouse Ultrasensitive Insulin ELISA kit (Alpco, Salem, NH, USA, 80-INSMSU-E10) according to manufacturer's instructions, and absorption at 450 nm was read on the microplate reader as an output of insulin concentration. Sample insulin concentrations were extrapolated from standard curves via 5 parameter logistic curves using the following standards with known insulin concentrations from the manufacturer: 0.188 ng/mL, 0.6 ng/mL, 1.25 ng/mL, 3.75 ng/mL, and 6.9 ng/mL. Limitation of detection for the ELISA assay was 0.025 ng/mL, and cross-reactivity includes 147% human insulin, <0.01% mouse c-peptide 1 and 2, 0.27% human proinsulin, as well as unknown reactivity to mouse proinsulin.

2.2.11 Measurements of islet cell oxygen consumption & glycolysis

The metabolic functions of WT and B7-H4 Tg islet cells were assessed indirectly through measurements of oxygen consumption and extracellular acidification. Isolated islets were dispersed and seeded in 96-well polystyrene XF cell culture microplates (Seahorse Biosciences, North Billerica, MA, USA, 102416-100) at approximately 60 islets per well. Islets were allowed to adhere to the plate for 3 days in complete 11.1 mM glucose RPMI-1640 prior to onset of assay. Assay medium (Seahorse Biosciences, 10253-100) was adjusted to pH 7.4, and prepared to a final concentration of 2 mM glutamine in combination with 2mM glucose. Cells were first

washed with 2 mM assay medium and incubated in non-CO_2 chamber for 1 hr prior to start of assay. Injection ports were loaded with assay medium of varying glucose concentration to achieve final concentrations of 5 mM and 10 mM glucose post-injections. Run protocol was programmed as follows: islets were incubated at basal glucose concentration of 2 mM for 20 min, followed by 5 mM glucose and 10 mM glucose, respectively. Mitochondrial oxidative consumption rates (OCR) and extracellular acidification rates (ECAR) were measured at each glucose concentration and normalized to total protein content, as quantified by Bradford assay.

2.2.12 Statistical analysis

Statistical analyses were performed on Graphpad Prism by 2-way ANOVA followed by Bonferroni post-hoc test, by 1-way ANOVA, or by Student's t-test. Both effects due to genotype and treatment were analyzed, and differences were considered significant when $p<0.05$. All data are represented as mean ± SEM. For area-under-the-curve (AUC) analysis of calcium responses, the incremental AUC (iAUC) was calculated as $AUC_{response} - AUC_{baseline}$.

CHAPTER 3: RESULTS

3.1 Confirmation of B7-H4 Expression Levels in Islets from B7-H4 Tg and KO Mice

We examined the β-cell specific roles of B7-H4 using a line of B7-H4 transgenic mice on the C57Bl/6 background previously that was established in our lab, which has a 150 fold increase in mRNA expression as well as elevated protein expression[109]. Briefly, the full length murine B7-H4 open reading frame was inserted under the rat insulin promoter (RIP) to generate β-cell-specific B7-H4 over-expression. All mice used for the experiments were genotyped for the B7-H4 transgene post-weaning to ensure that they have the proper genetic make-up (Figure 1A). As shown in Figure 1B, B7-H4 Tg islets exhibited significantly elevated expression of the B7-H4 gene, as verified via qPCR. Western blots were also performed to confirm B7-H4 protein overexpression in B7-H4 Tg islets. This β-cell -specific overexpression system enables us to study the role of B7-H4 in β-cells while bypassing its systemic effects in immune system modulation under *in vitro* experimental conditions.

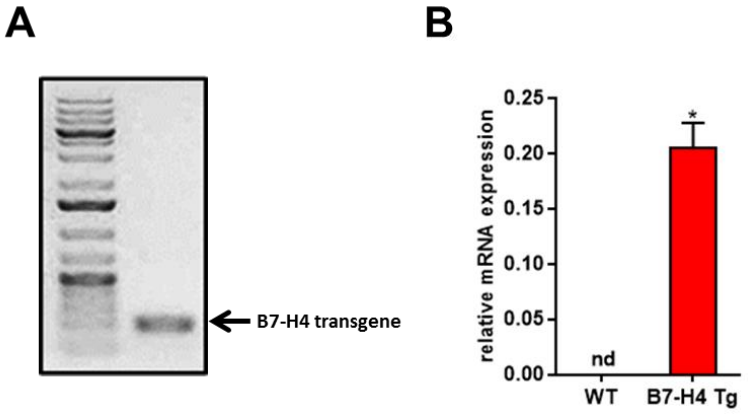

Figure 1. β-cell specific overexpression of B7-H4
(A) PCR products probed for the B7-H4 transgene post-weaning in isolated islets from B7-H4 Tg mice (B) Quantification of B7-H4 mRNA in islets from age-matched WT and B7-H4 Tg mice (nd. not detected). Gene expressions are normalized to GAPDH, 18s rRNA, and RPLP0. Data are represented as mean ± SEM; *p≤0.05 vs WT.

To further elucidate the role of B7-H4 within the islets, we have also obtained B7-H4 global knock-out mice from the lab of Dr. T.W. Mak (University of Toronto)[119]. B7-H4$^{-/-}$ mice were bred in our facility with C57BL/6 to generate heterozygotes. These mice were screened and set up as parent breeders to produce F2 generations with B7-H4 KO mice and WT littermate controls. All mice were genotyped post-weaning to verify genetic make-up as well as to set up correct breeder pairings (Fig 2A). As expected, B7-H4 KO islets showed significant reduction in the mRNA expression of B7-H4 as compared with littermate controls (Figure 2B), confirming efficient knock-down of our gene of interest. Residual B7-H4 mRNA expression in B7-H4 KO islets may need to be further verified by immunostaining.

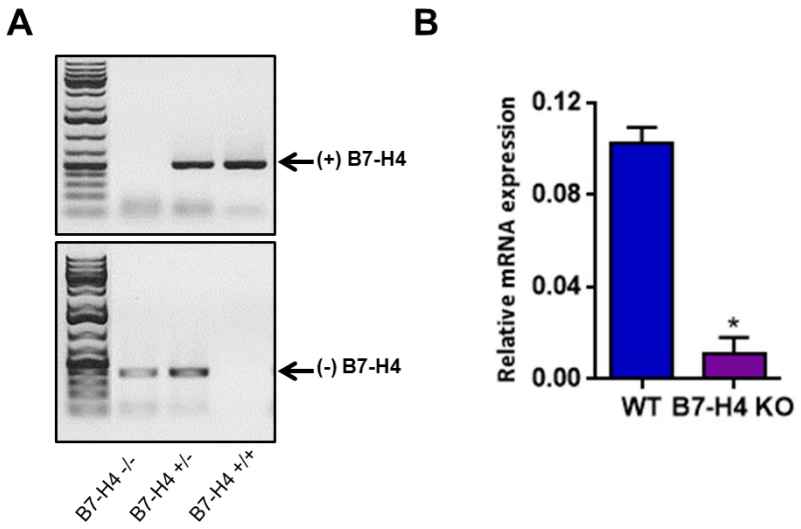

Figure 2. Global knock-out of the B7-H4 gene
(A) DNA gel electrophoresis of PCR amplified products were used to assign the corresponding genotypes (B7-H4$^{-/-}$, B7-H4$^{+/-}$, and B7-H4 $^{+/+}$) as shown. (B) B7-H4 gene expression normalized to GAPDH, 18s rRNA, and RPLP0. Newly-synthesized cDNA were amplified for the B7-H4 gene prior to qPCR reaction. Data are represented as mean ± SEM; *p≤0.05 vs WT.

3.2 Roles of B7-H4 in β-Cell Function

3.2.1 B7-H4 amplifies glucose-induced Ca^{2+} responses

Due to its inherent expression in pancreatic β-cells, we wanted to determine whether B7-H4 is involved in regulation of β-cell function. To examine this, we first compared glucose-induced cytosolic Ca^{2+} changes between B7-H4 Tg and WT islets *in vitro* (Figure 3). As mentioned previously, cytosolic Ca^{2+} influx from extracellular space is known to be a key event in glucose stimulated signal transduction that triggers, and correlates closely with, insulin secretion[64]. Isolated whole islets were subjected to transient glucose stimulation, and changes in $[Ca^{2+}]_i$ were measured by Fura-2 ratiometric imaging. Direct cellular depolarization by KCl was performed at the end of glucose stimulation to serve as a positive control for glucose-independent intracellular Ca^{2+} response. As illustrated by the representative recordings in Figure 3A, upon raising the glucose concentration from 3 mM to 15 mM, WT islets exhibited characteristic multiphasic responses, starting with phase 0, which corresponds to Ca^{2+} uptake into the ER via SERCA[61]. This was followed by an abrupt increase in $[Ca^{2+}]_i$ due to activation of extracellular Ca^{2+} influx through VGCCs, which progressed to steady-state oscillations. The presence of phase 0 responses and steady-state oscillations in response to glucose stimulation was significantly reduced in B7-H4 Tg islets (Figure 3A, 3B). Furthermore, B7-H4 Tg islets responded more rapidly to glucose with Ca^{2+} entry compared with WT islets as seen in the average traces in Figure 3C and the quantification of islet Ca^{2+} response time in Figure 3D. Despite the differences in the kinetics of the glucose-induced Ca^{2+} responses, AUC analysis did not reveal significant genotype-dependent differences in the integrated amount of cytosolic Ca^{2+} at basal 3 mM glucose, 15 mM glucose, 3 mM glucose recovery period, and during KCl stimulations (Figure 3E). However, B7-H4 Tg islets displayed a notable trend of higher

intracellular Ca^{2+} at basal glucose concentration (Figure 3C, 3E). These data demonstrate that B7-H4 kinetics of glucose-induced Ca^{2+} responses are altered in B7-H4 overexpressing islets, which may affect other aspects of β-cell function, including the ability to secrete insulin and respond to environmental stress.

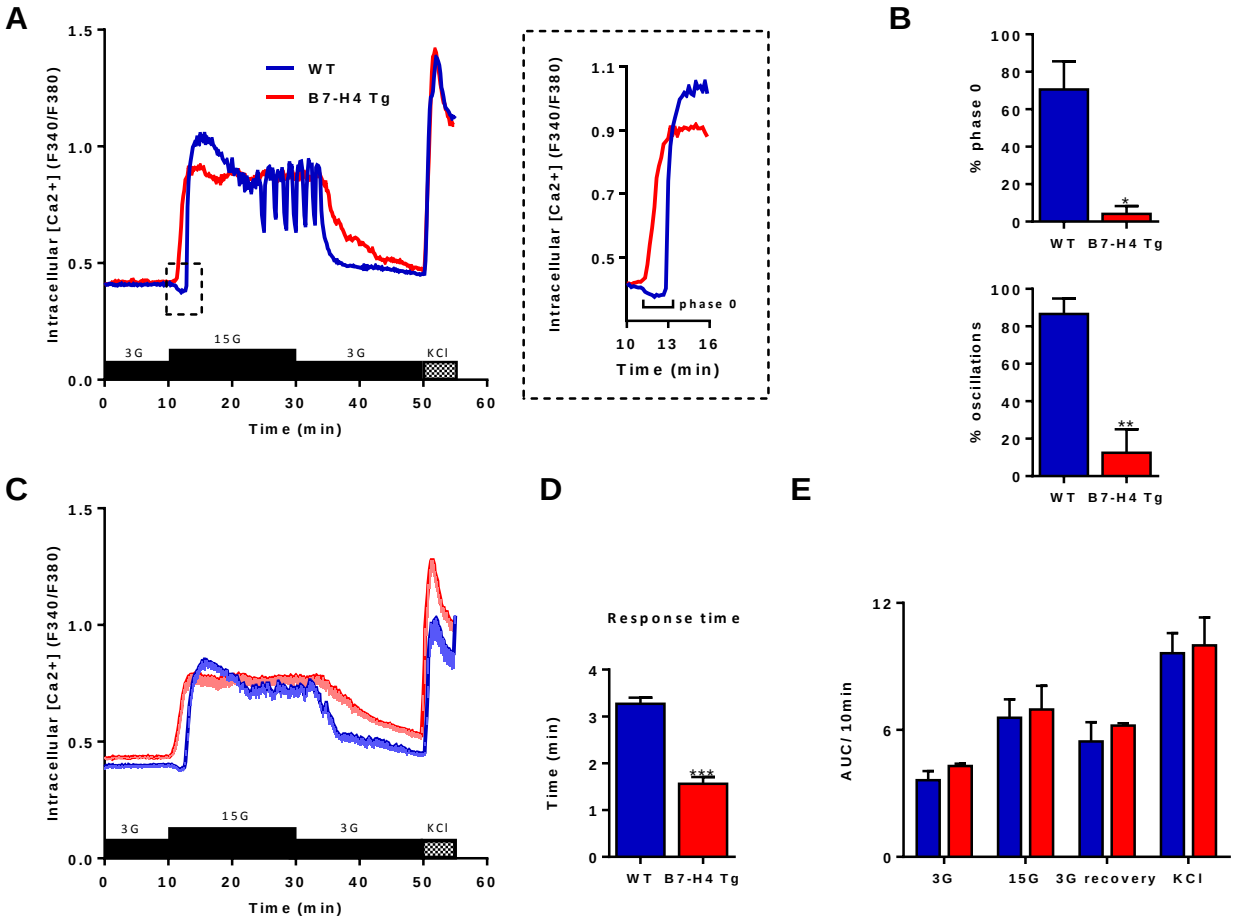

Figure 3. Cytosolic Ca^{2+} responses of WT and B7-H4 Tg islets to 15 mM glucose stimulation
(A) Representative traces of a single WT and B7-H4 Tg islet stimulated with 15 mM glucose (15G) and KCl with expanded phase 0 responses in dashed box. (B) The number of oscillating and phase 0-displaying islets from each WT and B7-H4 Tg animal were represented as a percentage of total number of islets (n=3-4 animals). (C) Average cytosolic Ca^{2+} responses of WT and B7-H4 Tg islets during glucose and KCl stimulations at indicated concentrations. (D) Islet response times to 15 mM glucose stimulation. The response threshold was set at F340/F380=0.5 and the response time calculated as the difference between time to reach response threshold and start of 15mM glucose perfusion. (E) AUC analysis per 10 min during each stimulus in panel C. Data are represented as ± SEM; *p≤0.05 vs WT; **p≤0.01 vs WT; ***p≤0.001 vs WT.

Since B7-H4 Tg islets have faster glucose-activated Ca^{2+} responses as compared with WT islets, we hypothesized that these islets may have heightened sensitivity to glucose. It has also been shown that loss of oscillations in phase 2 response generally occurs during very high glucose stimulations, such as at a concentration of approximately 20 mM[122]. It is therefore possible that B7-H4 Tg islets exhibited a left-shifted, i.e. sensitized glucose response compared with WT islets. To test this, we subjected both WT and B7-H4 Tg islets to a near-threshold stimulation of 5 mM glucose from basal concentration of 2 mM (Figure 4A). At this lower basal glucose concentration there were no apparent differences in $[Ca^{2+}]_i$ between genotypes. As hypothesized, we observed that B7-H4 Tg islets responded faster, and with significantly higher peak Ca^{2+} levels compared with to WT islets when stimulated with 5 mM glucose (Figure 4B, 4C). Furthermore, iAUC analyses confirmed that greater Ca^{2+} entry was induced over the duration of the stimulus in B7-H4 Tg islets compared with to WT islets (Figure 4D). These results suggest that B7-H4 can augment β-cell responses to glucose at the level of cellular Ca^{2+} flux, possibly reflecting a sensitization to glucose.

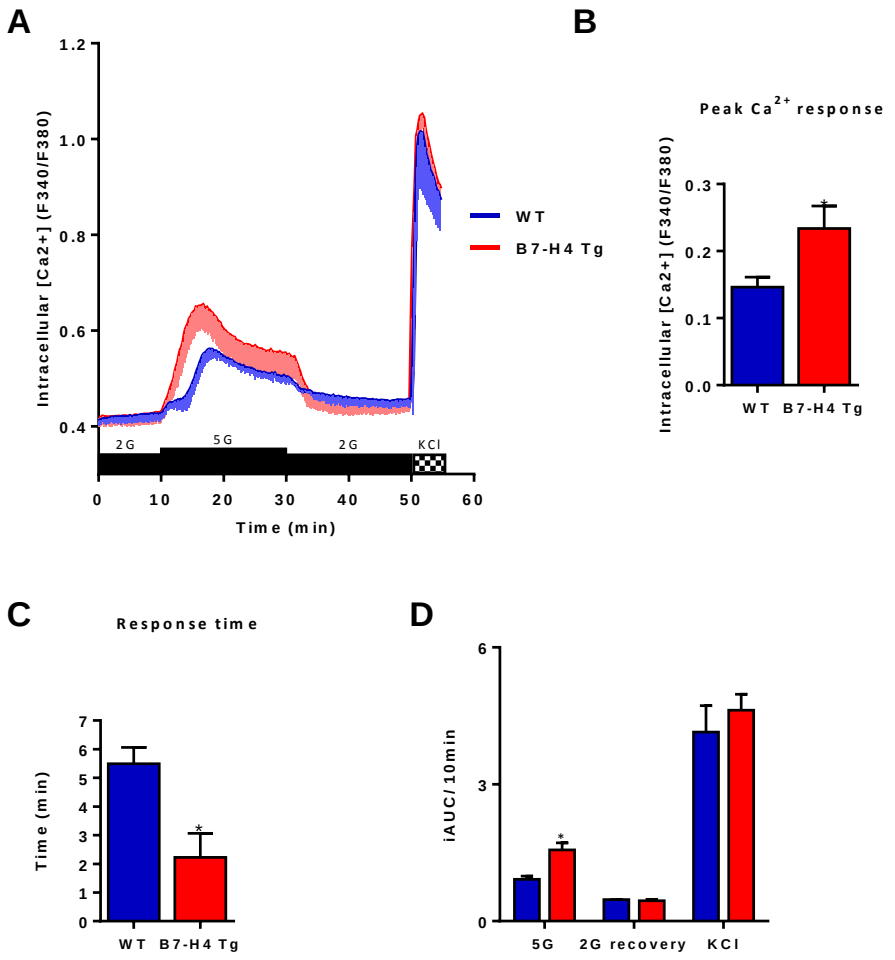

Figure 4. Cytosolic Ca^{2+} responses of WT and B7-H4 Tg islets to 5 mM glucose stimulation
(A) Average intracellular Ca^{2+} responses of WT and B7-H4 Tg islets during glucose and KCl stimulations (n=3 animals). (B) Peak intracellular Ca^{2+} concentrations in WT and B7-H4 Tg islets in response to 5 mM glucose (5G). Values shown are quantified as change in $[Ca^{2+}]_i$ relative to basal $[Ca^{2+}]_i$ at 2 mM glucose (2G). (C) Islet response times to 5 mM glucose stimulation. Response threshold was set at F340/F380=0.5, and response time was represented as the time to reach response threshold – start of 5 mM glucose perfusion. (D) iAUC analysis per 10 min during each stimulus in panel A, calculated as $AUC_{stimulus} - AUC_{baseline}$. Data are represented as ± SEM; *p≤0.05 vs WT.

To further investigate the effect of B7-H4 on glucose sensitivity in pancreatic β-cells, we compared the responses of WT and B7-H4 Tg islets to a step-wise glucose ramp (Figure 5A). WT islets were not able to generate Ca^{2+} responses following 4 mM glucose stimulations, rather, reductions in $[Ca^{2+}]_i$ were recorded (Figure 5A). It is likely that under these conditions, WT islets

were insufficiently depolarized via K_{ATP} channels to induce Ca^{2+} influx through VGCCs, but the phase 0 lowering of cytosolic Ca^{2+} remained due to SERCA activation. B7-H4 Tg islets, on the contrary, showed significantly elevated peak Ca^{2+} responses already at 4 mM glucose (Figure 5B). Compared to WT islets, the B7-H4 Tg islets also showed a higher overall $[Ca^{2+}]_i$ during 4 mM and 6 mM glucose stimulations, as quantified by iAUC (Figure 5D). Furthermore, the ability of B7-H4 Tg islets to respond to lower glucose stimulations was correlated with a significant reduction in the percentage of islets that show steady-state oscillations in response to 10 mM glucose (Figure 5C). Again, KCl-induced $[Ca^{2+}]_i$ changes were similar between WT and B7-H4 Tg islets, confirming that genotypic differences in Ca^{2+} responses were glucose dependent. In addition, the percentage of islets that oscillated at 10 mM glucose (WT: 92.2%; B7-H4 Tg: 19.5%) was slightly higher compared with with what was seen at 15 mM glucose (WT: 86.5%; B7-H4 Tg: 12.3%) (Figure 3B, Figure 5C), which likely reflects the increased percentage of islets that show a plateau response instead of oscillations at increased glucose concentration, as discussed previously. These data confirmed that B7-H4 Tg islets exhibit a lower threshold for glucose response in terms of cytosolic Ca^{2+} rises, which normally represent voltage-gated influx under these conditions.

We also repeated the glucose ramp in B7-H4 KO islets to assess whether loss of endogenous B7-H4 may lead to perturbations in Ca^{2+} homeostasis (Figure 5E). In contrast to the B7-H4 overexpressing islets, B7-H4 KO islets responded similarly to WT islets under these conditions in both peak Ca^{2+} responses and iAUCs (Figure 5F, 5H). In addition, steady-state oscillations occurred in B7-H4 KO islets, as in WT islets. It is possible that the relatively low levels of endogenous B7-H4 in WT mouse islets is not abundant enough to contribute a significant effect to glucose-stimulated Ca^{2+} responses.

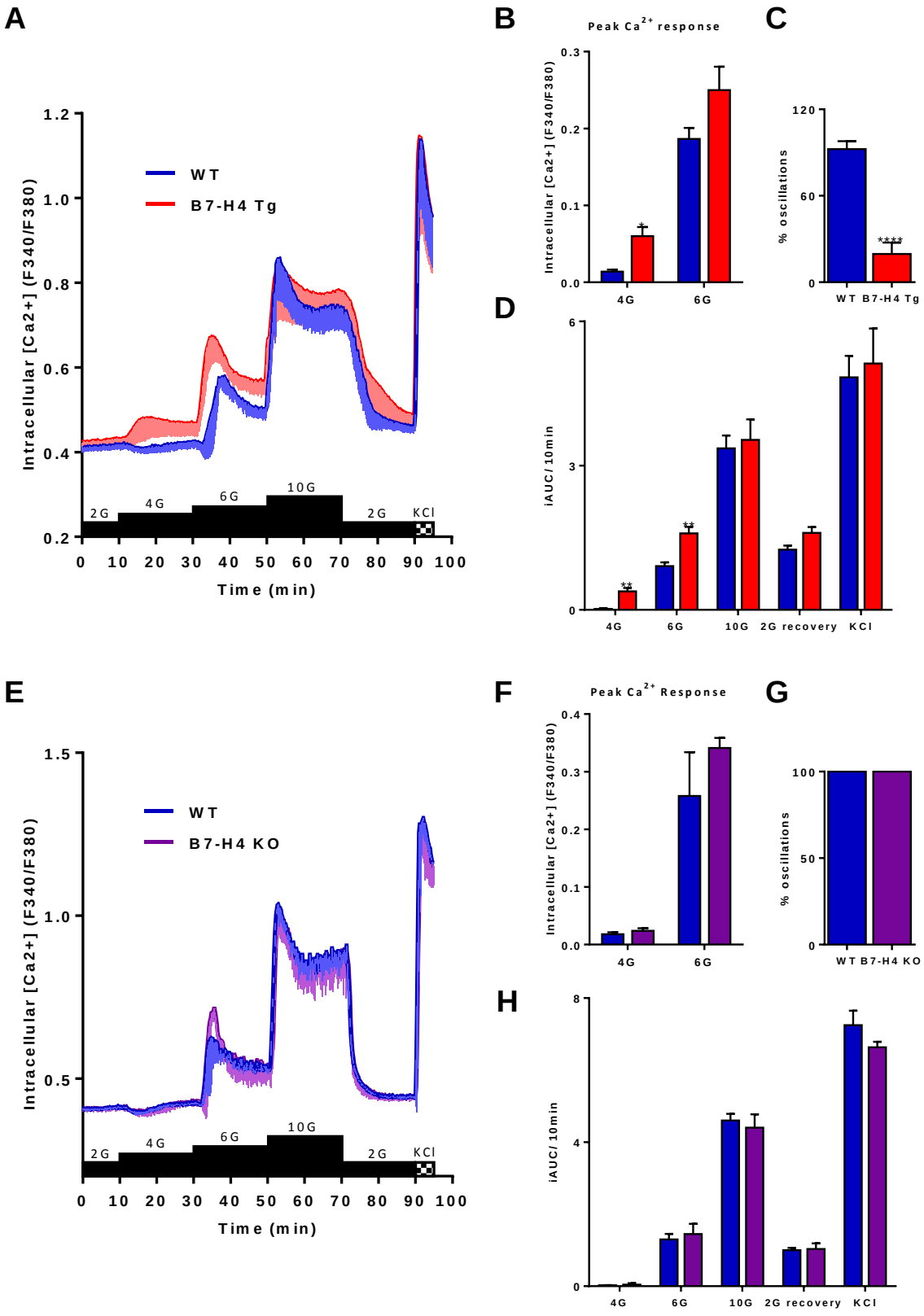
A
WT
B7-H4 Tg
Intracellular [Ca2+] (F340/F380)
Time (min)
2G
4G
6G
10G
2G
KCl
B
Peak Ca2+ response
Intracellular [Ca2+] (F340/F380)
4G
6G
C
% oscillations
WT B7-H4 Tg
D
iAUC/10min
4G
6G
10G
2G recovery
KCl
E
WT
B7-H4 KO
Intracellular [Ca2+] (F340/F380)
Time (min)
2G
4G
6G
10G
2G
KCl
F
Peak Ca2+ Response
Intracellular [Ca2+] (F340/F380)
4G
6G
G
% oscillations
WT B7-H4 KO
H
iAUC/10min
4G
6G
10G
2G recovery
KCl

Figure 5. Cytosolic Ca^{2+} responses of WT, B7-H4 Tg, and B7-H4 KO islets to glucose ramp stimulation
(A) Average intracellular Ca^{2+} responses of WT and B7-H4 Tg islets during glucose ramp and KCl stimulations (n=5-6 animals). (B) Peak intracellular Ca^{2+} concentrations in WT and B7-H4 Tg islets in response to 4 mM (4G) and 6 mM glucose (6G) stimulations. Values shown are quantified as change in $[Ca^{2+}]_i$, relative to basal $[Ca^{2+}]_i$ at 2 mM glucose. (C) Percentage of WT and B7-H4 Tg islets displaying steady-state oscillations at 10 mM glucose (10G). (D) iAUC analysis per 10 min during each stimulus in panel A. (E) Average intracellular Ca^{2+} responses of B7-H4 KO and WT littermate islets during glucose and KCl stimulations (n=2). (F) Peak intracellular Ca^{2+} concentrations in WT and B7-H4 KO islets in response to glucose stimulations. (G) Percentage of WT and B7-H4 KO islets exhibiting steady-state Ca^{2+} oscillations. (H) iAUC analysis per 10min during each stimulus in panel E. Data are represented as mean ± SEM; *p≤0.05 vs WT; **p≤0.01 vs WT; ****p≤0.0001 vs WT.

Lastly, we depolarized both WT and B7-H4 Tg islets with KCl, and monitored return of $[Ca^{2+}]_i$ back to basal concentration (Figure 6). We saw no significant differences in recovery times, which demonstrated that the ability of β-cells to return to basal Ca^{2+} levels was similar between genotypes.

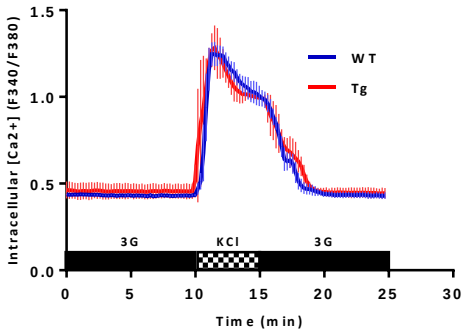

Figure 6. KCl stimulation of WT and B7-H4 Tg islets
Average intracellular Ca^{2+} responses of WT and B7-H4 Tg islets during 3 mM glucose (3G) and KCl stimulations (n=3 animals). Data are represented as mean ± SEM.

3.2.2 Role of B7-H4 in β-cell metabolism

Glycolysis and oxidative phosphorylation are important processes in glucose-stimulated Ca^{2+} responses and insulin secretion through the production of ATP. Therefore, increased glucose sensitivity in B7-H4 Tg islets raise the possibility that B7-H4 may affect pathways involved in glucose metabolism, thus generating differential output in Ca^{2+} responses. We used the Seahorse XF^e 96 system[123,124] for real-time measurements of extracellular flux in dispersed

islet cells to determine whether mitochondrial respiration and glycolysis are influenced by B7-H4 overexpression. Dispersed WT and B7-H4 Tg islet cells were subjected to a glucose ramp at 2 mM, 5mM, and 10 mM glucose. The oxygen consumption rate (OCR) and extracellular acidification rate (ECAR) were compared, which reflects mitochondrial respiration and glycolysis, respectively (Figure 7A, 7B). We observed distinct step-wide increases in OCR and ECAR with rising glucose concentrations in both genotypes, and B7-H4 overexpression did not significantly affect either OCR or ECAR, as shown by comparisons at each time point. In agreement with the lack of significant metabolic differences, expression levels of the enzyme GCK, as well as the glucose transporter Glut 2, were not different between WT and B7-H4 Tg islets (Figure 7C). Since all the Ca^{2+} imaging experiments were performed 6 days after islet isolation, gene expression was compared at both 1 and 6 days post-islet isolation in order to exclude confounding changes in gene expression as a result of culture time. These data suggest that the striking differences in Ca^{2+} response kinetics demonstrated by B7-H4 Tg islets is not due to obvious metabolic alterations.

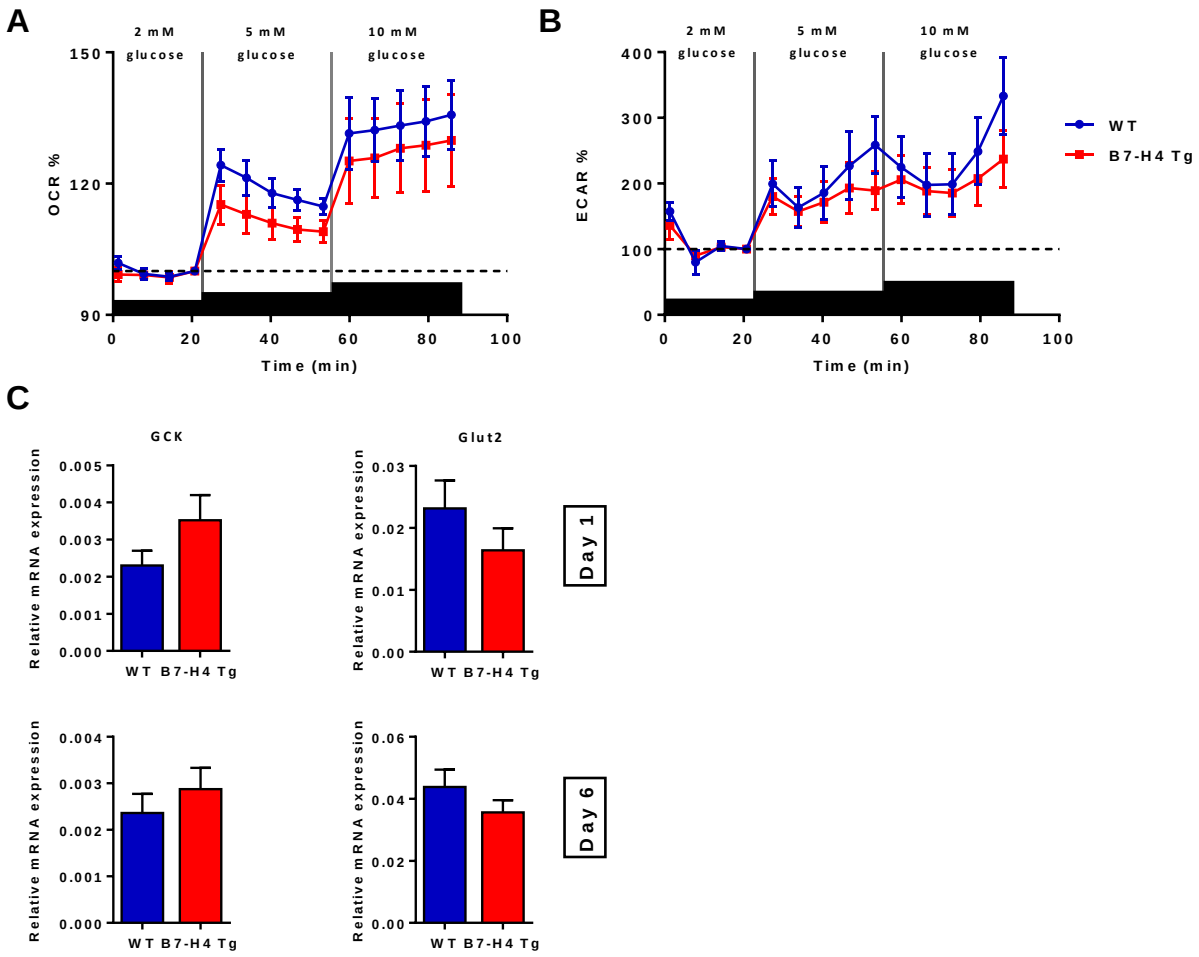

Figure 7. Real-time assessment of mitochondrial respiration and glycolysis in WT and B7-H4 Tg islet cells
(A, B) Simultaneous kinetic measurement of oxygen consumption (panel A) and extracellular acidification rate (panel B) in dispersed islet cells exposed to a step-wise glucose ramp stimulus (n=3). Values are represented as percentage of OCR or ECR normalized to basal rates and total protein content. (C) Gene expression of GCK and Glut2 at 1 and 6 days post-isolation in WT and B7-H4 Tg islets normalized to the house-keeping genes 18s rRNA, RPLP0, and GAPDH (n=6-10). Data are represented as mean ± SEM.

3.2.3 Regulation of β-cell ER Ca^{2+} by B7-H4

Since we found no significant metabolic differences, we next wanted to investigate whether the lack of phase 0 cytosolic Ca^{2+} lowering and steady-state oscillations in B7-H4 Tg islets may be due to differences in β-cells ER Ca^{2+} handling. To assess the contribution of ER Ca^{2+} buffering and/or release to the differences we observed in glucose-induced cytosolic Ca^{2+}

responses, we treated both WT and B7-H4 Tg islets with the specific SERCA inhibitor, thapsigargin, for 30 min prior to carrying out the glucose ramp stimulation described previously. WT islets demonstrated significant elevations in Ca^{2+} responses at 4 mM, 6 mM, and 10 mM of glucose following SERCA inhibition (Figure 8A, 8B). At 6 mM glucose, the Ca^{2+} responses in thapsigargin- treated WT islets were increased to such an extent that they were comparable to responses from the more glucose-sensitive B7-H4 Tg islets (untreated). Furthermore, thapsigargin pre-incubation significantly reduced the response time of WT islets (Figure 8C). It was also noted that SERCA inhibition in the WT islets resulted in loss of phase 0, similar to what was seen in the untreated B7-H4 Tg islets (Figure 8D). Since thapsigargin inhibits SERCA, the disappearance of phase 0 demonstrated that it indeed reflects ER Ca^{2+} uptake. In contrast, we did not observe any changes in the glucose-induced Ca^{2+} responses in B7-H4 Tg islets due to thapsigargin pre-treatment. It is possible that Ca^{2+} uptake into the ER was already minimal in B7-H4 Tg islets and therefore could not be substantially affected by SERCA inhibition. Taken together, these data show that inhibition of ER Ca^{2+} uptake in WT islets results in glucose-induced Ca^{2+} responses that closely mimics that of B7-H4 Tg islets, suggesting that the Ca^{2+} responses in B7-H4 Tg islets may be attributed to reduced SERCA activity. However, islet SERCA2b gene expression did not differ significantly between the two genotypes at both 1 and 6 days post-islet isolation, indicating that any such changes would be regulated either post-transcriptionally or post-translationally (Figure 8E).

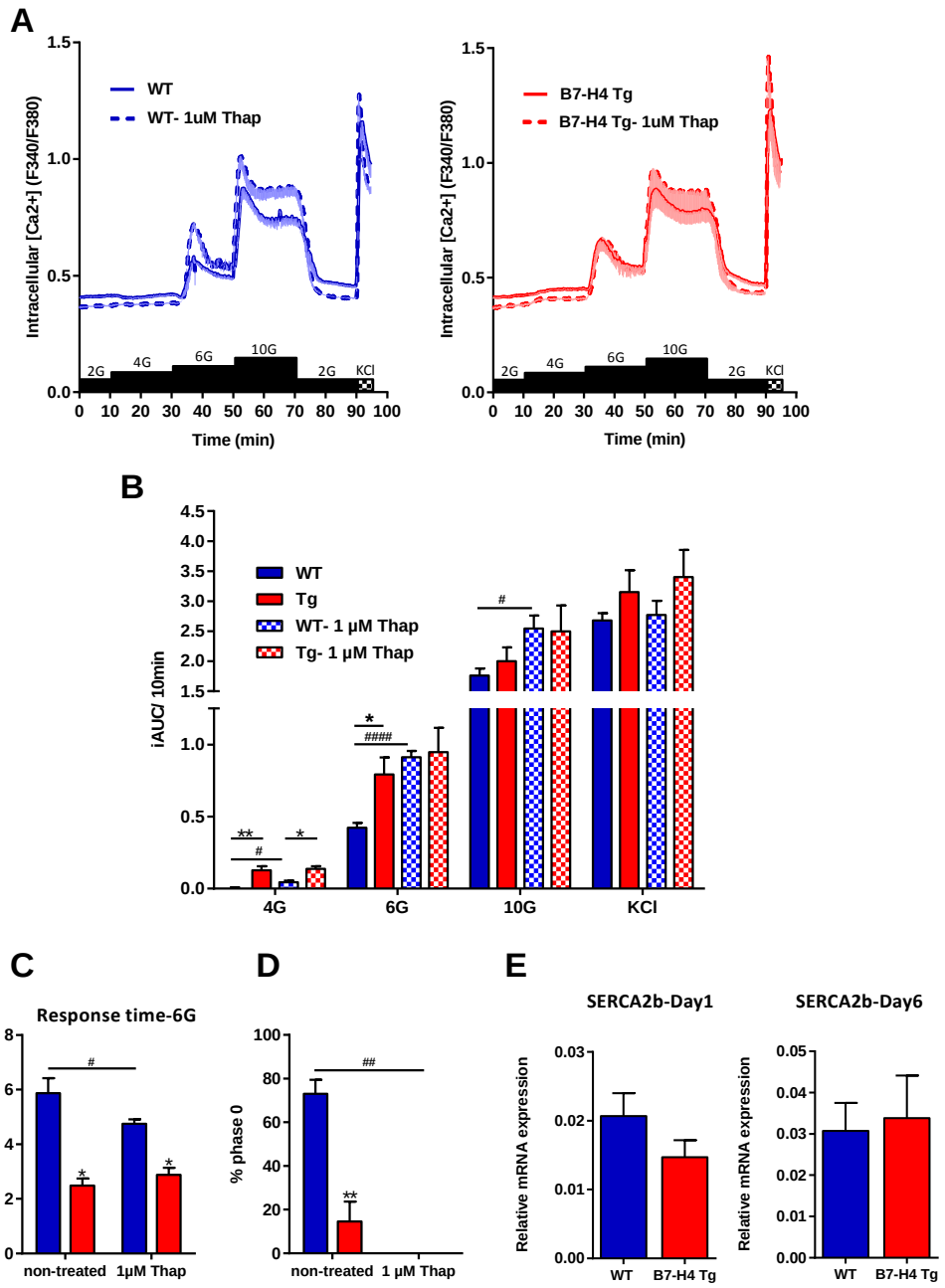

Figure 8. The effects of acute thapsigargin treatments on glucose-stimulated Ca^{2+} response
(A) Measurement of $[Ca^{2+}]_i$ during glucose ramp stimulation preceded by acute thapsigargin (Thap) treatment (n=3 animals). (B) iAUC quantification of Ca^{2+} responses at indicated glucose concentration in WT and B7-H4 islets. (C) Average response times of WT and B7-H4 Tg islets to 6 mM glucose (6G); response threshold set at F340/F380=0.5; response time defined as time to threshold – time of 6 mM glucose stimulation. (D) Percentage of islets displaying phase 0 responses during initial glucose stimulation at 4 mM glucose (4G) in each treatment group. (E) Gene expression (normalized to GAPDH, 18s rRNA, and RPLP0) of SERCA2b at 1 or 6 days post-islet isolation. Data are expressed as mean ± SEM; *p≤ 0.05 vs WT; **p≤0.01 vs WT, #p≤0.05 vs treatment, ##p≤0.01 vs treatment; ####p≤0.0001 vs treatment.

Since efficiency of Ca^{2+} sequestration into the ER would be expected to affect overall ER Ca^{2+} storage, we wanted to determine whether the ability to mobilize ER Ca^{2+} is altered in B7-H4 Tg islets. The cholinergic agonist carbachol was administered to islets in the presence of sub-stimulatory 3 mM glucose. Carbachol triggers the opening of IP_3R ER Ca^{2+} release channels via generation of the 2nd messenger IP_3[56]. Indeed, in the presence of 500 μM carbachol, a rapid spike and a subsequent second rising phase in cytoplasmic Ca^{2+} concentrations were evident in both WT and B7-H4 Tg islets (Figure 9A). It is known that mobilization of stored ER Ca^{2+} corresponds to the spike, and that deletion of ER Ca^{2+} stores will trigger extracellular Ca^{2+} entry through activation of store-operated Ca^{2+} (SOC) channels, which is reflected by the second phase[125]. As shown in Figure 9A, B7-H4 Tg islets exhibited elevated baseline in $[Ca^{2+}]_i$, which corresponded to those from previous glucose stimulations with 3 mM glucose in section 3.2.1. To isolate carbachol-induced changes in $[Ca^{2+}]_i$ responses, iAUC analyses were used to compare Ca^{2+} responses between genotypes. However, there were no significant differences between WT and B7-H4 Tg islets with carbachol stimulation (Figure 9B). To more directly compare the initial peak corresponding to ER Ca^{2+} release, the islet Ca^{2+} responses were also examined in the presence of carbachol in Ca^{2+}-free buffers. Quantification of iAUC during this second stimulus was comparable between WT and B7-H4 Tg islets. Taken together, these data suggest that B7-H4 does not affect mobilization of Ca^{2+} from ER stores. However, as the B7-H4 Tg islets did not fully recover back to base prior to the second stimulation in Ca^{2+}-free carbachol, this conclusion remains to be confirmed under more stringent experimental conditions.

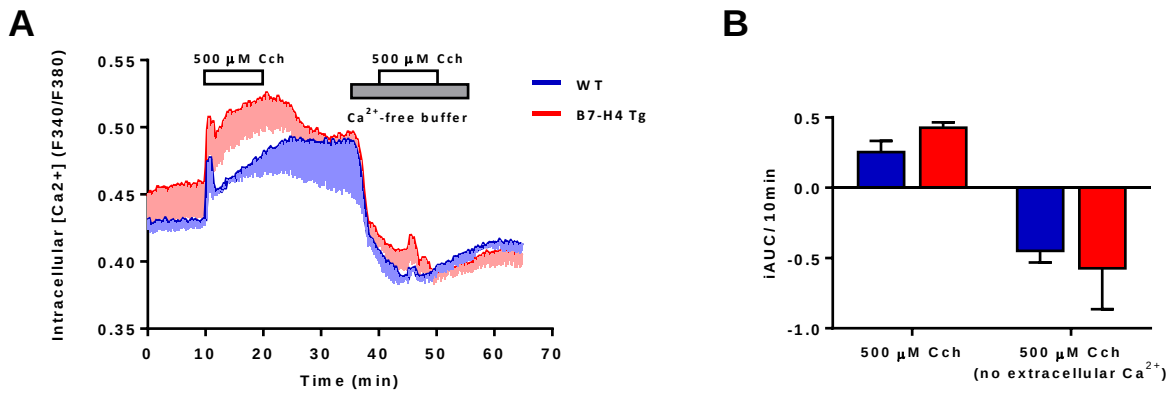

Figure 9. Calcium release from ER storage by carbachol
(A) $[Ca^{2+}]_i$ changes as measured via ratiometric Fura-2 imaging (n=3). Islets were perfused with 3 mM glucose (3G) Ringer's buffer for the duration of the run. Carbachol (Cch) and 3 mM Ca^{2+}-free buffer were added at indicated time periods. (B) iAUC analysis of overall Ca^{2+} responses in WT and B7-H4 Tg islets during carbachol stimulation +/- extracellular Ca^{2+}. Data are represented as mean ± SEM.

3.2.4 K_{ATP} channel involvement in B7-H4-induced changes in islet Ca^{2+} responses

To further examine the mechanisms of altered Ca^{2+} responses to glucose in B7-H4 Tg islets, we next treated islets with diazoxide (DZ), which prevents the closure of K_{ATP} channels. This inhibits ATP-dependent β-cell depolarization and activation of VGCCs without blocking glucose metabolism. Treatment with diazoxide allowed us to evaluate contributions from K_{ATP} channel-independent mechanisms during glucose stimulations, including a more direct evaluation of the phase 0 Ca^{2+} uptake into the ER in isolation from the depolarization-induced influx (Figure 10A). Upon diazoxide treatment, we uncovered the presence of phase 0 responses in B7-H4 Tg islets subsequent to glucose stimulation (Figure 10A), and the percentage of B7-H4 islets showing phase 0 responses was similar to WT islets (Figure 10B). The results imply that SERCA activation occurs during glucose stimulation in B7-H4 Tg islets, but is usually masked by accelerated cellular depolarization. As expected, diazoxide inhibited glucose-induced Ca^{2+}

responses in WT islets but surprisingly, B7-H4 Tg islets were still able to elicit a Ca^{2+} response during diazoxide treatment, albeit it was delayed and at a significantly lower level than non-treated islets (Figure 10A, 10C). To further explore the source of cytosolic Ca^{2+} rise during diazoxide treatment, we incubated islets with thapsigargin 30 min prior to, and during the glucose stimulation with diazoxide. Thapsigargin depletes ER Ca^{2+} storage, and would reveal if ER Ca^{2+} was required for the diazoxide-insensitive response. As previous observed, while Ca^{2+} responses in WT islets were drastically reduced following diazoxide treatment, and B7-H4 Tg islets showed pronounced rises in cytosolic Ca^{2+} during glucose stimulation despite the presence of thapsigargin (Figure 10D, 10E). This suggests that cytosolic changes in $[Ca^{2+}]_i$ during diazoxide treatment is not dependent on mobilization of Ca^{2+} from ER storage.

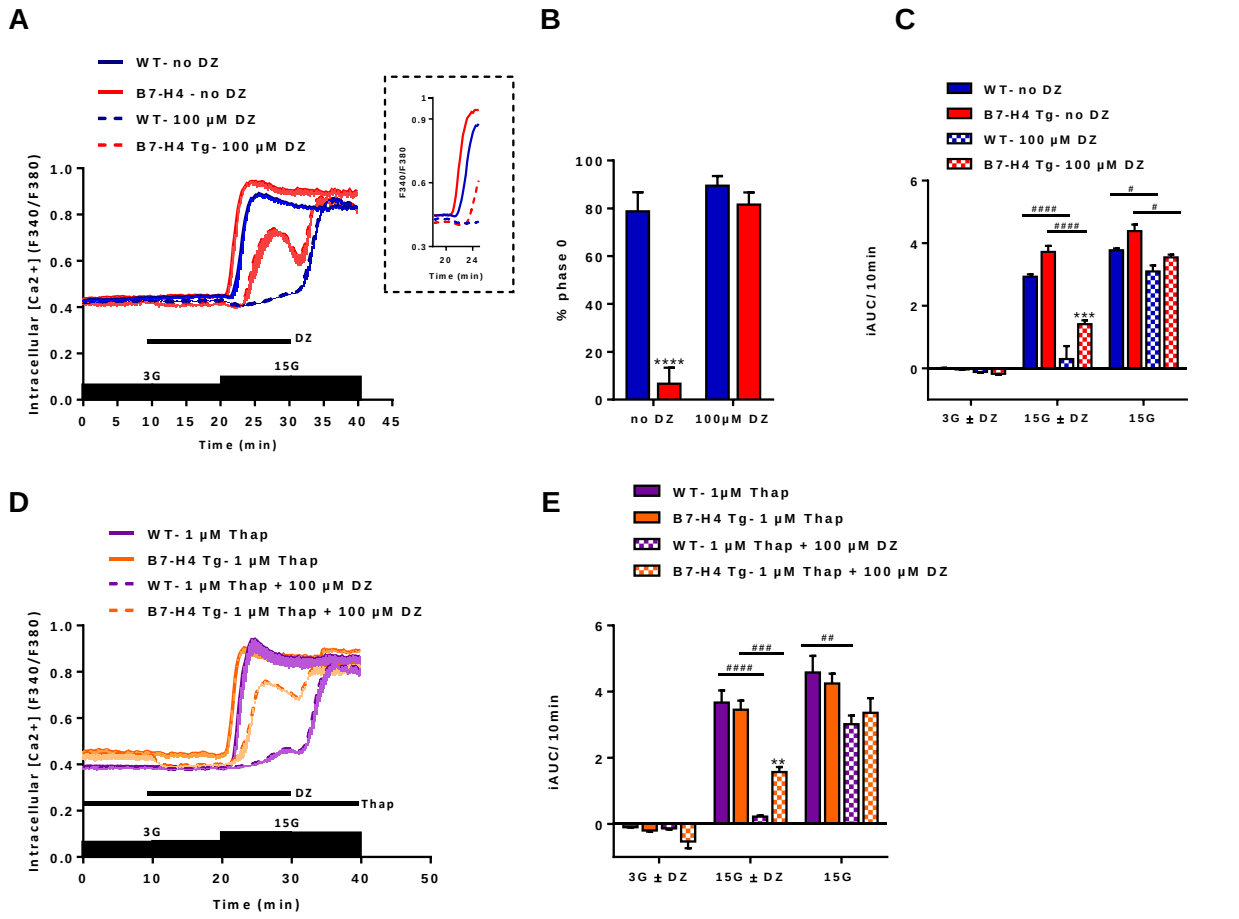

Figure 10. Sensitivity of WT and B7-H4 Tg islets to the K_{ATP} activator, diazoxide
(A) Cytosolic recordings of islets stimulated with 15 mM glucose (15G) in combination with 100 µM diazoxide (DZ) (n=3-4 animals). Enlarged phase 0 responses are shown in dashed box. (B) Percentage of islets displaying phase 0 response following 15 mM glucose stimulation with or without diazoxide. (C) iAUC analysis of average Ca^{2+} response per 10 min during at indicated conditions in panel A. (D) Average $[Ca^{2+}]_i$ changes to glucose + diazoxide stimulations in conjunction with ER Ca^{2+} depletion via thapsigargin (n=3). (E) iAUC analysis of average Ca^{2+} response per 10min at indicated conditions in panel A. Data are expressed as mean ± SEM; **p≤ 0.01 vs WT; ***p≤0.001 vs WT, #p≤0.05 vs treatment, ##p≤0.01 vs treatment; ###p≤0.001 vs treatment, ####p≤0.0001 vs treatment.

As demonstrated in the previous, B7-H4 Tg islets displayed a significant diazoxide-insensitive component in their Ca^{2+} response to glucose compared with to WT islets. It is possible that B7-H4 may directly affect K_{ATP} channel function. We next measured islet Ca^{2+} responses to pulses of increasing tolbutamide concentrations in order to determine whether B7-

H4 Tg islets respond differently to K_{ATP} channel inhibition than WT islets. Interestingly, B7-H4 Tg islets exhibited significantly augmented Ca^{2+} responses at lower concentrations of tolbutamide compared with WT islets (Figure 11A, Figure 11B). When the concentration of tolbutamide exceeded 25 µM, this difference was lost as a saturation point was reached (Figure 11A, Figure 11C), where all K_{ATP} channels on the islets were inhibited. To summarize, B7-H4 Tg islets demonstrate reduced sensitivity to diazoxide and increased sensitivity to sub-maximal concentrations of tolbutamide. Consequently, it is possible that B7-H4 can modulate K_{ATP} channel activity to exert an effect on down-stream Ca^{2+} responses.

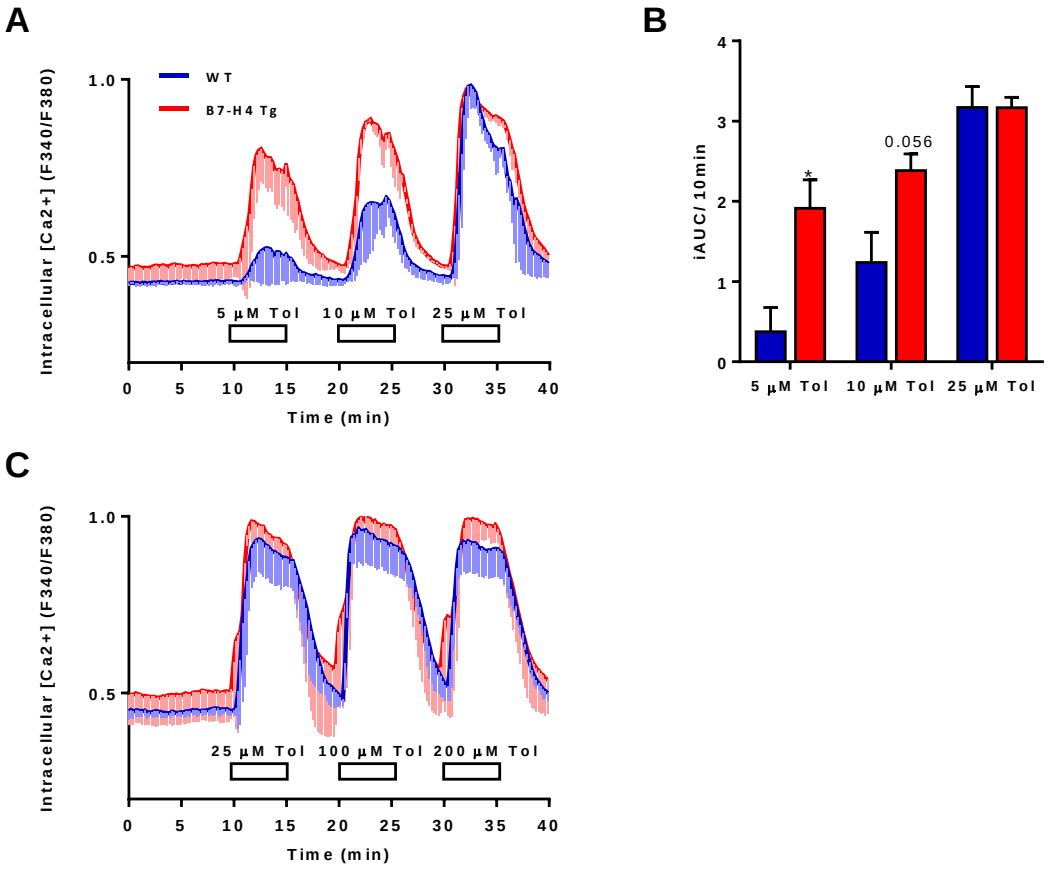

Figure 11. Inhibition of K_{ATP} channels in WT and B7-H4 Tg islets by tolbutamide
(A) Whole islets were perfused with 3 mM glucose (3G) Ringer's buffer, and changes in $[Ca^{2+}]_i$ were quantified by ratiometric Fura-2 imaging (n=3). Tolbutamide (Tol) of indicated concentration was given in 5- min pulses followed

by 5 minutes of washing out period in regular Ringer's buffer. (B) iAUC analysis of overall Ca^{2+} responses during each stimulus indicated in panel A. (C) Time kinetics of $[Ca^{2+}]_i$ at 3 mM glucose Ringer's buffer, stimulated with 5 min tolbutamide pulses (n=3). Data are represented as mean ± SEM, *p≤0.05 vs WT.

3.2.5 Role of B7-H4 in *in vitro* β-cell insulin secretion

As overexpression of B7-H4 led to striking differences in glucose-stimulated Ca^{2+} responses, islets from WT and B7-H4 Tg animals were collected and assayed for total insulin content and insulin secretion. Whole islets were incubated in 2 mM glucose and stimulated with a low glucose concentration of 5 mM as well as a higher glucose concentration of 10 mM, KCl was again used as a positive control. Based on data from glucose-stimulated Ca^{2+} responses, 5 mM glucose was identified as the stimulus threshold in WT islets, and induced only a small Ca^{2+} response. On the other hand, the same glucose stimulus is able to elicit a much more robust response in B7-H4 Tg islets. Surprisingly, there were no observable differences in insulin secretion between the genotypes under a 5 mM glucose stimulus (Figure 12A). It is possible that the differences in Ca^{2+} responses elicited under such low glucose stimulus may not be large enough to translate into differences in insulin secretion. WT and B7-H4 Tg islets showed comparable insulin secretion when stimulated with 10 mM glucose and KCl (Figure 12A), which in this case was consistent with the lack of differences in the Ca^{2+} profiles under these conditions. Furthermore, we did not detect differences in insulin content between the WT and B7-H4 Tg islets (Figure 12B). In support of this finding, mRNA expression of Pdx1 and Ins2 were comparable between WT and B7-H4 Tg islets at both 1 and 6 days post-islet isolation (Figure 12C). These results suggest that while B7-H4 alters glucose-induced Ca^{2+} influx in β-cells, it may not necessarily be coupled to insulin secretion.

Lastly, we measured insulin secretion in islets treated with diazoxide to determine whether the diazoxide-resistance of Ca^{2+} responses in B7-H4 Tg islets was reflected in enhanced insulin secretion. Indeed, while insulin secretion in WT islets were significantly blunted

following diazoxide treatment, insulin secretion in B7-H4 Tg islets was not significantly reduced compared with untreated islets (Figure 12D). Combined data from glucose-induced Ca^{2+} response and insulin secretion in the presence of diazoxide further suggest that B7-H4 may modulate insulin secretion in β-cells via the K_{ATP}-dependent pathway.

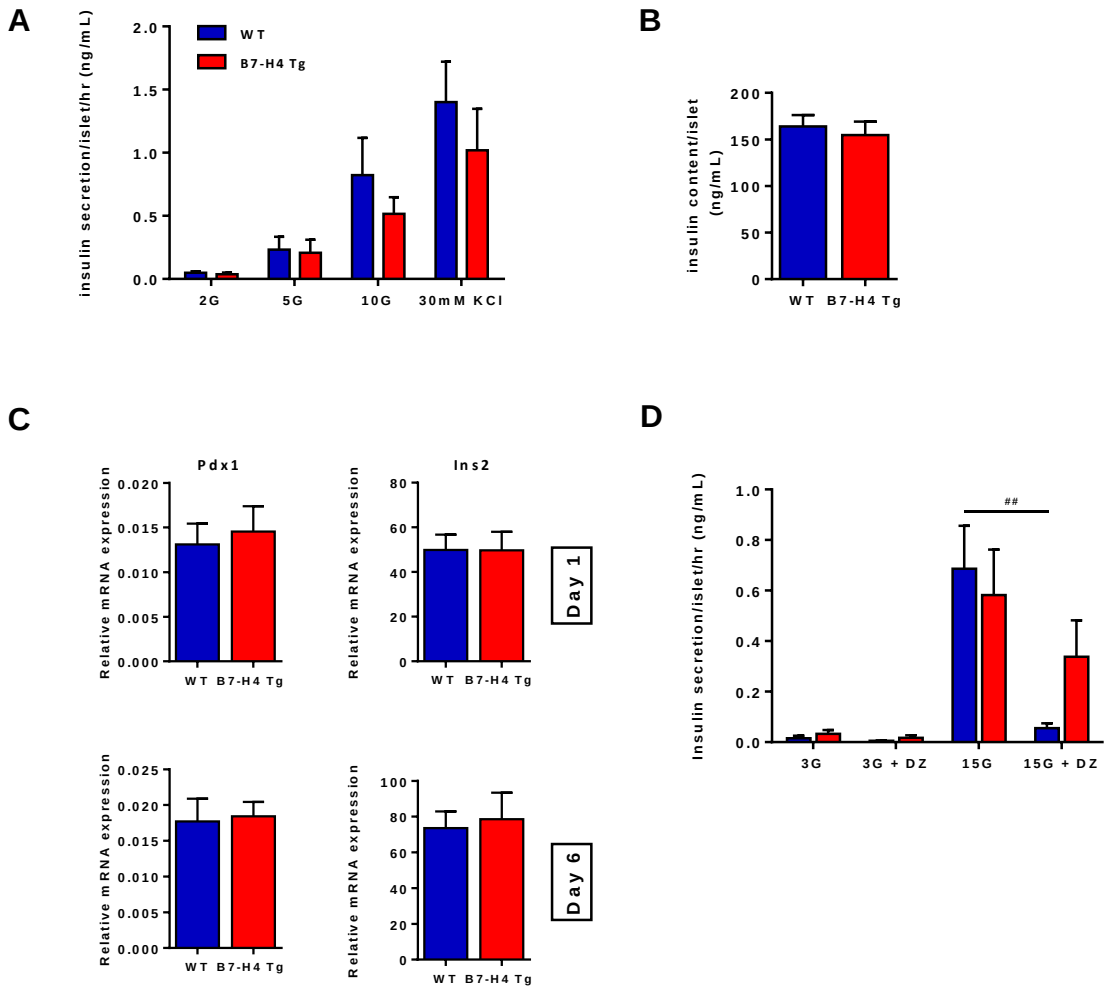

Figure 12. Role of B7-H4 on glucose-stimulated insulin content, secretion, and β-cell enriched genes
(A) Static glucose-stimulated insulin secretion- islets incubated at 2mM glucose (2G) for 1hr, followed by 5mM (5G), 10mM glucose (10G) (1hr each), and 30mM KCl (30min) stimulations (n=6). (B) Total insulin content per islet in WT and B7-H4 Tg mice (n=3). Values shown as fold change over basal secretion. (C) Relative gene expression of Pdx1 and Ins2 at 1 and 6 days post-islet isolation (n=6-10) normalized to house-keeping genes: 18s rRNA, GAPDH, RPLP0. (D) Static glucose-stimulated insulin secretion in islets incubated at 3 mM glucose (3G) ±100 µM diazoxide (DZ) followed by 15 mM glucose (15G) ±100 µM DZ. Data are expressed as mean ±SEM.

3.2.6 Effect of B7-H4 on glucose homeostasis *in vivo*

IPGTTs were carried out on WT and age-matched B7-H4 Tg mice to examine the effect of B7-H4 on glucose tolerance (Figure 13A). Another set of IPGTTs were administered to B7-H4 KO mice and their WT littermates (Figure 13B). Fasting glucose levels were similar between both sets of animals. B7-H4 Tg mice showed a slight reduction in blood glucose level 120min following glucose injection compared with WT mice. However there were no significant differences immediately following glucose administration. In addition, B7-H4 KO mice exhibited nearly identical glucose responsiveness as their WT counterparts. Taken together, we demonstrate that B7-H4 does not affect *in vivo* glucose tolerance and uptake in peripheral tissues.

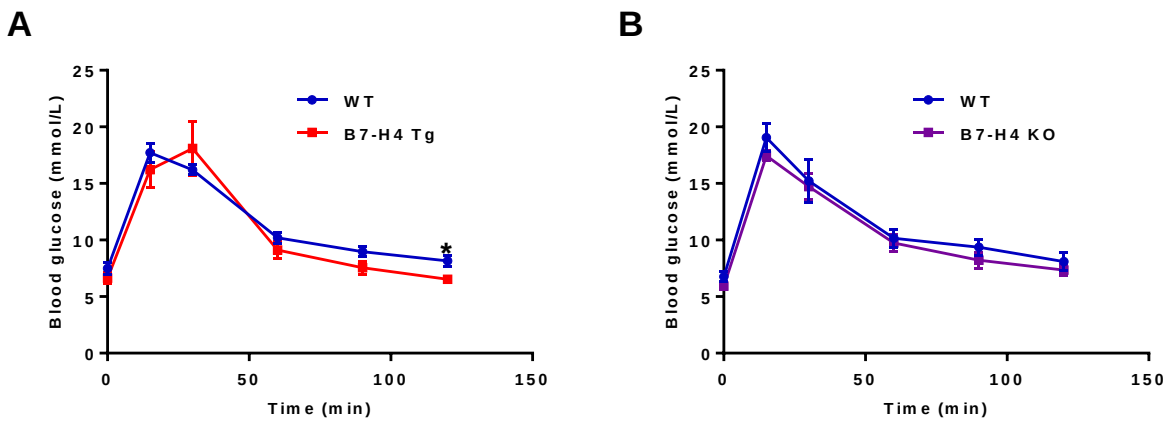

Figure 13. *In vivo* glucose tolerance of B7-H4 Tg, B7-H4 KO, and WT mice
(A,B) Intraperitoneal glucose tolerance in (A) B7-H4 Tg, age-matched WT (n=7-11) and (B) B7-H4-KO, WT littermate mice (n=7). Glucose (2 g/kg body weight) dissolved in saline were injected immediately following blood glucose measurement at time = 0. Data are represented as mean ±SEM, *p≤ 0.05.

3.3 Modulation of β-cell ER Stress Response by B7-H4

3.3.1 B7-H4 expression in human islets during ER stress

The UPR signaling pathways act to mitigate ER stress by altering the transcription and translation of numerous genes and proteins. It is currently unknown what the effect of ER stress is on the expression of B7-H4. Interestingly, we observed a small dose-dependent increase in B7-H4 mRNA expression when human islets were treated with thapsigargin for either 12 or 24 hrs (Figure 14A). Preliminary data suggest protein expression of B7-H4 is elevated as well in human islets following ER stress treatment (Figure 14B). During ER stress, with the exception of select proteins that are usually involved in restoration of ER homeostasis such as the chaperone proteins, the UPR generally down-regulates protein synthesis to decrease overall ER workload[81]. However, an increase in B7-H4 expression at the expense of eliciting protein-folding induced ER stress raises the question of whether B7-H4 is involved in the adaptive UPR. We have also assessed relative B7-H4 expression in human islets from normal, T1D, and T2D donors (Figure 14C). Preliminary results from T1D islets showed reduced B7-H4 expression compared with islets from normal donors. This can be attributed to loss of total β-cell mass as well as reduced B7-H4 expression in individual β-cells. Interestingly, mRNA expression of B7-H4 in islets was markedly elevated in islets from the T2D donor compared with those from the normal donor. This may support our finding that B7-H4 is upregulated under conditions of ER stress and suggests the consequences of this may be relevant in the context of T2D.

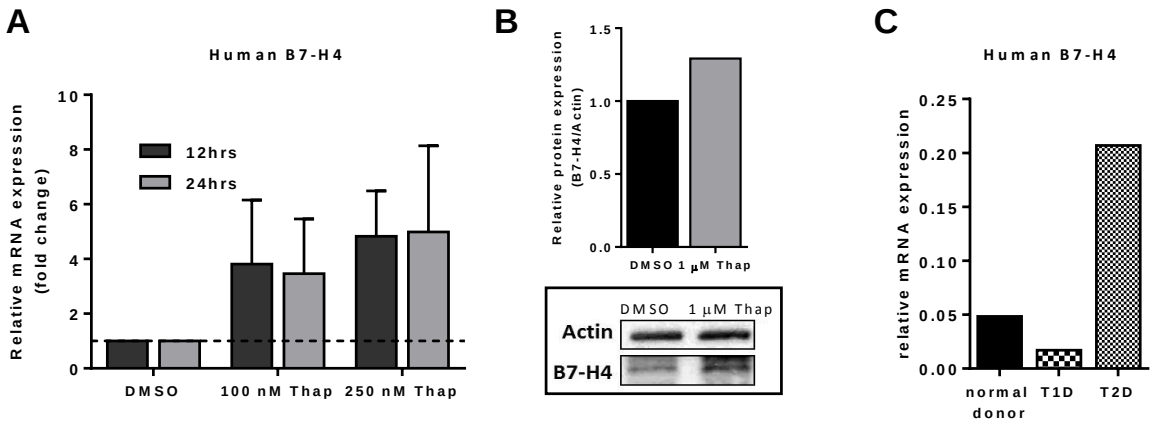

Figure 14. Mild ER stress induces B7-H4 expression in human pancreatic islets
(A) ER stress induced changes in human B7-H4 mRNA expression (n=3). Gene expression is normalized to HPRT, and expressed as fold change over DMSO. (B) Western blot analysis of B7-H4 protein expression in human islets after 24 hrs treatment with 1 uM thapsigargin (Thap) (n=1). B7-H4 protein expression is normalized to actin. (C) Endogenous mRNA expression of B7-H4 in islet from normal, T1D, and T2D donors (n=1). Data are expressed as mean ± SEM.

3.3.2 Amplification of the unfolded protein response by B7-H4

The ER is vital for β-cell function due to its importance in insulin synthesis. Functions of the ER can be affected by a multitude of factors, including the maintenance of intracellular Ca^{2+} homeostasis. Unpublished data from our lab showed that B7-H4 Ig treatment in NOD mice is associated with a reduction in CHOP and XBP1s. Because of this observation, and since we found B7-H4 to be an ER stress- inducible gene in human islets we wanted to inspect the effect of its increase on UPR signaling in β-cells. We first evaluated basal ER stress in both WT and B7-H4 Tg islets by quantitative analysis of the UPR genes- BiP, XBP1s, and CHOP. There were no differences in the expression of BiP and CHOP between genotypes (Figure 15A, Figure 15C). However, expression of XBP1s was significantly reduced in B7-H4 Tg islets compared with WT islets (Figure 15B). Furthermore, there was no evidence of oxidative stress in B7-H4 Tg islets, as

quantified by gene expression of NF-E2-related factor 2 (Nrf2) and heme oxygenase (Hmox) (Figure 15D, 15E). Together, the lack of difference in UPR and oxidative stress gene expression in B7-H4 Tg islets suggests that our B7-H4 overexpression model does not induce ER stress, and may even mitigate ER stress under basal conditions.

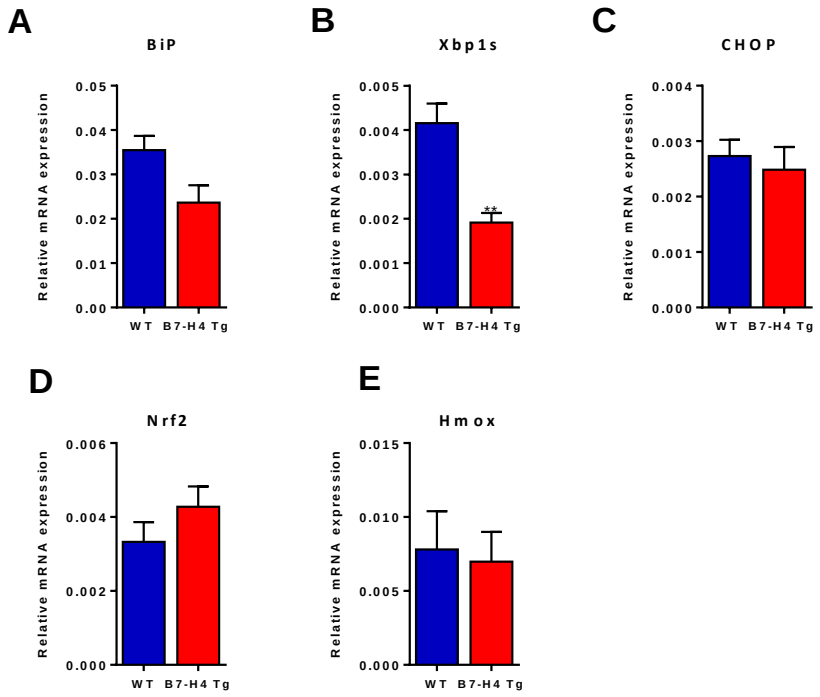

Figure 15. UPR and oxidative stress genes in WT and B7-H4 Tg islets
Relative gene expression of (A) BiP, (B) XBP1s, (C) CHOP, (D) Nrf2, and (E) Hmox in isolated islets (n=3-6). Expression levels are normalized to the house-keeping genes: 18s rRNA, GAPDH, RPLP0. Data represented as mean ± SEM; **p≤0.01 vs WT.

To determine if B7-H4 regulates the UPR under conditions of mild ER stress, we treated WT and B7-H4 Tg mouse islets with 100 nM thapsigargin for 12 hrs. RNA was isolated, and probed for expression of BiP, XBP1s, as well as CHOP. As expected, we saw an elevation in all 3 UPR genes in response to thapsigargin-induced ER stress (Figure 16A, 16B, 16C). In agreement with our basal UPR gene expression profile, BiP and CHOP expressions were

comparable between genotypes while B7-H4 Tg islets demonstrated significantly lower levels of XBP1s in the DMSO treated control samples. In contrast, there was greater activation of the UPR during mild ER stress in B7-H4 Tg islets compared with their WT counterparts, as illustrated by higher gene expression of BiP, XBP1s, and CHOP. We can therefore conclude that B7-H4 overexpression may suppress UPR signaling for XBP1s at least under basal conditions, while it amplifies the UPR under moderate ER stress.

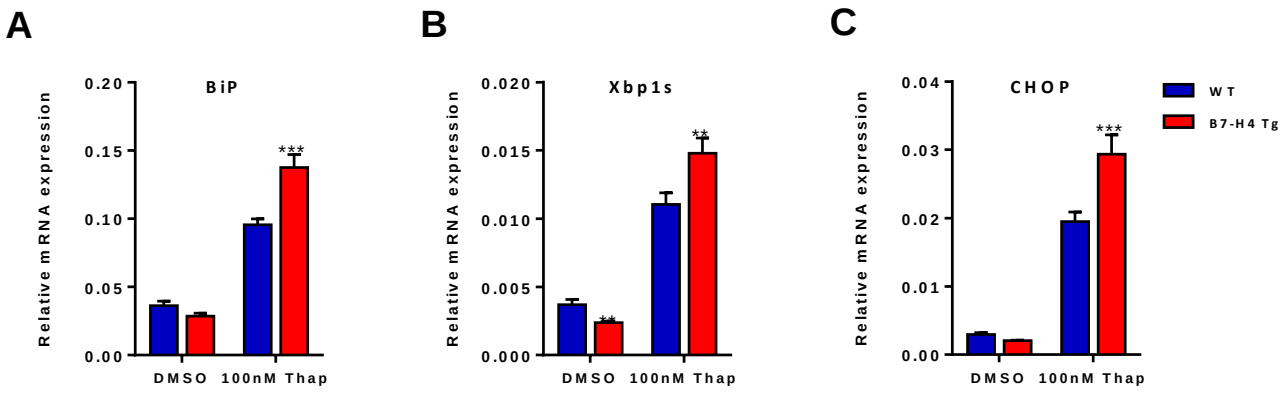

Figure 16. Expression of UPR genes during mild ER stress
Isolated islets from WT and B7-H4 Tg mice were treated with 100nM thapsigargin (Thap) or DMSO control for 12 hrs, and gene expression of (A) BiP, (B) XBP1s, (C) CHOP were determined (n=5). mRNA expression of each gene is normalized to 18s rRNA, GAPDH, and RPLP0. Data are expressed as mean ± SEM; **p≤0.01 vs WT, ***p≤0.001 vs WT.

3.3.3 The effect of B7-H4 on UPR-activated cell death

UPR signals can be both adaptive and pro-apoptotic, and induction of CHOP has especially been associated with increased cell death in response to impaired ER function[91,126]. However, B7-H4 has shown to be protective in islet transplantation settings, where ER stress is known to participate in graft dysfuncion[109,127]. It is therefore possible that B7-H4 up-regulation during ER stress can contribute to pro-survival UPR signaling to attenuate cell death. To

determine whether B7-H4 can be protective during irreversible ER stress, we subjected dispersed islet cells to prolonged and more severe stress conditions, and compared percentage of cell death as quantified by PI staining. We first investigated the effect of B7-H4 on apoptosis in general using a potent cell death inducer, staurosporine, which has been shown to activate apoptosis in various cell types[128]. Indeed, cell death was significantly increased in both genotypes after 45 hrs of staurosporine treatment compared with to DMSO control, and reached 50% at 72 hrs post-treatment. However, there were no significant differences in percentage of cell death between the genotypes, suggesting that B7-H4 does not protect β-cells from staurosporine-induced cell death (Figure 17A). If anything, B7-H4 Tg islets trended towards higher percentage of cell death compared with WT islets at earlier time points. We next treated dispersed islet cells with 15 μM of thapsigargin to elicit ER stress-induced cell death (Figure 17B). Following 72 hrs of treatment, the percentage of dead cells still remained negligible, and was not significantly increased compared with to DMSO controls. Similarly, 15 μM thapsigargin in combination with high glucose at 25 mM was not sufficient to induce significant cell death in both WT and B7-H4 Tg islets, and there were no genotype-dependent differences at any of the time points examined (Figure 17C). Due to the resistance of mouse islet cells to ER stress-induced cell death, the ability of B7-H4 to affect this process remains to be conclusively established.

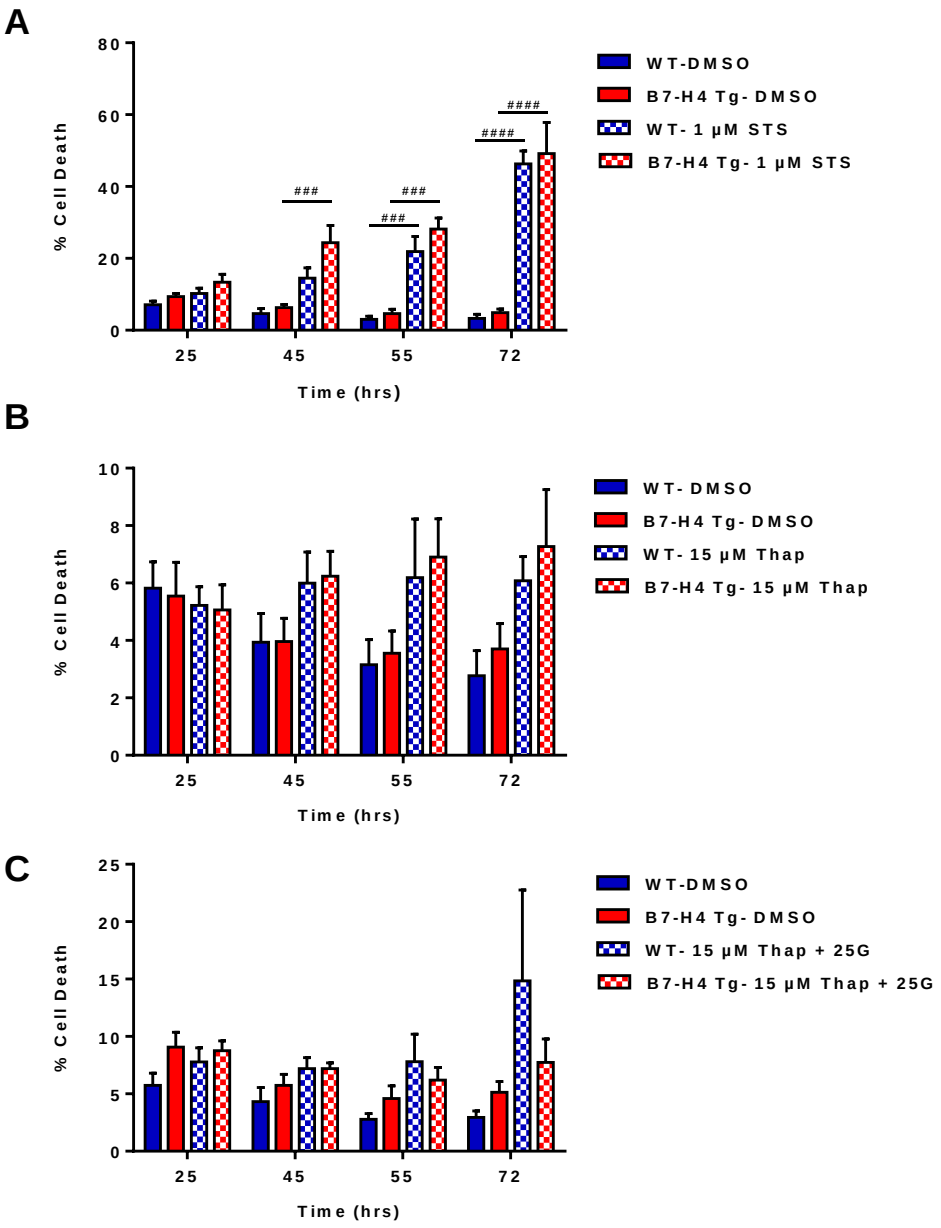

Figure 17. Assessment of β-cell death in WT and B7-H4 Tg islets under ER stress
Cell death analysis of WT and B7-H4 Tg islets treated with (A) stautosporine in 11.1 mM glucose (STS), (B) thapsigargin in 11.1 mM glucose (Thap), and (C) thapsigargin + 25 µM glucose (Thap + 25G), or DMSO vehicle control (n=5-8). Dead islet cells are quantified at indicated time points, and are presented as percentage of PI-positive cells over Hoechst-positive cells. Data are represented as mean ± SEM, ###p≤0.001 vs DMSO control; ####p<0.0001 vs DMSO control.

CHAPTER 4: DISCUSSION

4.1 Roles of B7-H4 in β-Cell Function

The negative co-signaling molecule B7-H4 has well-defined roles in immune regulation, and showed therapeutic potential for prevention and arrest of autoreactive T cell attacks in disease models such as experimental autoimmune encephalomyelitis, rheumatoid arthritis, and T1D[92,129,130]. Recent studies demonstrated that B7-H4 is present in the endocrine pancreas[111,129], however, the specific function of endogenous B7-H4 in pancreatic β-cells is an unexplored avenue of research. In our study, we aim to determine whether B7-H4 affects β-cell functionality and its response to ER stress. In agreement with previous observations by Cheung *et al.*,[111] our preliminary results suggest that B7-H4 expression is reduced in T1D human islets. Furthermore, we observed up-regulated B7-H4 mRNA in islets from T2D donors as compared with those from normal donors. It is therefore possible that any functional roles of B7-H4 in β-cells may be altered in the diabetic state.

As a first assessment of β-cell function, we utilized Fura-2 ratiometric Ca^{2+} imaging to determine the effect of B7-H4 on glucose-responsiveness of mouse islets. B7-H4 Tg islets exhibited cytosolic Ca^{2+} rises in response to 4 mM glucose in contrast to WT islets, which did not respond at this concentration. Further, B7-H4 Tg islets showed larger cytosolic Ca^{2+} rises when stimulated with 5 mM and 6 mM glucose, compared with WT control islets. Stimulations with 10 mM and 15 mM glucose demonstrated that the difference in glucose sensitivity between WT and B7-H4 Tg islets was eliminated at higher glucose concentrations. Lastly, direct cellular depolarization with KCl confirmed that differential Ca^{2+} responses between WT and B7-H4 Tg islets were indeed glucose dependent. These *in vitro* data demonstrated that B7-H4 Tg islets have a lowered threshold for glucose-induced activation and respond with larger Ca^{2+} rises to a sub-

maximal glucose stimulus, supporting our hypothesis that B7-H4 contributes to β-cell functionality. The observed difference in glucose-responsiveness at the level of cytosolic Ca^{2+} concentrations could stem from several factors, including alterations in Ca^{2+} homeostasis, changes in glucose metabolism, and activities of plasma membrane ion channels. We address several aspects of these possible mechanisms for the effect of B7-H4 on β-cell function, which will be discussed in the following.

4.1.1 Effects of B7-H4 on β-cell Ca^{2+} homeostasis

Maintenance of Ca^{2+} homeostasis is crucial for proper cell function and survival. In pancreatic β-cells, glucose induced changes in cytosolic Ca^{2+} level are closely coupled to insulin release. We demonstrated that overexpression of B7-H4 resulted in accelerated Ca^{2+} responses to glucose. This was accompanied by changes in the Ca^{2+} response kinetics, as evidenced by an absence of the initial phase 0 dip in intracellular Ca^{2+} and a lack of steady-state oscillations in B7-H4 Tg islets. The cell possesses a number of mechanisms that reduce cytosolic Ca^{2+} to maintain intracellular homeostasis, one of which is sequestration of Ca^{2+} into the ER by SERCA[61,131]. The transient Ca^{2+} lowering effect of glucose in phase 0 has been attributed to SERCA activity, and can be abolished by administration of the specific SERCA antagonist, thapsigargin[61,122,132]. To determine whether changes in Ca^{2+} response kinetics in B7-H4 Tg islets might involve ER Ca^{2+} pools/mechanisms, we compared the effects of thapsigargin on the glucose responses of WT and B7-H4 Tg islets. Acute pre-treatment with thapsigargin in WT islets mimicked the phenotype seen in B7-H4 Tg islets, as exemplified by a sensitized Ca^{2+} response, rise in basal $[Ca^{2+}]_i$, loss of phase 0 responses, and reduction in the prevalence of steady-state oscillations. These characteristics reflected those observed in previous studies where

thapsigargin treatment caused gradual increase in basal $[Ca^{2+}]_i$ and abolished steady-state oscillations during glucose stimulation[61]. Conversely, glucose-induced Ca^{2+} responses of B7-H4 Tg islets seemed unaffected by administration of thapsigargin. In the type 2 diabetic GK and neonatal streptozotocin-treated rats, nSTZ rats, which possess defective SERCA activity, the glucose-stimulated transient drop in cytosolic Ca^{2+} was absent, and Ca^{2+} responses were unaffected by thapsigargin treatment[133]. It was therefore possible that B7-H4 Tg islets may experience defective glucose-dependent cytosolic handling of Ca^{2+} due to changes in SERCA activity. To more directly study the effect of glucose on islet ER uptake of cytosolic Ca^{2+} without interference from voltage-dependent Ca^{2+} entry, we also stimulated WT and B7-H4 Tg islets with 15 mM glucose while keeping them in a hyperpolarized state with the K_{ATP} channel opener, diazoxide. Consequently, changes in $[Ca^{2+}]_i$ would be directly reflective of signaling events upstream of β-cell depolarization including glucose metabolism and ATP-dependent SERCA activation, which are unaffected by diazoxide. As expected, phase 0 responses in WT islets were observed in the presence of diazoxide, confirming that uptake of cytosolic Ca^{2+} occurs prior to, and independently of cellular depolarization and activation of VGCCs. Importantly, diazoxide treatment unmasked the presence of a glucose-induced drop in cytosolic Ca^{2+} in B7-H4 Tg islets, with a similar proportion of B7-H4 Tg and WT islets displaying this phase 0 ER Ca^{2+} filling response. Contrary to the indications from the thapsigargin-treated islets, these data suggest that SERCA activity may not be significantly affected by B7-H4 expression. This conclusion was further supported by quantitative analysis of SERCA2b gene expression, which did not yield differences between B7-H4 Tg and WT islets.

Aside from inadequate ER Ca^{2+} sequestration, the ability of ER to mobilize Ca^{2+} can also affect cytosolic Ca^{2+} homeostasis, and therefore conceivably also the effect of B7-H4 on the islet

glucose response. To assess whether ER Ca^{2+} release was altered in B7-H4 Tg islets, carbachol was added to the perfusion buffer at 3 mM glucose. It has been established that binding of carbachol to the M3 muscarinic receptor induces a bi-phasic increase in intracellular Ca^{2+} concentration. The first transient phase corresponds to Ca^{2+} release from intracellular IP_3-sensitive ER store, while the second sustained phase arises from extracellular Ca^{2+} influx via store-operated channels[134]. Analysis by iAUC did not reveal any differences in Ca^{2+} responses to carbachol between WT and B7-H4 Tg islets. By depleting Ca^{2+} from the extracellular bath and eliminating 2^{nd} phase response, we aimed to isolate ER Ca^{2+} release. Our results again showed comparable Ca^{2+} response between both genotypes following carbachol stimulation.

Together, these data suggest that B7-H4 does not significantly affect ER Ca^{2+} flux in pancreatic islets. By extension, it is unlikely that the ER contributes to the differences in glucose-induced cytosolic Ca^{2+} responses despite the fact that thapsigargin pre-treatment of WT islets resulted in Ca^{2+} kinetics that were qualitatively similar to those of untreated B7-H4 Tg islets. Rather, it is likely the apparent lack of phase 0 in B7-H4 Tg islets is due to it being overridden by a more rapidly occurring rise in Ca^{2+} levels by the cause of alternative factors that influence the rate of glucose-dependent β-cell depolarization

4.1.2 β-cell glucose metabolism

Pancreatic β-cells are unique in their coupling of nutrient sensing to Ca^{2+} signaling and the induction of insulin secretion. The process of fuel-induced insulin secretion is largely dependent on glucose metabolism[41]. As B7-H4 islets demonstrated increased Ca^{2+} responsiveness to glucose stimuli at low concentrations and an accelerated response at higher concentrations, it was possible their glucose metabolism was altered. Furthermore, since mouse

islets normally show a steady-state oscillatory response to intermediate glucose concentrations and shift to a plateau response at higher (~20 mM) glucose concentrations, the observation that B7-H4 Tg islets showed plateau Ca^{2+} responses already at intermediate glucose concentrations could also reflect metabolic amplifications. To determine whether B7-H4 Tg islets were in fact more metabolically active than WT islets, we measured real-time OCR and ECAR in dispersed WT and B7-H4 Tg islets as an output of mitochondrial respiration and glycolysis, respectively. While both WT and B7-H4 Tg islet cells displayed amplified metabolic activities in response to glucose[28,41], we did not observe genotype-dependent differences in either glycolysis or mitochondrial respiration. Our results differs from a study by Kim *et al.*[118], which alluded to roles of B7-H4 in regulation of mitochondrial function in cancer cells. They reported that knock-down of B7-H4 resulted in suppression of oxygen consumption rate, reduced ATP production, and generation of reactive oxygen species, which synergistically led to cell apoptosis[118]. While this provided some direct evidence for immune-independent roles of B7-H4, these metabolic differences may be specific for cancer cells, which vary drastically in their biology and behavior compared with normal cells. In light of our data, it seems that cell-autonomous functions of B7-H4 may be cell-type-specific, and that B7-H4 does not increase glucose sensitivity of β-cells by impacting glucose metabolism.

4.1.3 K_{ATP} channel activity

In the β-cell, Ca^{2+} responses to glucose are closely coupled to glucose metabolism through K_{ATP} channels. The β-cell K_{ATP} channels are composed of two different types of protein subunits: Kir6.2 and SUR-1[135,136]. The 4 Kir6.2 subunits form the channel pore, and possess binding sites for ATP. Each Kir6.2 subunit is associated with a regulatory SUR-1 subunit, which

grants the channel sensitivity to sulfonylureas and K^+ channel openers[34,35,136]. Binding of ATP to any Kir 6.2 subunit exerts an inhibitory effect on the K_{ATP} channels , rendering it closed[137]. The principal physiological activator of K_{ATP} channels, Mg-ADP, interacts with the SUR-1 subunit to counteract the effect of ATP inhibition[137]. In an effort to unmask the phase 0 response in B7-H4 Tg islets, we used the K^+ channel activator, diazoxide, to prevent glucose-induced depolarization and extracellular Ca^{2+} influx. This led to the surprising discovery that B7-H4 Tg islets showed partial resistance to diazoxide-induced suppression, and were able to respond to glucose with significantly elevated cytosolic Ca^{2+} and insulin secretion in the presence of the drug. This was in contrast to WT islets, in which diazoxide completely prevented glucose-stimulated Ca^{2+} responses and insulin secretion. Furthermore, the reduced sensitivity of B7-H4 Tg islets to diazoxide was accompanied by augmented responses to tolbutamide, a potent sulphonylurea. Tolbutamide stimulated dose-dependent increases in cytosolic Ca^{2+} in both WT and B7-H4 Tg islets, but the B7-H4 Tg islet responses were significantly larger than WT islets, at sub-maximal concentrations of 5 μM and 10 μM tolbutamide. The specificity of diazoxide and tolbutamide for K_{ATP} channels suggests that variations in K_{ATP} channel activity between WT and B7-H4 Tg islets may underlie the differences seen cytosolic Ca^{2+} following sub-maximal glucose stimulation. It is possible that B7-H4 may interact directly with K_{ATP} channels or exert regulatory control over synthesis of channel subunits. Functional studies using site-directed mutagenesis has identified a number of residues in Kir6.2 that may affect channel sensitivity to ATP when mutated[34,136]. In congenital hyperinsulinism, a rare disorder characterized by excessive insulin secretion, loss-of-function mutations in Kir6.2 and SUR-1may induce a predominantly closed state and reduced activity of the channel[34]. For example, point mutation G1479R in the nucleotide binding domain of SUR-1 reduces channel responsiveness to ADP[137]. Another feature in some congenital

hyperinsulinism cases is insensitivity to diazoxide, which has largely been attributed to K_{ATP} channel mutations [35,138,139]. Physiological modulation of K_{ATP} channels can occur via protein-protein interactions with SUR-1. It has been demonstrated that K_{ATP} channel activity can be suppressed by binding of SNARE protein syntaxin 1A to the nuclear binding domain of SUR-1[140,141]. In addition, this interaction can counter the stimulatory effects of diazoxide[141]. It is therefore possible that the sensitized glucose response and diazoxide resistant phenotype we observed in B7-H4 Tg islets may be due to molecular interactions or modifications that modulate K_{ATP} channel activity.

4.1.4 Insulin secretion and glucose tolerance

The exocytotic fusion of insulin granules to the plasma membrane and insulin release is facilitated by cytosolic Ca^{2+}. Interestingly, while B7-H4 Tg islets generated more robust Ca^{2+} responses at low glucose stimulations compared with WT islets, static insulin secretion assay did not reveal differences in insulin secretion. *In vivo* mouse studies also demonstrated that glucose tolerance was not affected by β-cell specific B7-H4 overexpression or global knockout. It is possible that the Ca^{2+} -induced changes in insulin secretion were too small to be detected with our *in vitro* assay. Alternatively, the rise in intracellular Ca^{2+} during low glucose stimulations may not be sufficiently coupled to granule exocytosis to promote insulin release in B7-H4 Tg islets. Activation of exocytotic proteins such as synaptogamin require very high concentrations of Ca^{2+}, in the range of tens of micromoles[142,143]. In order to achieve such high concentrations, the immediately releasable pools of insulin granules in β-cells are largely located in the vicinity of Ca^{2+} channels to facilitate coupling between Ca^{2+} influx and granule docking[143]. It has been proposed that β-cells contain approximately 450 Ca^{2+} channels arranged in triplets[144]. However,

it was estimated that the immediately releasable pool consist of only 60 granules per cell, which indicates that the excess Ca^{2+} channel clusters are not associated with primed granules[144]. Therefore, it is possible that during low glucose stimulations, the microenvironment at the granule docking sites may not reach threshold of activation for vesicle fusion in B7-H4 Tg islets due to either insufficient Ca^{2+} influx and/or granule coupling due to spatial separation between Ca^{2+} channels and insulin granules. Furthermore, syntaxin 1A may deviate from their function in insulin exocytosis if they are already involved in regulating K_{ATP} channel activity in B7-H4 Tg islets. Assessments of insulin content in islets from both WT and B7-H4 Tg islets revealed no difference in overall insulin content, suggesting that total amount of insulin in islets is similar between genotypes. Future studies may include measuring K^+ current and intracellular ATP levels during glucose stimulations to confirm changes in K_{ATP} channel activity in B7-H4 Tg islets. Additionally, patch-clamp recording of K_{ATP} channels can provide more direct information regarding its electrical properties and density on the β-cell plasma membrane. Lastly,islet perifusion experiments can be carried out to determine if B7-H4 overexpression might result in a difference in the kinetics of insulin release that is not apparent in the static incubation assay.

4.2 The Unfolded Protein Response and Apoptosis

Our data have demonstrated cell-autonomous role of B7-H4 in aspects of β-cell function. This in turn may have consequences on cellular response to stress, and vice versa. It is known that cytosolic Ca^{2+} can not only trigger key cellular functions such as hormone secretion, but is also an important second messenger linked to regulation of cell survival. For instance, a family of Ca^{2+}-dependent proteases known as calpains has been shown to be a mediator of β-cell apoptosis[145]. Conversely, glucose-stimulated Ca^{2+} entry may also promote insulin receptor

substrate 2 expression, which is important for β-cell plasticity mass expansion, and survival[146,147]. Interestingly, expression of B7-H4 has been found to be upregulated in a various types of cancer, and may contribute to disease progress through increased cell proliferation, decreased caspase activity, and reduced cell apoptosis[116,117,148]. We found that the broad protein kinase inhibitor staurosporine induced robust cell death in both WT and B7-H4 Tg islets, and that B7-H4 overexpression did not reduce staurosporine-induced cell death. This suggests that B7-H4 overexpression does not have an effect on the execution of β-cell apoptosis, per se. However, it needs to be acknowledged that massive overexpression of protein may itself lead to cellular dysfunction.

To specifically address putative roles of B7-H4 in β-cell stress, we first assessed whether B7-H4 overexpression has an effect on β-cell stress under basal conditions by gene expression analysis of ER stress genes as well as the oxidative stress genes, Hmox and Nrf2. Nrf2 is a transcription factor which has been shown to be a key regulator of anti-oxidant enzyme genes such as Hmox[149,150]. Under unstressed conditions, Nrf2 activity is repressed via degradation through the proteasome pathway. However, exposure to electrophiles and reactive species disrupts the ubiquination system for Nrf degration, thus facilitating its translocation into the nucleus[149,150]. We saw a significant reduction in the UPR gene XBP1s in B7-H4 Tg islets compared with WT islets. Other oxidative (Hmox, Nrf2) and ER stress (BiP, CHOP) genes were comparable between genotypes. These results suggest that B7-H4 overexpression does not induce ER stress due to the overexpression system, but it may ameliorate stress under basal conditions. No changes in β-cell specific genes such as Ins2 and Pdx1 were observed, which can be down-regulated during oxidative stress, further indicating that B7-H4 overexpression does not impart significant oxidative stress. Next, we used thapsigargin as a model of ER stress to

investigate whether B7-H4 has an effect on β-cell stress response. Analysis of the UPR genes revealed higher expression of BiP, XBP1s, and CHOP in B7-H4 Tg islets compared with WT islets following 12 hrs treatment with 100 nM thapsigargin. The results illustrate that B7-H4 can alter β-cell stress response via modulation of the UPR. Currently it is not clear whether these changes in UPR genes exert a protective or adverse effect on β-cell health.

To examine whether up-regulation of UPR activity by B7-H4 overexpression may protect β-cells from ER stress-mediated apoptosis, we treated dispersed islets with 15 μM thapsigargin for up to 72 hrs to induce chronic ER stress. We were not able to detect a difference in cell death between WT and B7-H4 Tg islets under these conditions, but these comparisons were made somewhat difficult by the fact that thapsigargin induced surprisingly low levels of islet cell death. Following 72 hrs of treatment, cell death remained below 10% and was not significantly elevated compared with to control conditions in cells from both genotypes. The relative low percentage of cell death in islets with thapsigargin treatment was also observed in other studies. For example, Martinez *et al.*[151] demonstrated that following a 24 hrs treatment with 100 nM thapsigargin, cell death was below 10% in MIN6 cells. In primary mouse islet cells, treatment with 20 μM thapsigargin for 56 hours was only able to induce approximately 30% cell death[152] Additionally, a combination of thapsigargin and high glucose was only able to elevate cell death to approximately 15% during the course of our experiment. It is possible that a higher dose and/or longer incubation time is needed to elicit cell death, at which point comparisons between the genotypes would be more relevant. Furthermore, future studies using an *in vivo* high-fat diet model may be able to elucidate the role of B7-H4 in the UPR-dependent apoptosis induced by conditions of chronic ER stress that mimics conditions of T2D more closely.

Based on the lack of cell death observed with 15 µM thapsigargin over the course of 72 hours, we hypothesize that mouse islets exposed to 100 nM thapsigargin experience a mild ER stress associated primarily with activation of the protective UPR, and by extension that B7-H4 Tg islets may therefore show a faster and more efficient adaptive response to ER stress. While BiP and XBP1s are well-known for their beneficial roles in the UPR, such as increase efficiency for protein folding, ERAD, and protein quality control[81], CHOP has traditionally been labeled as an apoptosis inducer. However, CHOP has also been shown to have important roles in cellular recovery during acute ER stress through transcriptional control of target genes or microRNAs such as GADD34, ODZ4, and miR708[153,154 155]. The amplified CHOP expression we observed in B7-H4 Tg islets could therefore also have protective roles.

In human islets undergoing ER stress we detected elevated B7-H4 mRNA expression, and preliminary data suggested that this was true at the protein level as well. Importantly, we also saw indications that B7-H4 expression is increased in T2D human islets, which are known to experience heightened levels of ER stress[78,79]. If, as we propose, B7-H4 facilitates activation of the compensatory UPR, the up-regulation of endogenous B7-H4 synthesis during ER stress could conceivably function as an adaptive mechanism to restore ER homeostasis in human islets.

To summarize, we established that B7-H4 gene expression is up-regulated during ER stress, and that B7-H4 overexpression amplifies the UPR. Whether these changes act to overcome perturbations to ER homeostasis or further advance cell death pathways remains to be established.

CHAPTER 5: CONCLUSION

In this study we have established that B7-H4 has cell-autonomous roles in pancreatic β-cells. We found that B7-H4 overexpression resulted in greater glucose sensitivity in β-cells as measured by cytosolic Ca^{2+} concentration. This was associated with resistance to the effect of diazoxide and hypersensitivity to sulfonylurea treatment, which implies that B7-H4 may modulate K_{ATP} channel activity. Further investigations on these novel roles of B7-H4 may offer insights into the functionality of B7-H4 in β-cell physiology under normal conditions as well as where its expression is increased, such as during ER stress. Mechanistic studies regarding its impact on K_{ATP} channels may also reveal underlying defects and therapeutic targets for diazoxide-resistant congenital hyperinsulinism. In the present study we have provided evidence that B7-H4 overexpression amplifies the early ER stress response in β-cells, possibly through all 3 branches of the UPR. However the specific pathway by which B7-H4 regulates the UPR and whether it can exert a protective role during β-cell ER stress remains to be established. Overall, B7-H4 may be an important player in β-cell function and survival that can be relevant in the context of T2D, in addition to its established roles in T1D where it has been shown to promote tolerance induction, graft protection, and reversal of T1D. Additional studies need to be carried out in order to determine its cell-autonomous effects in a physiological setting.

Bibliography

1 *International Diabetes Federation. IDF Diabetes Atlas update poster, 6th edn.*, (International Diabetes Federation, 2014 [http://www.idf.org/diabetesatlas]).

2 Cnop, M., Welsh, N., Jonas, J.-C., Jörns, A., Lenzen, S. & Eizirik, D. Mechanisms of pancreatic beta-cell death in type 1 and type 2 diabetes: many differences, few similarities. *Diabetes* **54 Suppl 2**, 107, doi:10.2337/diabetes.54.suppl_2.S97 (2005).

3 Jain, R. & Lammert, E. Cell-cell interactions in the endocrine pancreas. *Diabetes, obesity & metabolism* **11 Suppl 4**, 159-167, doi:10.1111/j.1463-1326.2009.01102.x (2009).

4 Caicedo, A. Paracrine and autocrine interactions in the human islet: more than meets the eye. *Seminars in cell & developmental biology* **24**, 11-21, doi:10.1016/j.semcdb.2012.09.007 (2012).

5 Karra, E. & Batterham, R. L. The role of gut hormones in the regulation of body weight and energy homeostasis. *Molecular and cellular endocrinology* **316**, 120-128, doi:10.1016/j.mce.2009.06.010 (2010).

6 Forbes, J. & Cooper, M. Mechanisms of diabetic complications. *Physiological Reviews* **93**, 137-188, doi:10.1152/physrev.00045.2011 (2013).

7 van Belle, T., Coppieters, K. & von Herrath, M. Type 1 diabetes: etiology, immunology, and therapeutic strategies. *Physiological Reviews* **91**, 79-118, doi:10.1152/physrev.00003.2010 (2011).

8 Bluestone, J., Herold, K. & Eisenbarth, G. Genetics, pathogenesis and clinical interventions in type 1 diabetes. *Nature* **464**, 1293-1300, doi:10.1038/nature08933 (2010).

9 Malecki, M. T. & Mlynarski, W. Monogenic diabetes: implications for therapy of rare types of disease. *Diabetes*, doi:10.1111/j.1463-1326.2007.00736.x (2008).

10 Kim, C., Newton, K. M. & Knopp, R. H. Gestational Diabetes and the Incidence of Type 2 Diabetes A systematic review. *Diabetes care* (2002).

11 Knip, M. & Simell, O. Environmental triggers of type 1 diabetes. *Cold Spring Harbor perspectives in medicine* **2**, doi:10.1101/cshperspect.a007690 (2012).

12 Kaufman, F. Type 2 diabetes in children and young adults: a " new epidemic" . *Clinical Diabetes* **20**, 217-218, doi:10.2337/diaclin.20.4.217 (2002).

13 Prentki, M. & Nolan, C. Islet beta cell failure in type 2 diabetes. *Journal of Clinical Investigation* **116**, 1802-1812, doi:10.1172/JCI29103 (2006).

14 Nolan, C., Damm, P. & Prentki, M. Type 2 diabetes across generations: from pathophysiology to prevention and management. *Lancet* **378**, 169-181, doi:10.1016/S0140-6736(11)60614-4 (2011).

15 Olokoba, A., Obateru, O. & Olokoba, L. Type 2 diabetes mellitus: a review of current trends. *Oman medical journal* **27**, 269-273, doi:10.5001/omj.2012.68 (2012).

16 Engin, F., Yermalovich, A., Nguyen, T., Ngyuen, T., Hummasti, S., Fu, W., Eizirik, D., Mathis, D. & Hotamisligil, G. Restoration of the unfolded protein response in pancreatic β cells protects mice against type 1 diabetes. *Science translational medicine* **5**, 211ra156, doi:10.1126/scitranslmed.3006534 (2013).

17 Marhfour, I., Lopez, X., Lefkaditis, D., Salmon, I., Allagnat, F., Richardson, S., Morgan, N. & Eizirik, D. Expression of endoplasmic reticulum stress markers in the islets of

patients with type 1 diabetes. *Diabetologia* **55**, 2417-2420, doi:10.1007/s00125-012-2604-3 (2012).
18 Tersey, S., Nishiki, Y., Templin, A., Cabrera, S., Stull, N., Colvin, S., Evans-Molina, C., Rickus, J., Maier, B. & Mirmira, R. Islet β-cell endoplasmic reticulum stress precedes the onset of type 1 diabetes in the nonobese diabetic mouse model. *Diabetes* **61**, 818-827, doi:10.2337/db11-1293 (2012).
19 Oyadomari, S., Takeda, K., Takiguchi, M., Gotoh, T., Matsumoto, M., Wada, I., Akira, S., Araki, E. & Mori, M. Nitric oxide-induced apoptosis in pancreatic beta cells is mediated by the endoplasmic reticulum stress pathway. *Proceedings of the National Academy of Sciences of the United States of America* **98**, 10845-10850, doi:10.1073/pnas.191207498 (2001).
20 Cardozo, A., Ortis, F., Storling, J., Feng, Y.-M., Rasschaert, J., Tonnesen, M., Van Eylen, F., Mandrup-Poulsen, T., Herchuelz, A. & Eizirik, D. Cytokines downregulate the sarcoendoplasmic reticulum pump Ca2+ ATPase 2b and deplete endoplasmic reticulum Ca2+, leading to induction of endoplasmic reticulum stress in pancreatic beta-cells. *Diabetes* **54**, 452-461, doi:10.2337/diabetes.54.2.452 (2005).
21 Tihamer Orban, B. B., Dorothy J Becker, Linda A DiMeglio, Stephen E Gitelman, Robin Goland, Peter A Gottlieb, Carla J Greenbaum, Jennifer B Marks, Roshanak Monzavi, Antoinette Moran, Philip Raskin, Henry Rodriguez, William E Russell, Desmond Schatz, Diane Wherrett, Darrell M Wilson, Jeffrey P Krischer, Jay S Skyler, and the Type 1 Diabetes TrialNet Abatacept Study Group. Co-stimulation modulation with abatacept in patients with recent-onset type 1 diabetes: a randomised, double-blind, placebo-controlled trial. *The Lancet* **378**, doi:10.1016/s0140-6736(11)60886-6 (2011).
22 Shapiro, A. M., Ricordi, C., Hering, B. J., Auchincloss, H., Lindblad, R., Robertson, R. P., Secchi, A., Brendel, M. D., Berney, T., Brennan, D. C., Cagliero, E., Alejandro, R., Ryan, E. A., DiMercurio, B., Morel, P., Polonsky, K. S., Reems, J.-A. A., Bretzel, R. G., Bertuzzi, F., Froud, T., Kandaswamy, R., Sutherland, D. E., Eisenbarth, G., Segal, M., Preiksaitis, J., Korbutt, G. S., Barton, F. B., Viviano, L., Seyfert-Margolis, V., Bluestone, J. & Lakey, J. R. International trial of the Edmonton protocol for islet transplantation. *The New England journal of medicine* **355**, 1318-1330, doi:10.1056/NEJMoa061267 (2006).
23 Warnock, G. L., Thompson, D. M., Meloche, R. M., Shapiro, R. J., Ao, Z., Keown, P., Johnson, J. D., Verchere, C. B., Partovi, N., Begg, I. S., Fung, M., Kozak, S. E., Tong, S. O., Alghofaili, K. M. & Harris, C. A multi-year analysis of islet transplantation compared with intensive medical therapy on progression of complications in type 1 diabetes. *Transplantation* **86**, 1762-1766, doi:10.1097/TP.0b013e318190b052 (2008).
24 Ryan, E. A., Paty, B. W., Senior, P. A., Bigam, D., Alfadhli, E., Kneteman, N. M., Lakey, J. R. & Shapiro, A. M. Five-year follow-up after clinical islet transplantation. *Diabetes* **54**, 2060-2069 (2005).
25 Rutter, G. A., Pullen, T. J., Hodson, D. J. & Martinez-Sanchez, A. Pancreatic β-cell identity, glucose sensing and the control of insulin secretion. *The Biochemical journal* **466**, 203-218, doi:10.1042/bj20141384 (2015).
26 Rorsman, P. & Renström, E. Insulin granule dynamics in pancreatic beta cells. *Diabetologia* **46**, 1029-1045, doi:10.1007/s00125-003-1153-1 (2003).

27 Henquin, J.-C. C. The dual control of insulin secretion by glucose involves triggering and amplifying pathways in β-cells. *Diabetes research and clinical practice* **93 Suppl 1**, 31, doi:10.1016/s0168-8227(11)70010-9 (2011).
28 Jitrapakdee, S., Wutthisathapornchai, A., Wallace, J. C. & MacDonald, M. J. Regulation of insulin secretion: role of mitochondrial signalling. *Diabetologia* **53**, 1019-1032, doi:10.1007/s00125-010-1685-0 (2010).
29 Newsholme, P., Cruzat, V., Arfuso, F. & Keane, K. Nutrient regulation of insulin secretion and action. *The Journal of endocrinology* **221**, 20, doi:10.1530/joe-13-0616 (2014).
30 Porter, J. R. & Barrett, T. G. Monogenic syndromes of abnormal glucose homeostasis: clinical review and relevance to the understanding of the pathology of insulin resistance and β cell failure. *Journal of medical genetics* (2005).
31 MacDonald, P. E., Joseph, J. W. & Rorsman, P. Glucose-sensing mechanisms in pancreatic beta-cells. *Philosophical transactions of the Royal Society of London. Series B, Biological sciences* **360**, 2211-2225, doi:10.1098/rstb.2005.1762 (2005).
32 Gut, A., Kiraly, C. E., Fukuda, M. & Mikoshiba, K. Expression and localisation of synaptotagmin isoforms in endocrine (β)-cells: their function in insulin exocytosis. *Journal of Cell Science* (2001).
33 Meldolesi, J. & Chieregatti, E. Fusion has found its calcium sensor. *Nature cell biology* **6**, 476-478, doi:10.1038/ncb0604-476 (2004).
34 Remedi, M. S. & Koster, J. C. KATP channelopathies in the pancreas. *Pflügers Archiv-European Journal of Physiology* (2010).
35 Saint-Martin, C., Arnoux, J. B. & de Lonlay, P. KATP channel mutations in congenital hyperinsulinism. *Seminars in Pediatric Surgery* (2011).
36 Villareal, D. T., Koster, J. C., Robertson, H., Akrouh, A., Miyake, K., Bell, G. I., Patterson, B. W., Nichols, C. G. & Polonsky, K. S. Kir6.2 variant E23K increases ATP-sensitive K+ channel activity and is associated with impaired insulin release and enhanced insulin sensitivity in adults with normal glucose tolerance. *Diabetes* **58**, 1869-1878, doi:10.2337/db09-0025 (2009).
37 Gembal, M., Gilon, P. & Henquin, J. C. Evidence that glucose can control insulin release independently from its action on ATP-sensitive K+ channels in mouse B cells. *The Journal of clinical investigation* **89**, 1288-1295, doi:10.1172/jci115714 (1992).
38 Panten, U., Schwanstecher, M., Wallasch, A. & Lenzen, S. Glucose both inhibits and stimulates insulin secretion from isolated pancreatic islets exposed to maximally effective concentrations of sulfonylureas. *Naunyn-Schmiedeberg's Archives of Pharmacology* **338**, doi:10.1007/bf00172128 (1988).
39 Seghers, V., Nakazaki, M., DeMayo, F., Aguilar-Bryan, L. & Bryan, J. Sur1 knockout mice. A model for K(ATP) channel-independent regulation of insulin secretion. *The Journal of biological chemistry* **275**, 9270-9277 (2000).
40 Shiota, C., Larsson, O., Shelton, K. D., Shiota, M., Efanov, A. M., Hoy, M., Lindner, J., Kooptiwut, S., Juntti-Berggren, L., Gromada, J., Berggren, P.-O. O. & Magnuson, M. A. Sulfonylurea receptor type 1 knock-out mice have intact feeding-stimulated insulin secretion despite marked impairment in their response to glucose. *The Journal of biological chemistry* **277**, 37176-37183, doi:10.1074/jbc.M206757200 (2002).

41 Prentki, M., Matschinsky, F. M. & Madiraju, S. R. Metabolic signaling in fuel-induced insulin secretion. *Cell metabolism* **18**, 162-185, doi:10.1016/j.cmet.2013.05.018 (2013).
42 Pralong, W. F., Bartley, C. & Wollheim, C. B. Single islet beta-cell stimulation by nutrients: relationship between pyridine nucleotides, cytosolic Ca2+ and secretion. *The EMBO journal* **9**, 53 (1990).
43 Ivarsson, R., Quintens, R., Dejonghe, S. & Tsukamoto, K. Redox control of exocytosis regulatory role of NADPH, thioredoxin, and glutaredoxin. *Diabetes*, doi:10.2337/diabetes.54.7.2132 (2005).
44 Reinbothe, T. M., Ivarsson, R., Li, D. Q. & Niazi, O. Glutaredoxin-1 mediates NADPH-dependent stimulation of calcium-dependent insulin secretion. *Molecular Endocrinology* (2009).
45 Chen, S., Ogawa, A., Ohneda, M., Unger, R. H. & Foster, D. W. More direct evidence for a malonyl-CoA–carnitine palmitoyltransferase I interaction as a key event in pancreatic β-cell signaling. *Diabetes*, doi:10.2337/diab.43.7.878 (1994).
46 Herrero, L., Rubí, B., Sebastián, D., Serra, D. & Asins, G. Alteration of the malonyl-CoA/carnitine palmitoyltransferase I interaction in the β-cell impairs glucose-induced insulin secretion. *Diabetes*, doi:10.2337/diabetes.54.2.462 (2005).
47 Olofsson, C. S., Salehi, A. & Holm, C. Palmitate increases L-type Ca2+ currents and the size of the readily releasable granule pool in mouse pancreatic β-cells. *The Journal of Physiology* doi:10.1113/jphysiol.2004.066258 (2004).
48 Deeney, J. T., Gromada, J., Høy, M., Olsen, H. L., Rhodes, C. J., Prentki, M., Berggren, P. O. & Corkey, B. E. Acute stimulation with long chain acyl-CoA enhances exocytosis in insulin-secreting cells (HIT T-15 and NMRI beta-cells). *The Journal of biological chemistry* **275**, 9363-9368 (2000).
49 Maechler, P. & Wollheim, C. B. Mitochondrial glutamate acts as a messenger in glucose-induced insulin exocytosis. *Nature* **402**, 685-689, doi:10.1038/45280 (1999).
50 Li, M., Li, C., Allen, A., Stanley, C. A. & Smith, T. J. The structure and allosteric regulation of mammalian glutamate dehydrogenase. *Archives of biochemistry and biophysics* (2012).
51 Stanley, C. A. Regulation of glutamate metabolism and insulin secretion by glutamate dehydrogenase in hypoglycemic children. *The American journal of clinical nutrition*, doi:10.3945/ajcn.2009.27462AA (2009).
52 Bertrand, G., Ishiyama, N., Nenquin, M., Ravier, M. A. & Henquin, J.-C. C. The elevation of glutamate content and the amplification of insulin secretion in glucose-stimulated pancreatic islets are not causally related. *The Journal of biological chemistry* **277**, 32883-32891, doi:10.1074/jbc.M205326200 (2002).
53 Chandra, R. & Liddle, R. A. Neurohormonal regulation of pancreatic secretion. *Current opinion in gastroenterology* **28**, 483-487, doi:10.1097/MOG.0b013e3283567f16 (2012).
54 Deacon, C. F. & Ahrén, B. Physiology of incretins in health and disease. *The review of diabetic studies : RDS* **8**, 293-306, doi:10.1900/rds.2011.8.293 (2010).
55 Gilon, P. & Henquin, J. C. Mechanisms and physiological significance of the cholinergic control of pancreatic beta-cell function. *Endocrine reviews* **22**, 565-604, doi:10.1210/edrv.22.5.0440 (2001).

56 Renuka, T. R., Robinson, R. & Paulose, C. S. Increased insulin secretion by muscarinic M1 and M3 receptor function from rat pancreatic islets in vitro. *Neurochemical research* **31**, 313-320, doi:10.1007/s11064-005-9022-6 (2006).
57 Seino, Y., Fukushima, M. & Yabe, D. GIP and GLP-1, the two incretin hormones: Similarities and differences. *Journal of diabetes investigation* **1**, 8-23, doi:10.1111/j.2040-1124.2010.00022.x (2010).
58 MacDonald, P. E., El-Kholy, W., Riedel, M. J., Salapatek, A. M., Light, P. E. & Wheeler, M. B. The multiple actions of GLP-1 on the process of glucose-stimulated insulin secretion. *Diabetes* **51 Suppl 3**, 42 (2002).
59 Pederson, R. A. & Brown, J. C. The insulinotropic action of gastric inhibitory polypeptide in the perfused isolated rat pancreas. *Endocrinology* **99**, 780-785, doi:10.1210/endo-99-3-780 (1976).
60 McIntosh, C. H., Widenmaier, S. & Kim, S.-J. J. Glucose-dependent insulinotropic polypeptide (Gastric Inhibitory Polypeptide; GIP). *Vitamins and hormones* **80**, 409-471, doi:10.1016/s0083-6729(08)00615-8 (2008).
61 Roe, M. W., Mertz, R. J., Lancaster, M. E., Worley, J. F. & Dukes, I. D. Thapsigargin inhibits the glucose-induced decrease of intracellular Ca2+ in mouse islets of Langerhans. *The American journal of physiology* **266**, 62 (1994).
62 Roe, M. W., Lancaster, M. E., Mertz, R. J., Worley, J. F. & Dukes, I. D. Voltage-dependent intracellular calcium release from mouse islets stimulated by glucose. *The Journal of biological chemistry* **268**, 9953-9956 (1993).
63 Bertram, R., Sherman, A. & Satin, L. S. Electrical, Calcium, and Metabolic Oscillations in Pancreatic Islets. *Islets of Langerhans* (2015).
64 Gilon, P., Shepherd, R. M. & Henquin, J.-C. Oscillations of secretion driven by oscillations of cytoplasmic Ca2+ as evidences in single pancreatic islets. *Journal of Biological Chemistry* **268**, 22265-22268 (1993).
65 Henquin, J. C. Regulation of insulin secretion: a matter of phase control and amplitude modulation. *Diabetologia* **52**, 739-751, doi:10.1007/s00125-009-1314-y (2009).
66 Cerasi, E. & Luft, R. The plasma insulin response to glucose infusion in healthy subjects and in diabetes mellitus. *Acta endocrinologica* **55**, 278-304, doi:10.1530/acta.0.0550278 (1967).
67 Mitsuhisa, K., Yoshihiko, S., Toru, A. & Kiyoshi, H. KATP Channel-Independent Glucose Action: An Elusive Pathway in Stimulus-Secretion Coupling of Pancreatic .BETA.-cell. *Endocrine Journal* **48**, 275-288, doi:10.1507/endocrj.48.275 (2001).
68 Zarkovic, M. Synchronization and entrainment of cytoplasmic Ca2+ oscillations in cell clusters prepared from single or multiple mouse pancreatic islets. *AJP: Endocrinology and Metabolism* **287**, doi:10.1152/ajpendo.00069.2004 (2004).
69 Evans-Molina, C., Hatanaka, M. & Mirmira, R. G. Lost in translation: endoplasmic reticulum stress and the decline of β-cell health in diabetes mellitus. *Diabetes, obesity & metabolism* **15 Suppl 3**, 159-169, doi:10.1111/dom.12163 (2013).
70 Mekahli, D., Bultynck, G. & Parys, J. B. Endoplasmic-reticulum calcium depletion and disease. *Cold Spring Harbor perspectives in medicine* (2011).
71 Takei, D., Ishihara, H., Yamaguchi, S. & Yamada, T. WFS1 protein modulates the free Ca 2+ concentration in the endoplasmic reticulum. *FEBS letters*, doi:10.1016/j.febslet.2006.09.007 (2006).

72 Cunha, D. A., Hekerman, P. & Ladrière, L. Initiation and execution of lipotoxic ER stress in pancreatic β-cells. *Journal of Cell Science*, doi:10.1242/jcs.026062 (2008).
73 Wagner, M. & Moore, D. D. Endoplasmic reticulum stress and glucose homeostasis. *Current opinion in clinical nutrition and metabolic care* **14**, 367-373, doi:10.1097/MCO.0b013e32834778d4 (2011).
74 Cnop, M., Foufelle, F. & Velloso, L. A. Endoplasmic reticulum stress, obesity and diabetes. *Trends in molecular medicine* (2012).
75 Maganti, A., Evans-Molina, C. & Mirmira, R. From immunobiology to β-cell biology: the changing perspective on type 1 diabetes. *Islets* **6**, doi:10.4161/isl.28778 (2013).
76 Marhfour, I., Lopez, X., Lefkaditis, D., Salmon, I., Allagnat, F., Richardson, S. J., Morgan, N. G. & Eizirik, D. L. Expression of endoplasmic reticulum stress markers in the islets of patients with type 1 diabetes. *Diabetologia* (2012).
77 Tersey, S. A., Nishiki, Y., Templin, A. T. & Cabrera, S. M. Islet β-cell endoplasmic reticulum stress precedes the onset of type 1 diabetes in the nonobese diabetic mouse model. *Diabetes* (2012).
78 Back, S. H., Kang, S.-W. W., Han, J. & Chung, H.-T. T. Endoplasmic reticulum stress in the β-cell pathogenesis of type 2 diabetes. *Experimental diabetes research* **2012**, 618396, doi:10.1155/2012/618396 (2011).
79 Back, S. H. & Kaufman, R. J. Endoplasmic reticulum stress and type 2 diabetes. *Annual review of biochemistry* **81**, 767-793, doi:10.1146/annurev-biochem-072909-095555 (2011).
80 Szegezdi, E., Logue, S. E., Gorman, A. M. & Samali, A. Mediators of endoplasmic reticulum stress-induced apoptosis. *EMBO reports* **7**, 880-885, doi:10.1038/sj.embor.7400779 (2006).
81 Hetz, C. The unfolded protein response: controlling cell fate decisions under ER stress and beyond. *Nature reviews. Molecular cell biology* **13**, 89-102, doi:10.1038/nrm3270 (2012).
82 Harding, H. P., Zeng, H., Zhang, Y., Jungries, R., Chung, P., Plesken, H., Sabatini, D. D. & Ron, D. Diabetes mellitus and exocrine pancreatic dysfunction in perk-/- mice reveals a role for translational control in secretory cell survival. *Molecular cell* **7**, 1153-1163 (2001).
83 Zhang, P., McGrath, B., Li, S. a., Frank, A., Zambito, F., Reinert, J., Gannon, M., Ma, K., McNaughton, K. & Cavener, D. R. The PERK eukaryotic initiation factor 2 alpha kinase is required for the development of the skeletal system, postnatal growth, and the function and viability of the pancreas. *Molecular and cellular biology* **22**, 3864-3874 (2002).
84 Lipson, K. L., Fonseca, S. G., Ishigaki, S., Nguyen, L. X. & Foss, E. Regulation of insulin biosynthesis in pancreatic beta cells by an endoplasmic reticulum-resident protein kinase IRE1. *Cell metabolism* (2006).
85 Iwawaki, T., Akai, R. & Kohno, K. IRE1α disruption causes histological abnormality of exocrine tissues, increase of blood glucose level, and decrease of serum immunoglobulin level. *PloS one* **5**, doi:10.1371/journal.pone.0013052 (2009).
86 Teodoro, T., Odisho, T., Sidorova, E. & Volchuk, A. Pancreatic β-cells depend on basal expression of active ATF6α-p50 for cell survival even under nonstress conditions. *American journal of physiology. Cell physiology* **302**, 1003, doi:10.1152/ajpcell.00160.2011 (2012).

87 Cunha, D. A., Igoillo-Esteve, M., Gurzov, E. N., Germano, C. M., Naamane, N., Marhfour, I., Fukaya, M., Vanderwinden, J.-M. M., Gysemans, C., Mathieu, C., Marselli, L., Marchetti, P., Harding, H. P., Ron, D., Eizirik, D. L. & Cnop, M. Death protein 5 and p53-upregulated modulator of apoptosis mediate the endoplasmic reticulum stress-mitochondrial dialog triggering lipotoxic rodent and human β-cell apoptosis. *Diabetes* **61**, 2763-2775, doi:10.2337/db12-0123 (2012).

88 Taylor, R. C., Cullen, S. P. & Martin, S. J. Apoptosis: controlled demolition at the cellular level. *Nature reviews. Molecular cell biology* **9**, 231-241, doi:10.1038/nrm2312 (2008).

89 Tait, S. W. & Green, D. R. Mitochondria and cell death: outer membrane permeabilization and beyond. *Nature reviews. Molecular cell biology* **11**, 621-632, doi:10.1038/nrm2952 (2010).

90 Oyadomari, S., Koizumi, A., Takeda, K., Gotoh, T., Akira, S., Araki, E. & Mori, M. Targeted disruption of the Chop gene delays endoplasmic reticulum stress-mediated diabetes. *The Journal of clinical investigation* **109**, 525-532, doi:10.1172/jci14550 (2002).

91 Song, B., Scheuner, D., Ron, D., Pennathur, S. & Kaufman, R. J. Chop deletion reduces oxidative stress, improves beta cell function, and promotes cell survival in multiple mouse models of diabetes. *The Journal of clinical investigation* **118**, 3378-3389, doi:10.1172/jci34587 (2008).

92 Prasad, D., Richards, S., Mai, X. & Dong, C. B7S1, a novel B7 family member that negatively regulates T cell activation. *Immunity* **18**, 863-873, doi:10.1016/S1074-7613(03)00147-X (2003).

93 Sica, G., Choi, I., Zhu, G., Tamada, K., Wang, S., Tamura, H., Chapoval, A., Flies, D., Bajorath, J. & Chen, L. B7-H4, a molecule of the B7 family, negatively regulates T cell immunity. *Immunity* **18**, 849-861, doi:10.1016/S1074-7613(03)00152-3 (2003).

94 Choi, I.-H., Zhu, G., Sica, G., Strome, S., Cheville, J., Lau, J., Zhu, Y., Flies, D., Tamada, K. & Chen, L. Genomic organization and expression analysis of B7-H4, an immune inhibitory molecule of the B7 family. *Journal of Immunology* **171**, 4650-4654 (2003).

95 Collins, M., Ling, V. & Carreno, B. M. The B7 family of immune-regulatory ligands. *Genome biology* **6**, 223, doi:10.1186/gb-2005-6-6-223 (2004).

96 Greenwald, R. J., Freeman, G. J. & Sharpe, A. H. The B7 family revisited. *Annual review of immunology* **23**, 515-548, doi:10.1146/annurev.immunol.23.021704.115611 (2004).

97 Radvanyi, L. G., Shi, Y., Vaziri, H., Sharma, A., Dhala, R., Mills, G. B. & Miller, R. G. CD28 costimulation inhibits TCR-induced apoptosis during a primary T cell response. *Journal of immunology (Baltimore, Md. : 1950)* **156**, 1788-1798 (1996).

98 Krummel, M. F. & Allison, J. P. CTLA-4 engagement inhibits IL-2 accumulation and cell cycle progression upon activation of resting T cells. *The Journal of experimental medicine* **183**, 2533-2540 (1996).

99 Rainbow, D., Moule, C., Fraser, H., Clark, J., Howlett, S., Burren, O., Christensen, M., Moody, V., Steward, C., Mohammed, J., Fusakio, M., Masteller, E., Finger, E., Houchins, J., Naf, D., Koentgen, F., Ridgway, W., Todd, J., Bluestone, J., Peterson, L., Mattner, J. & Wicker, L. Evidence that Cd101 is an autoimmune diabetes gene in nonobese diabetic mice. *Journal of Immunology* **187**, 325-336, doi:10.4049/jimmunol.1003523 (2011).

100 Hollenbaugh, D. & Aruffo, A. Construction of immunoglobulin fusion proteins. *Current protocols in immunology / edited by John E. Coligan ... [et al.]* **Chapter 10**, doi:10.1002/0471142735.im1019as48 (2002).
101 Wang, X., Hao, J., Metzger, D., Mui, A., Ao, Z., Akhoundsadegh, N., Langermann, S., Liu, L., Chen, L., Ou, D., Verchere, C. & Warnock, G. Early treatment of NOD mice with B7-H4 reduces the incidence of autoimmune diabetes. *Diabetes* **60**, 3246-3255, doi:10.2337/db11-0375 (2011).
102 Zang, X., Loke, P. n., Kim, J., Murphy, K., Waitz, R. & Allison, J. B7x: a widely expressed B7 family member that inhibits T cell activation. *Proc. Natl. Acad. Sci. U. S. A.* **100**, 10388-10392, doi:10.1073/pnas.1434299100 (2003).
103 Wang, X., Hao, J., Metzger, D. L., Ao, Z., Chen, L., Ou, D., Verchere, C. B., Mui, A. & Warnock, G. L. B7-H4 Treatment of T Cells Inhibits ERK, JNK, p38, and AKT Activation. *PloS one* **7**, doi:10.1371/journal.pone.0028232 (2011).
104 Lee, I. F., Wang, X., Hao, J., Akhoundsadegh, N., Chen, L., Liu, L., Langermann, S., Ou, D. & Warnock, G. B7-H4.Ig inhibits the development of type 1 diabetes by regulating Th17 cells in NOD mice. *Cell. Immunol.* **282**, 1-8, doi:10.1016/j.cellimm.2013.03.005 (2013).
105 Wei, J., Loke, P. n., Zang, X. & Allison, J. P. Tissue-specific expression of B7x protects from CD4 T cell-mediated autoimmunity. *Journal of Experimental Medicine* **208**, 1683-1694, doi:10.1084/jem.20100639 (2011).
106 Wang, X., Hao, J., Metzger, D. L., Mui, A., Ao, Z., Verchere, C. B., Chen, L., Ou, D. & Warnock, G. L. Local expression of B7-H4 by recombinant adenovirus transduction in mouse islets prolongs allograft survival. *Transplantation* **87**, 482-490, doi:10.1097/TP.0b013e318195e5fa (2009).
107 Yuan, C.-L. L., Xu, J.-F. F., Tong, J., Yang, H., He, F.-R. R., Gong, Q., Xiong, P., Duan, L., Fang, M., Tan, Z., Xu, Y., Chen, Y.-F. F., Zheng, F. & Gong, F.-L. L. B7-H4 transfection prolongs beta-cell graft survival. *Transplant immunology* **21**, 143-149, doi:10.1016/j.trim.2009.03.007 (2009).
108 Wang, X., Hao, J., Metzger, D. L., Ao, Z., Meloche, M., Verchere, C. B., Chen, L., Ou, D., Mui, A. & Warnock, G. L. B7-H4 Pathway in Islet Transplantation and β-Cell Replacement Therapies. *Journal of transplantation* **2011**, 418902, doi:10.1155/2011/418902 (2010).
109 Wang, X., Hao, J., Metzger, D. L., Mui, A., Lee, I. F. F., Akhoundsadegh, N., Ao, Z., Chen, L., Ou, D., Verchere, C. B. & Warnock, G. L. Endogenous expression of B7-H4 improves long-term murine islet allograft survival. *Transplantation* **95**, 94-99, doi:10.1097/TP.0b013e318277229d (2013).
110 Wang, X., Hao, J., Metzger, D. L., Mui, A., Ao, Z., Verchere, C. B., Chen, L., Ou, D. & Warnock, G. L. B7-H4 induces donor-specific tolerance in mouse islet allografts. *Cell transplantation* **21**, 99-111, doi:10.3727/096368911x582750 (2011).
111 Cheung, S., Ou, D., Metzger, D., Meloche, M., Ao, Z., Ng, S., Owen, D. & Warnock, G. B7-H4 expression in normal and diseased human islet β cells. *Pancreas* **43**, 128-134, doi:10.1097/MPA.0b013e31829695d2 (2014).
112 Salceda, S., Tang, T., Kmet, M., Munteanu, A., Ghosh, M., Macina, R., Liu, W., Pilkington, G. & Papkoff, J. The immunomodulatory protein B7-H4 is overexpressed in

breast and ovarian cancers and promotes epithelial cell transformation. *Experimental Cell Research* **306**, 128-141, doi:10.1016/j.yexcr.2005.01.018 (2005).
113 Simon, I., Katsaros, D., Rigault de la Longrais, I., Massobrio, M., Scorilas, A., Kim, N. W., Sarno, M. J., Wolfert, R. L. & Diamandis, E. P. B7-H4 is over-expressed in early-stage ovarian cancer and is independent of CA125 expression. *Gynecologic oncology* **106**, 334-341, doi:10.1016/j.ygyno.2007.03.035 (2007).
114 Awadallah, N. S., Shroyer, K. R., Langer, D. A., Torkko, K. C., Chen, Y. K., Bentz, J. S., Papkoff, J., Liu, W., Nash, S. R. & Shah, R. J. Detection of B7-H4 and p53 in pancreatic cancer: potential role as a cytological diagnostic adjunct. *Pancreas* **36**, 200-206, doi:10.1097/MPA.0b013e318150e4e0 (2008).
115 Simon, I., Zhuo, S., Corral, L., Diamandis, E. P., Sarno, M. J., Wolfert, R. L. & Kim, N. W. B7-h4 is a novel membrane-bound protein and a candidate serum and tissue biomarker for ovarian cancer. *Cancer research* **66**, 1570-1575, doi:10.1158/0008-5472.can-04-3550 (2006).
116 Qian, Y., Hong, B., Shen, L., Wu, Z., Yao, H. & Zhang, L. B7-H4 enhances oncogenicity and inhibits apoptosis in pancreatic cancer cells. *Cell and tissue research* **353**, 139-151, doi:10.1007/s00441-013-1640-8 (2013).
117 Zhang, L., Wu, H., Lu, D., Li, G., Sun, C., Song, H., Li, J., Zhai, T., Huang, L., Hou, C., Wang, W., Zhou, B., Chen, S., Lu, B. & Zhang, X. The costimulatory molecule B7-H4 promote tumor progression and cell proliferation through translocating into nucleus. *Oncogene* **32**, 5347-5358, doi:10.1038/onc.2012.600 (2013).
118 Kim, H. K., Song, I.-S. S., Lee, S. Y., Jeong, S. H., Lee, S. R., Heo, H. J., Thu, V. T., Kim, N., Ko, K. S., Rhee, B. D., Jeong, D. H., Kim, Y. N. & Han, J. B7-H4 downregulation induces mitochondrial dysfunction and enhances doxorubicin sensitivity via the cAMP/CREB/PGC1-α signaling pathway in HeLa cells. *Pflügers Archiv : European journal of physiology* **466**, 2323-2338, doi:10.1007/s00424-014-1493-3 (2014).
119 Suh, W.-K. K., Wang, S., Duncan, G. S., Miyazaki, Y., Cates, E., Walker, T., Gajewska, B. U., Deenick, E., Dawicki, W., Okada, H., Wakeham, A., Itie, A., Watts, T. H., Ohashi, P. S., Jordana, M., Yoshida, H. & Mak, T. W. Generation and characterization of B7-H4/B7S1/B7x-deficient mice. *Molecular and cellular biology* **26**, 6403-6411, doi:10.1128/mcb.00755-06 (2006).
120 Warnock, G. L., Meloche, R. M., Thompson, D., Shapiro, R. J., Fung, M., Ao, Z., Ho, S., He, Z., Dai, L.-J. J., Young, L., Blackburn, L., Kozak, S., Kim, P. T., Al-Adra, D., Johnson, J. D., Liao, Y.-H. T. H., Elliott, T. & Verchere, C. B. Improved human pancreatic islet isolation for a prospective cohort study of islet transplantation vs best medical therapy in type 1 diabetes mellitus. *Archives of surgery (Chicago, Ill. : 1960)* **140**, 735-744, doi:10.1001/archsurg.140.8.735 (2005).
121 Vandesompele, J., Preter, D. K. & Pattyn, F. Accurate normalization of real-time quantitative RT-PCR data by geometric averaging of multiple internal control genes. *Genome biology*, doi:10.1186/gb-2002-3-7-research0034 (2002).
122 Roe, M. W., Philipson, L. H. & Frangakis, C. J. Defective glucose-dependent endoplasmic reticulum Ca2+ sequestration in diabetic mouse islets of Langerhans. *Journal of Biological Chemistry* (1994).
123 Marchi, U., Thevenet, J., Hermant, A., Dioum, E. & Wiederkehr, A. Calcium co-regulates oxidative metabolism and ATP synthase-dependent respiration in pancreatic

beta cells. *Journal of Biological Chemistry* **289**, 9182-9194, doi:10.1074/jbc.M113.513184 (2014).
124 Wikstrom, J. D., Sereda, S. B., Stiles, L., Elorza, A. & Allister, E. M. A novel high-throughput assay for islet respiration reveals uncoupling of rodent and human islets. *PloS one*, doi:10.1371/journal.pone.0033023 (2012).
125 Dyachok, O. & Gylfe, E. Store-operated influx of Ca2+ in pancreatic β-cells exhibits graded dependence on the filling of the endoplasmic reticulum. *Journal of Cell Science* (2001).
126 Zinszner, H., Kuroda, M., Wang, X., Batchvarova, N., Lightfoot, R. T., Remotti, H., Stevens, J. L. & Ron, D. CHOP is implicated in programmed cell death in response to impaired function of the endoplasmic reticulum. *Genes & development* **12**, 982-995 (1998).
127 Negi, S., Park, S. H., Jetha, A., Aikin, R., Tremblay, M. & Paraskevas, S. Evidence of endoplasmic reticulum stress mediating cell death in transplanted human islets. *Cell transplantation* **21**, 889-900, doi:10.3727/096368911x603639 (2011).
128 Belmokhtar, C. A., Hillion, J. & Ségal-Bendirdjian, E. Staurosporine induces apoptosis through both caspase-dependent and caspase-independent mechanisms. *Oncogene* **20**, 3354-3362, doi:10.1038/sj.onc.1204436 (2001).
129 Wei, J., Loke, P. n., Zang, X. & Allison, J. P. Tissue-specific expression of B7x protects from CD4 T cell-mediated autoimmunity. *The Journal of experimental medicine* **208**, 1683-1694, doi:10.1084/jem.20100639 (2011).
130 Azuma, T., Zhu, G., Xu, H., Rietz, A. C., Drake, C. G., Matteson, E. L. & Chen, L. Potential role of decoy B7-H4 in the pathogenesis of rheumatoid arthritis: a mouse model informed by clinical data. *PLoS medicine* **6**, doi:10.1371/journal.pmed.1000166 (2009).
131 Guerrero-Hernandez, A. & Verkhratsky, A. Calcium signalling in diabetes. *Cell calcium* **56**, 297-301, doi:10.1016/j.ceca.2014.08.009 (2014).
132 Worley, J. F., McIntyre, M. S., Spencer, B., Mertz, R. J., Roe, M. W. & Dukes, I. D. Endoplasmic reticulum calcium store regulates membrane potential in mouse islet beta-cells. *The Journal of biological chemistry* **269**, 14359-14362 (1994).
133 Marie, J. C., Bailbé, D., Gylfe, E. & Portha, B. Defective glucose-dependent cytosolic Ca2+ handling in islets of GK and nSTZ rat models of type 2 diabetes. *The Journal of endocrinology* **169**, 169-176 (2001).
134 Edelman, J. L., Kajimura, M., Woldemussie, E. & Sachs, G. Differential effects of carbachol on calcium entry and release in CHO cells expressing the m3 muscarinic receptor. *Cell calcium* **16**, 181-193 (1994).
135 Tarasov, A., Dusonchet, J. & Ashcroft, F. Metabolic Regulation of the Pancreatic Beta-Cell ATP-Sensitive K+ Channel A Pas de Deux. *Diabetes*, doi:10.2337/diabetes.53.suppl_3.S113 (2004).
136 Lin, C. W., Lin, Y. W., Yan, F. F., Casey, J. & Kochhar, M. Kir6. 2 Mutations Associated With Neonatal Diabetes Reduce Expression of ATP-Sensitive K+ channels Implications in Disease Mechanism and Sulfonylurea Therapy. *Diabetes* (2006).
137 Quan, Y., Barszczyk, A., Feng, Z. & Sun, H. Current understanding of KATP channels in neonatal diseases: focus on insulin secretion disorders. *Acta Pharmacologica Sinica*, doi:10.1038/aps.2011.57 (2011).

138 MacMullen, C. M., Zhou, Q., Snider, K. E. & Tewson, P. H. Diazoxide-unresponsive congenital hyperinsulinism in children with dominant mutations of the β-cell sulfonylurea receptor SUR1. *Diabetes* (2011).
139 Bellanné-Chantelot, C., Saint-Martin, C., Ribeiro, M. J. J., Vaury, C., Verkarre, V., Arnoux, J. B. B., Valayannopoulos, V., Gobrecht, S., Sempoux, C., Rahier, J., Fournet, J. C. C., Jaubert, F., Aigrain, Y., Nihoul-Fékété, C. & de Lonlay, P. ABCC8 and KCNJ11 molecular spectrum of 109 patients with diazoxide-unresponsive congenital hyperinsulinism. *Journal of medical genetics* **47**, 752-759, doi:10.1136/jmg.2009.075416 (2010).
140 Pasyk, E. A., Kang, Y., Huang, X., Cui, N., Sheu, L. & Gaisano, H. Y. Syntaxin-1A binds the nucleotide-binding folds of sulphonylurea receptor 1 to regulate the KATP channel. *Journal of Biological Chemistry* **279**, 4234-4240, doi:10.1074/jbc.M309667200 (2004).
141 Ng, B., Kang, Y., Elias, C. L., He, Y., Xie, H. & Hansen, J. B. The Actions of a Novel Potent Islet β-Cell–Specific ATP-Sensitive K+ Channel Opener Can Be Modulated by Syntaxin-1A Acting on Sulfonylurea Receptor 1. *Diabetes*, doi:10.2337/db07-0030 (2007).
142 Satin, L. S. Localized calcium influx in pancreatic beta-cells: its significance for Ca2+-dependent insulin secretion from the islets of Langerhans. *Endocrine* **13**, 251-262, doi:10.1385/endo:13:3:251 (2000).
143 Pedersen, M. G. & Sherman, A. Newcomer insulin secretory granules as a highly calcium-sensitive pool. *Proceedings of the National Academy of Sciences of the United States of America* **106**, 7432-7436, doi:10.1073/pnas.0901202106 (2009).
144 Barg, S., Ma, X., Eliasson, L., Galvanovskis, J., Göpel, S. O., Obermüller, S., Platzer, J., Renström, E., Trus, M., Atlas, D., Striessnig, J. & Rorsman, P. Fast exocytosis with few Ca(2+) channels in insulin-secreting mouse pancreatic B cells. *Biophysical journal* **81**, 3308-3323, doi:10.1016/s0006-3495(01)75964-4 (2001).
145 Huang, C., Gurlo, T., Haataja, L., Costes, S. & Daval, M. Calcium-activated calpain-2 is a mediator of beta cell dysfunction and apoptosis in type 2 diabetes. *Journal of Biological Chemistry*, doi:10.1074/jbc.M109.024190 (2010).
146 Weir, G. C. & Bonner-Weir, S. A dominant role for glucose in β cell compensation of insulin resistance. *Journal of Clinical Investigation*, doi:10.1172/jci30862 (2007).
147 Persaud, S. J., Liu, B., Sampaio, H. B., Jones, P. M. & Muller, D. S. Calcium/calmodulin-dependent kinase IV controls glucose-induced Irs2 expression in mouse beta cells via activation of cAMP response element-binding protein. *Diabetologia*, doi:10.1007/s00125-011-2050-7 (2011).
148 Tihamer Orban, B. B., Dorothy J Becker, Linda A DiMeglio, Stephen E Gitelman, Robin Goland, Peter A Gottlieb, Carla J Greenbaum, Jennifer B Marks, Roshanak Monzavi, Antoinette Moran, Philip Raskin, Henry Rodriguez, William E Russell, Desmond Schatz, Diane Wherrett, Darrell M Wilson, Jeffrey P Krischer, Jay S Skyler, and the Type 1 Diabetes TrialNet Abatacept Study Group. The immunomodulatory protein B7-H4 is overexpressed in breast and ovarian cancers and promotes epithelial cell transformation. *Experimental Cell Research* **306**, 128141, doi:10.1016/j.yexcr.2005.01.018 (2005).
149 Uruno, A., Furusawa, Y., Yagishita, Y., Fukutomi, T., Muramatsu, H., Negishi, T., Sugawara, A., Kensler, T. W. & Yamamoto, M. The Keap1-Nrf2 system prevents onset

of diabetes mellitus. *Molecular and cellular biology* **33**, 2996-3010, doi:10.1128/mcb.00225-13 (2013).

150 Yagishita, Y., Fukutomi, T., Sugawara, A., Kawamura, H., Takahashi, T., Pi, J., Uruno, A. & Yamamoto, M. Nrf2 protects pancreatic β-cells from oxidative and nitrosative stress in diabetic model mice. *Diabetes* **63**, 605-618, doi:10.2337/db13-0909 (2014).

151 Martinez, S. C., Tanabe, K. & Cras-Méneur, C. Inhibition of Foxo1 protects pancreatic islet β-cells against fatty acid and endoplasmic reticulum stress–induced apoptosis. *Diabetes*, doi:10.2337/db07-0595 (2008).

152 Carrington, E. M., McKenzie, M. D., Jansen, E., Myers, M., Fynch, S., Kos, C., Strasser, A., Kay, T. W., Scott, C. L. & Allison, J. Islet -cells deficient in Bcl-xL develop but are abnormally sensitive to apoptotic stimuli. *Diabetes* **58**, 2316-2323, doi:10.2337/db08-1602 (2009).

153 Wang, X. Z., Kuroda, M., Sok, J. & Batchvarova, N. Identification of novel stress-induced genes downstream of chop. *The EMBO journal*, doi:10.1093/emboj/17.13.3619 (1998).

154 Behrman, S., Acosta-Alvear, D. & Walter, P. A CHOP-regulated microRNA controls rhodopsin expression. *The Journal of cell biology* **192**, 919-927, doi:10.1083/jcb.201010055 (2011).

155 Qi, Y. & Xia, P. Cellular inhibitor of apoptosis protein-1 (cIAP1) plays a critical role in β-cell survival under endoplasmic reticulum stress: promoting ubiquitination and degradation of C/EBP homologous protein (CHOP). *The Journal of biological chemistry* **287**, 32236-32245, doi:10.1074/jbc.M112.362160 (2012).